

University of Alberta

Rapid Dampening Suspension for Ultra Class Haulers
by

Ramil Santos

A thesis submitted to the Faculty of Graduate Studies and Research in partial
fulfilment of the requirements for the degree of

Master of Science

in



Mining Engineering

Department of *Civil and Environmental Engineering*

Edmonton, Alberta

Spring 2007



Library and
Archives Canada

Bibliothèque et
Archives Canada

Published Heritage
Branch

Direction du
Patrimoine de l'édition

395 Wellington Street
Ottawa ON K1A 0N4
Canada

395, rue Wellington
Ottawa ON K1A 0N4
Canada

Your file *Votre référence*
ISBN: 978-0-494-30016-9
Our file *Notre référence*
ISBN: 978-0-494-30016-9

NOTICE:

The author has granted a non-exclusive license allowing Library and Archives Canada to reproduce, publish, archive, preserve, conserve, communicate to the public by telecommunication or on the Internet, loan, distribute and sell theses worldwide, for commercial or non-commercial purposes, in microform, paper, electronic and/or any other formats.

The author retains copyright ownership and moral rights in this thesis. Neither the thesis nor substantial extracts from it may be printed or otherwise reproduced without the author's permission.

AVIS:

L'auteur a accordé une licence non exclusive permettant à la Bibliothèque et Archives Canada de reproduire, publier, archiver, sauvegarder, conserver, transmettre au public par télécommunication ou par l'Internet, prêter, distribuer et vendre des thèses partout dans le monde, à des fins commerciales ou autres, sur support microforme, papier, électronique et/ou autres formats.

L'auteur conserve la propriété du droit d'auteur et des droits moraux qui protègent cette thèse. Ni la thèse ni des extraits substantiels de celle-ci ne doivent être imprimés ou autrement reproduits sans son autorisation.

In compliance with the Canadian Privacy Act some supporting forms may have been removed from this thesis.

Conformément à la loi canadienne sur la protection de la vie privée, quelques formulaires secondaires ont été enlevés de cette thèse.

While these forms may be included in the document page count, their removal does not represent any loss of content from the thesis.

Bien que ces formulaires aient inclus dans la pagination, il n'y aura aucun contenu manquant.


Canada

ABSTRACT

In the last decade continuously growing demand for production in bulk mining operations has influenced ultra class truck payloads to reach 400+ tons. Due to the additional weight of these larger units while maintaining an older suspension design proven for smaller units, there is a growing concern as to the increased number of high shock loading events. This results in bottoming out causing metal to metal contact and detrimental damage. Repeated bottoming out reduces the life of truck components and posed a risk to the operator's health and safety. The focus of this thesis is the introduction of a conceptual damper design to mitigate shock loading effects in a simple mechanical manner that can be introduced through a field adaptation. The project consisted of two parts; numerical modeling and physical testing of a damper. The results showed that by applying the metering pin and plate concept there is a potential increase in damping force that reduces the occurrence of bottoming out.

TABLE OF CONTENTS

CHAPTER 1 Background.....	1
1.1 Introduction.....	1
1.2 Suspension System.....	2
1.2.1 Suspension Stiffness	3
1.2.2 Dampening.....	4
1.2.3 Suspension Components	4
1.2.3.1 Spring.....	4
1.2.3.2 Damper.....	7
1.2.4 Energy Transfer	11
1.2.5 Damper Design	11
1.2.6 Suspension System Classification	12
1.2.6.1 Passive Suspension	13
1.2.6.2 Active.....	14
1.2.6.3 Semi-active	15
1.3 Suspension Systems for Ultra Class Haul Trucks.....	17
1.3.1 Oil-pneumatic Suspension Cylinder.	18
1.3.2 Basic Operation of an Oil-pneumatic Suspension Cylinder.	20
1.4 Measurement of Suspension Properties.....	23
1.4.1 Spring Rater.	23
1.4.2 Shock Dynamometer.....	24
1.4.3 Vehicle Dynamic Simulation.....	25
1.5 Fluid Mechanics Considerations.....	27
1.5.1 Gas Spring.....	27
1.5.2 Flow across an orifice	27
1.5.3 Hydraulic Dampening Force.....	30
1.5.4 Total Dampening Force	31
1.6 Suspension System Alternatives	32
1.6.1 New Suspension System Design.....	32
1.6.2 Changing Spring Rate	33
1.6.3 Damper Type	34

1.6.4 Possible Solution.....	34
1.6.5 The Concept for an Alternative Ultra Haul Class Hauler Suspension.....	34
CHAPTER 2 Thesis Project.....	37
2.1 Methodology	37
2.1.1 Computer Modeling.....	37
2.1.2 Scaled Down Damper.	39
2.2 Test Methodology	47
2.2.1 Test Frame	47
2.2.2 Servo Controller.....	47
2.2.3 Sensors	50
2.2.3.1 Linear variable Differential Transformer (LVDT)	52
2.2.3.2 Load Cell.....	52
2.2.3.3 Pressure Transducer	54
2.2.4 Data Acquisition System	56
2.2.5 Software	58
2.3 Testing.....	60
2.3.1 Set up	60
2.3.2 Test Run.....	62
2.3.3 Test Procedure	63
CHAPTER 3 Results and Discussion	65
3.1 Results and Raw Trends.....	65
3.1.1 Displacement-Time Plot	65
3.1.2 Hydraulic Dampening Force Plot	67
3.1.3 Pressure Plot	69
3.2 Analysis.....	71
3.2.1 Stroke and Velocity Parameters.....	71
3.2.2 Analysis Plots	72
3.2.2.1 Force - Velocity Plot.....	72
3.2.2.2 Force – Stroke Plot.....	73
3.2.2.3 Pressure Differential	73
3.2.2.4 Model versus Test.....	74

3.3 Discussion	76
3.3.1 Force versus Velocity	76
3.3.2 Force versus Stroke.....	79
3.3.3 Pressure Differential versus Stroke.....	82
3.3.4 Model versus Test data	84
3.3.5 Full Scale Prediction.....	86
CHAPTER 4 Conclusions and Recommendations	90
REFERENCES.....	93
APPENDICES	95
APPENDIX A	96
APPENDIX B	98
APPENDIX C	100
APPENDIX D	109
APPENDIX E	118
APPENDIX F.....	122
APPENDIX G.....	124

LIST OF TABLES

Table 2.1: Damper Parameters.....	39
Table 2.2 Shur-Lift Cylinder Spec.....	41
Table 2.3 Scaled OEM Damper Input.....	44
Table 2.4 Metering Pin Parameters.....	44
Figure 2.7 Metering Pin.....	45
Table 2.5 Variables and Sensors.....	50
Table 2.6 LVDT Parameters.....	52
Table 2.7 Load Cell Parameters.....	53
Table 2.8 Pressure Transducer Parameters.....	55
Table 2.9 Data Acquisition Components.....	56
Table 2.10: Channels.....	59
Table 3.1 Cycle Time.....	66
Table 3.2 Hydraulic Dampening Force Attained For Each Frequency Cycle.....	69
Table 3.3 Pressure Attained For Each Cycle Rate.....	69
Table 3.4 Regression Analysis Results – R ² Values.....	85
Table 3.5 789B Suspension Damper Parameters.....	87

LIST OF FIGURES

Figure 1.1 Quarter-Car Model	2
Figure 1.2 Coil Spring.....	5
Figure 1.3 Leaf Spring.....	6
Figure 1.4 Effect of Dampening (after Gillespie, 1992).....	7
Figure 1.5 Compression Curve (after Thede, 1996)	9
Figure 1.6 Rebound Curve (after Thede, 1996).....	10
Figure 1.7 Dampening Curve (after Thede, 1996).....	10
Figure 1.8 Simple Damper.....	13
Figure 1.9 Active Suspension System (after Wong, 1993).....	15
Figure 1.10 Semi-active Suspension System (after Wong, 1993)	16
Figure 1.11 Rear Suspension Setup	17
Figure 1.12 Example of the Oil-pneumatic Suspension Cylinder	18
Figure 1.13 Components of an Oil-pneumatic Cylinder.....	19
Figure 1.14 Damper Orientations (after Caterpillar, 2006)	20
Figure 1.15 Compression (after Caterpillar, 2001).....	21
Figure 1.16 Rebound (after Caterpillar, 2001).....	22
Figure 1.17 Spring Rater (after Roehrig Engineering, 2005)	23
Figure 1.18 Shock Dynamometer (after Roehrig Engineering, 2005).....	24
Figure 1.19 Components of a Shock Dynamometer (after Hanley, 2004)	25
Figure 1.20 Shaker Rig (Cambiaghi et al, 1998)	26
Figure 1.21 Orifice (Furesz et al. 1998).....	30
Figure 1.22 Ball Check Valve (Furesz et al. 1998).....	30
Figure 1.23 Oleo-pneumatic Damper (after Chai and Mason, 1997)	35
Figure 1.24 Modified Damper	36
Figure 2.1 Model Flow	38
Figure 2.2 Example of Modeled Dampening Characteristic	39
Figure 2.3 Shur-Lift Hydraulic Cylinder.	41
Figure 2.4 Modified Piston	42
Figure 2.5 Spacer	43
Figure 2.6 Fluid Flow of the Scaled OEM Damper.....	43
Table 2.8 Modified piston and Plate.....	45

Table 2.9 Fluid Flow of the Scaled Modified Damper	46
Figure 2.10 Test Frame	48
Figure 2.11 K7500 Servo Controller	49
Figure 2.12 K7500 Interface	49
Figure 2.13 Sensor Setup	51
Figure 2.14 LVDT	53
Figure 2.15 Load Cell	54
Figure 2.16 Pressure Transducer.....	55
Figure 2.17 Flow of Information	58
Figure 2.18 LabView Interface	59
Figure 3.1 Example of Displacement-Time Plot	66
Figure 3.2 Hydraulic Dampening Force at 0.15 Hz.....	67
Figure 3.3 Hydraulic Dampening Force at 0.7 Hz (OEM)	68
Figure 3.4 Hydraulic Dampening Force at 0.7 Hz (Modified)	68
Figure 3.5 Example of Pressure Plot.....	70
Figure 3.6 Sample of a Force -Velocity Plot	72
Figure 3.7 Sample of a Force-Stroke Plot.....	73
Figure 3.8 Example of Pressure Differential Plot.....	74
Figure 3.9 Example of Modeled versus Test	75
Figure 3.10 Dampening Force at 0.15 Hz.....	77
Figure 3.11 Dampening Force at a High Velocity at 0.7 Hz	78
Figure 3.12 OEM Force vs. Velocity Curves	78
Figure 3.13 Dampening Force at 0.15 Hz.....	79
Figure 3.14 Dampening Force at 0.35 HZ.....	80
Figure 3.15 Dampening Force at 0.7 Hz.....	80
Figure 3.16 Velocity Versus Stroke Plots.....	81
Figure 3.17 Orifice Opening Vs. Stroke	82
Figure 3.18 Pressure Differential at 0.7 Hz (OEM).....	83
Figure 3.19 Pressure Differential at 0.7Hz (Modified).....	84
Figure 3.20 Modeled versus Test Data at 0.15 Hz.....	85
Figure 3.21 Modeled versus Test Data at 0.7 Hz.....	86

SYMBOLS, NOMENCLATURE, AND ABBREVIATIONS

A	=	area
A_1	=	area of tube
A_2	=	area of orifice
C_s	=	suspension coefficient
D	=	diameter
F	=	force
F_{damp}	=	hydraulic damping force
F_{total}	=	total damping force
F_s	=	spring force
F_q	=	frequency
g force	=	g force
k	=	specific heat ratio
K	=	stiffness
K_s	=	suspension stiffness
k_t	=	tire stiffness
\dot{m}	=	mass flow rate
M_s	=	sprung mass
M_u	=	unsprung mass
OEM	=	original equipment manufactured
P	=	pressure
ΔP	=	pressure differential
Q	=	volumetric flow rate
R^2	=	coefficient of regression
R_t	=	hydraulic resistance
RR	=	ride rate
T	=	time
v	=	velocity
V	=	volume
W_{truck}	=	the effective weight of the truck resting on a damper
x_t	=	total stroke
x_{actuator}	=	total stroke of the hydraulic actuator
ξ	=	resistance coefficient
ξ_{orifice}	=	resistance coefficient of the orifice
$\xi_{\text{ballcheck}}$	=	resistance coefficient of the ball check valve
γ	=	specific weight
ρ	=	density
ω_n	=	bounce natural frequency
ω_d	=	damped natural frequency
χ	=	displacement
χ_s	=	stroke
ζ_s	=	damping ratio

CHAPTER 1 Background

1.1 Introduction

As a result of increasing demand for commodities, mining operations are continually ramping up production. In order to achieve targets, equipment manufacturers are designing bigger ultra class haul trucks, to increase payload. However, a downfall of larger capacity trucks is an increase in shock loading due to the combined weight of the truck and payload. Shock loading occurs when a vehicle is exposed to extremely high loads for a short period of time. High levels of shock loading result in a phenomenon called bottoming out.

Bottoming out is a term referred to when a suspension component reaches the end of its travel under compression. When a suspension system bottoms out metal to metal contact of the components occurs, hindering its function. Due to the additional weight of larger ultra class haul trucks, there is a greater tendency to bottom out as compared to smaller scale predecessors. Repeated occurrences of bottoming out will lead to premature failure of truck components and pose a danger to the operator's health and safety.

In order to gain a better understanding of the bottoming out phenomenon, the research will focus on the suspension system of ultra class haul trucks. The current system being used is simply a scaled up version of those used on older and smaller units. It is apparent that the current suspension system design is outdated and does not provide the adequate performance required for present day trucks. A modification is proposed to improve the suspension system to mitigate the increasing problems due to shock loading.

1.2 Suspension System

A simple suspension system is illustrated in Figure 1.1. The system consists of a sprung mass (M_s) supported by the suspension, which in turn is connected to the unsprung mass (M_u). The sprung mass is essentially any mass connected above the suspension system; the frame, body, engine and occupants. The unsprung mass is any mass connected below the suspension; axle, rim, and tire. The suspension has stiffness (K_s) and dampening (C_s) coefficients. In addition to suspension stiffness, the rubber tires (K_t) also provide some stiffness due to their essentially elastic nature.

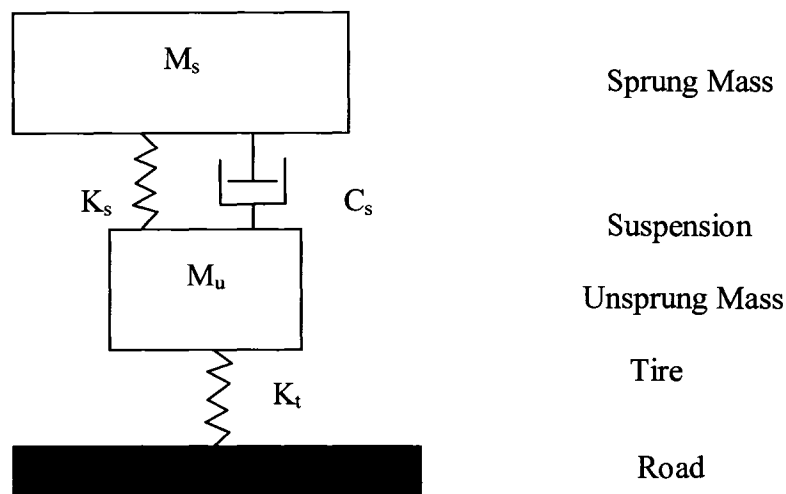


Figure 1.1 Quarter-Car Model

The primary function of a suspension system is to isolate a vehicle's sprung mass from vibrations due to irregularities of the road surface (ground conditions, bumps, road undulations, etc.). Humans are comfortable at frequencies ranging between 1.5 to 2.3 Hz. Frequencies lower than 1 Hz can cause dizziness and sickness, while higher frequencies can cause serious damage to the human body (Bastow, 1980).

Without a suspension system to absorb the vibrations, loading would be transmitted directly to the sprung mass, such as the frame and its occupants. As a result, excessive loading on the frame would occur which would then lead to fatigue

failure. Furthermore, the occupants of the vehicle would be exposed to excessive vibration.

Other functions of the suspension are related to the vehicle's handling, stability, and steering. The secondary functions of a suspension system are listed below (Gillespie, 1992).

- Maintain the wheels in the proper steer and camber attitudes to the road
- React to the control forces produced by the tires
- Resist body roll of the frame

The suspension's primary function, ride isolation, is accomplished with the use of springs and dampers. The secondary function involves utilizing mechanical linkages to control the relative motion between the unsprung mass and the sprung mass.

1.2.1 Suspension Stiffness

Stiffness (K) is the amount a body deflects (x) when a force (F) is applied to it (Eq.1.1). In a suspension system the spring provides the stiffness properties. Tires also have some stiffness properties. The combined rate of the tire and spring in series is referred to as the ride rate (RR) (Eq.1.2).

$$K = \frac{F}{x} \quad (1.1)$$

$$RR = \frac{K_s K_t}{K_s + K_t} \quad (1.2)$$

Disturbance of the sprung mass causes the spring to oscillate up and down. The oscillation is referred to as the bounce natural frequency, which can be determined from Equation 1.3.

$$\omega_n = \sqrt{\frac{RR}{M_s}} \quad (1.3)$$

1.2.2 Dampening

Dampening is the reduction of random or periodic oscillations. In the case of a vehicle's suspension, dampening reduces and controls the natural frequency (Gillespie, 1992). In the presence of dampening, the natural frequency of the suspension system is referred to as the damped natural frequency (ω_d). The relationship between the natural and damped frequency are displayed through Equation 1.4.

$$\omega_d = \omega_n \sqrt{1 - \zeta_s^2} \quad (1.4)$$

Where:

$$\zeta_s = \text{Dampening ratio} = \frac{C_s}{\sqrt{4K_s M_s}} \quad (1.5)$$

1.2.3 Suspension Components

Due to the hundreds of different vehicles available today, there are quite a number of different suspension systems. This is due to the fact that each suspension system is a compromise between comfort, road handling, and cost. Although there are numerous systems, the two essential components that are found common to all are the spring and damper.

1.2.3.1 Spring

The function of the spring is to absorb the force loading caused by the bump (Garrett et al., 1996). When a vehicle rolls over a bump the wheel will rise. Without a spring, both wheels and frame would act a single ridge unit and accelerate upwards. As a result, a considerable amount of force would be transmitted onto the frame and

onto the occupants inside the vehicle. With the spring, the actual force transferred to the frame is equal to the force required to compress the spring enough to roll over the bump. The result is a lower upward acceleration force experienced by the frame.

The type of spring used in a suspension system is dependent on the suspension setup. The coil spring and leaf spring are the more widespread styles. Coil springs are the most commonly used and can be found on almost every production vehicle (Figure 1.2).

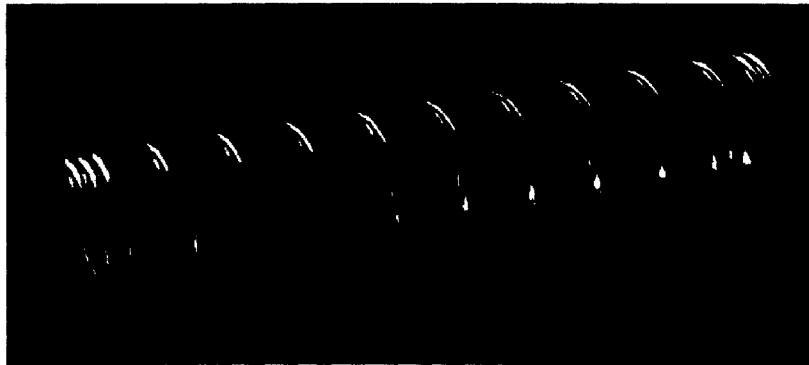


Figure 1.2 Coil Spring

Leaf springs, depicted in Figure 1.3, are arc-shaped steel bars stacked on top of each other in several layers. The stiffness is determined by the number of layers used as a composite. Leaf springs are used in heavy commercial vehicles such as trucks and vans. The advantage of a leaf spring is that the load is spread over a larger area of the vehicle's frame, whereas the coil spring transfers to a single point.



Figure 1.3 Leaf Spring

A third type of spring is a gas spring. In its simplest form, it is a volume of gas enclosed in a cylinder with a movable piston. Under a static load, the gas inside the cylinder is pressurized to a predetermined point. For a dynamic load, the piston moves up and down, causing the volume of gas to increase and decrease respectively. As the volume of gas decreases, the pressure of the gas builds up. Gas springs are generally used on vehicles with loads that vary significantly in weight such as semi-trailer trucks and motor coaches.

The force generated by the spring is dependent on its position in the stroke (Pettitt, 1999). It is not affected by how fast it compresses or extends. The deflection of a spring is dependent only on the load applied. The duration that the load is applied has no bearing on how much the spring will deflect. For example if the stiffness of a spring is rated at 1 kN/m, it will require 1 kN of force to deflect the spring 1 m. The spring will deflect 1 m regardless of the amount of time that the 1 kN force has been applied.

The amount of force that a spring can exert is called the spring rate. The spring rate can be either linear or progressive. A linear spring rate follows Hooke's Law, where the spring stiffness is constant. The spring will deflect proportional to the force applied to it. Hooke's Law holds true as long as the spring is within its elastic limits. When the spring is outside of its elastic limit, the spring behaves non-linearly.

With a progressive spring rate, the spring stiffness increases as the spring is deflected. A coil and leaf spring can exhibit a linear or progressive rate, where as a gas spring can only have progressive rates due to the gas law.

1.2.3.2 Damper

The function of the suspension damper, also referred to as a shock absorber, is to control excess motion of the sprung mass. Dampers reduce the tendency of the sprung mass to continue to bounce up and down on the springs after going over a disturbance. Dampers also prevent excessive build up of vibration caused by a series of irregularities on the road.

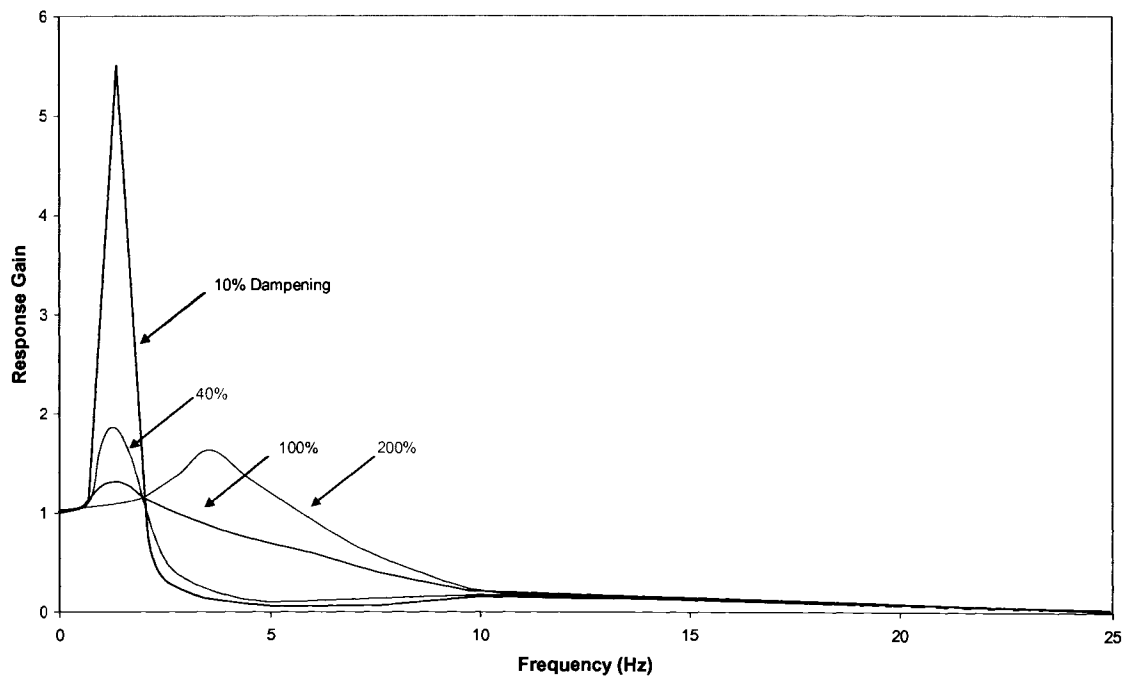


Figure 1.4 Effect of Dampening (after Gillespie, 1992)

Figure 1.4 above illustrates the effect of dampening for a quarter-car model with respect to damping ratio (Gillespie, 1992). The percent dampening is determined from the dampening ratio equation (Eq. 1.5). For a light dampening (~ 10%) the plot shows a spike at 1 Hz. This peak is the natural bounce frequency and results in a high response gain, meaning that the sprung mass oscillation is amplified by any irregularities on the road. This provides no control of vertical movement, which is

undesirable. However, for frequencies greater than the natural bounce frequency (1Hz) there is a high reduction of oscillation in the system.

At 40% dampening ratio, the resonant frequency is in the range of 1.5 to 2.0 Hz, which is the comfort range for humans. The 40% dampening curve is representative of most cars. At the critical dampening point (100%), the low frequency oscillations of the sprung mass are well controlled. However, at higher frequencies the ride isolation suffers, which is opposite to the behavior of a light dampening ratio. If the dampening ratio is greater than the critical dampening point, the resulting damper would be so stiff that it no longer moves causing the vehicle to bounce on its tires, resonating in the 3 to 4 Hz range. In effect, the damper could be used to add stiffness to the system.

Dampers are velocity sensitive devices. They are not dependent on the vehicle's traveling speed, but on the vertical velocity of the damper's movement. For this thesis the velocity is referred to as the vertical movement of the damper. The velocity produced by road irregularities is more dependent on the shape of the irregularity rather than the size (Theede, 1996). For instance, if there were two 1 inch bumps, one being square edged and the other a rounded edge, the square edged would produce a greater velocity than the smoother round edge. Figures 1.5 and 1.6 depict the typical relationship between the dampening force and the velocity for compression and rebound. The plots show that the relationship is a function of the square of its velocity. At low velocities there is little or no dampening force to resist the motion of the damper, thus the damper is relatively free to move at low speeds. At high speeds, the dampening force increases rapidly to resist the motion of the damper.

Figure 1.7 displays the whole dampening curve. As the damper goes through one complete cycle it passes through zero velocity twice (at the top and bottom of the stroke). When a wheel hits a bump, the damper accelerates to a maximum velocity then slows down and stops compressing. When the damper stops compressing, the vertical velocity is zero. After reaching this point, the damper accelerates in the

opposite direction (rebound) until it once again reaches a maximum velocity and slows down back to zero velocity.

Another important aspect of suspension dampers is that the compression and rebound dampening are not equal. During compression the damper will experience a wide range of loading which is composed largely of impact loading. As shown in Figure 1.4 a moderate dampening ratio is best suited to control impact loading. Since the loading is not as violent during the rebound stroke, a greater dampening rate is used to dissipate the energy stored in the spring. Thus, the dampening rate during compression is less than in rebound. The ratio between rebound and compression dampening is approximately 3 to 1 (Gillespie,1992).

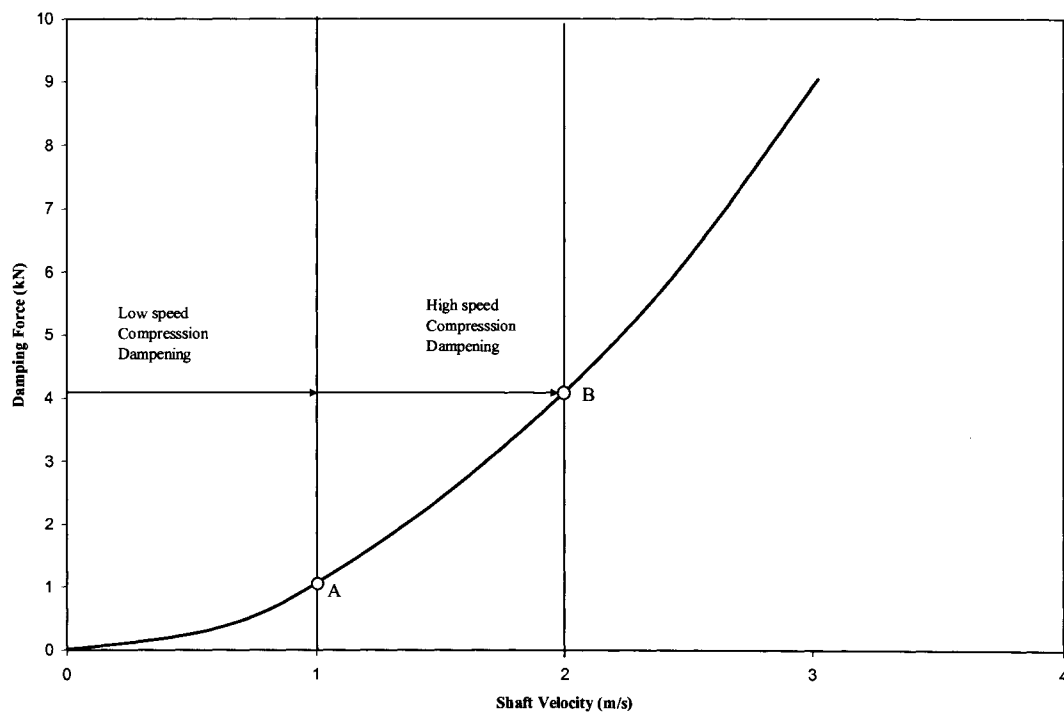


Figure 1.5 Compression Curve (after Thede, 1996)

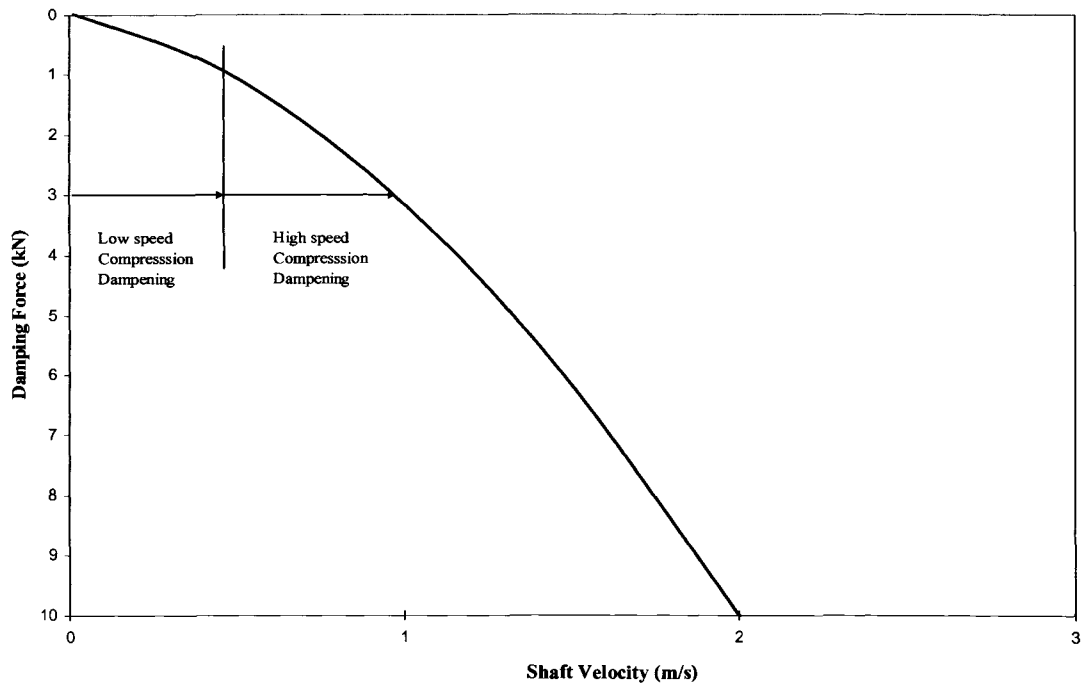


Figure 1.6 Rebound Curve (after Thede, 1996)

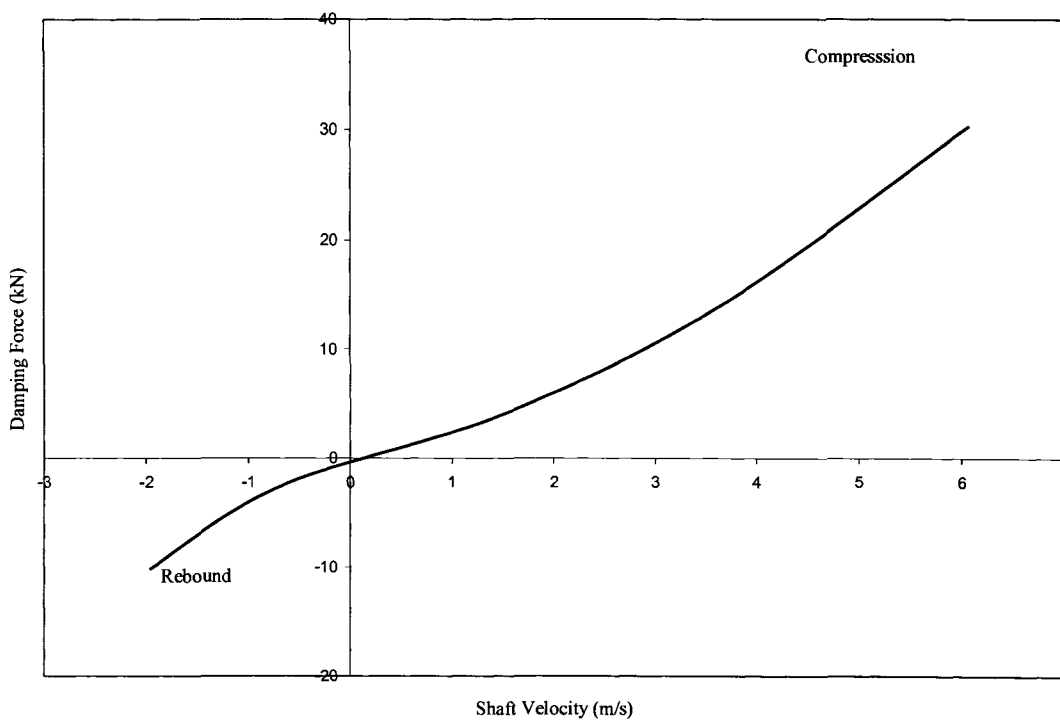


Figure 1.7 Dampening Curve (after Thede, 1996)

1.2.4 Energy Transfer

The key to any good suspension system is energy transfer. A spring's main function is to store and release energy caused by road irregularities, while the damper dissipates the energy (Theede, 2005). When a tire comes into contact with a bump in the road, the suspension compresses enough to let the tire roll over the bump. The compression of the suspension causes the spring to compress, thus storing potential energy. At the same time, the damper creates compression dampening which dissipates some of the mechanical energy. When the suspension spring has absorbed all of the energy caused by the bump, it will stop compressing and begin the rebound stroke. During rebound, the spring releases stored potential energy and extends the damper. As the damper extends, rebound dampening is created to dissipate the release energy. Because the rebound dampening is greater than the compression, the majority of the mechanical energy is dissipated during the rebound phase. The damper dissipates energy by converting mechanical energy into heat. The heat from the fluid is transferred to the damper's metallic body by conduction and cooled off by the passing air flow.

1.2.5 Damper Design

All dampers incorporate a piston moving inside a cylinder filled with a fluid, usually oil. The piston has small holes bored through it, referred to as orifices. A shaft connected to the piston on one end, connected to the vehicle frame, and the axle assembly on the other end provides the movement range of the piston. Figure 1.8 illustrates a simple damper. As the piston moves, the fluid is pressurized and flows through the orifice. The piston's resistance to move through the fluid is effectively the dampening force.

The amount of dampening is controlled by the orifice area, number, and geometry (Garrett et al., 1996). If the area of the piston is constant, the dampening decreases or increases respectively with a larger or smaller orifice area. Since the target ratio of the rebound to compression dampening is 3:1, the effective area for the

fluid to flow through must be higher during compression than it is during rebound. To get a 3:1 ratio, one way valves are typically used to restrict the flow during rebound.

The viscosity of the fluid also affects the dampening characteristics of the damper. A piston moving in a more viscous fluid will have a higher resistance to movement. Therefore, a more viscous fluid will result in greater dampening force.

1.2.6 Suspension System Classification

The classification of a suspension system is dependent on how ride isolation and handling is achieved. The three classes that a system can fall into are passive, active and semi-active. The majority of passenger and commercial vehicles use a passive system. Further improvement to ride quality has resulted in the development of active and semi-active suspension systems.

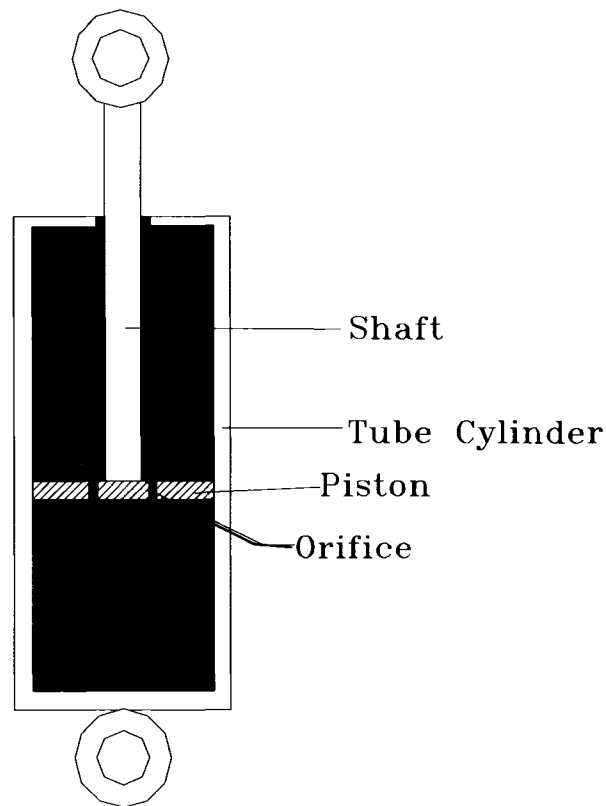


Figure 1.8 Simple Damper

1.2.6.1 Passive Suspension

The passive suspension system has been around since the invention of the automobile and is the simplest of the three systems. Figure 1.1 shows the schematic for a passive suspension. The spring and dampening characteristics of a passive system are fixed. Thus, once the system has been installed in the vehicle, there are minimal changes to its suspension properties. The advantage of a passive system is that it is predictable, therefore an operator can adapt to the limitations and capabilities of the suspension.

The system is designed as a compromise between ride isolation and handling performance. A soft spring will yield a better ride isolation over a wide range of frequencies, while a stiffer spring will provide better road-holding capabilities. The passive system is only optimized for a certain range of operating conditions. Once the

suspension has reached its limits, it has no way of compensating beyond its design parameters.

1.2.6.2 Active

The concept of an active system emerged in order to eliminate the compromise between the ride and handling in a passive system (Chalasan, 1986). The active system has the ability to adjust according to the operating conditions, resulting in a better and safer ride. An active system is depicted in Figure 1.9. In an active system, the conventional spring and damper is replaced with a force actuator. Sensors are used to continuously monitor the operating conditions of the vehicle. Based on the signals from the sensor and the programmed control strategy, the force in the actuator is modulated to achieve a superior ride with optimal handling and performance. The optimal control strategy is one that minimizes the root-mean square (rms) values for the sprung mass acceleration, suspension travel, and the tire dynamic deflection (Wong, 1993) In addition to providing a superior ride and handling qualities, an active suspension is used to control ride height, roll, and pitch of the vehicle body while in motion. The downside of an active system is the complexity, reliability, and cost. This type of system is only found in high end vehicles.

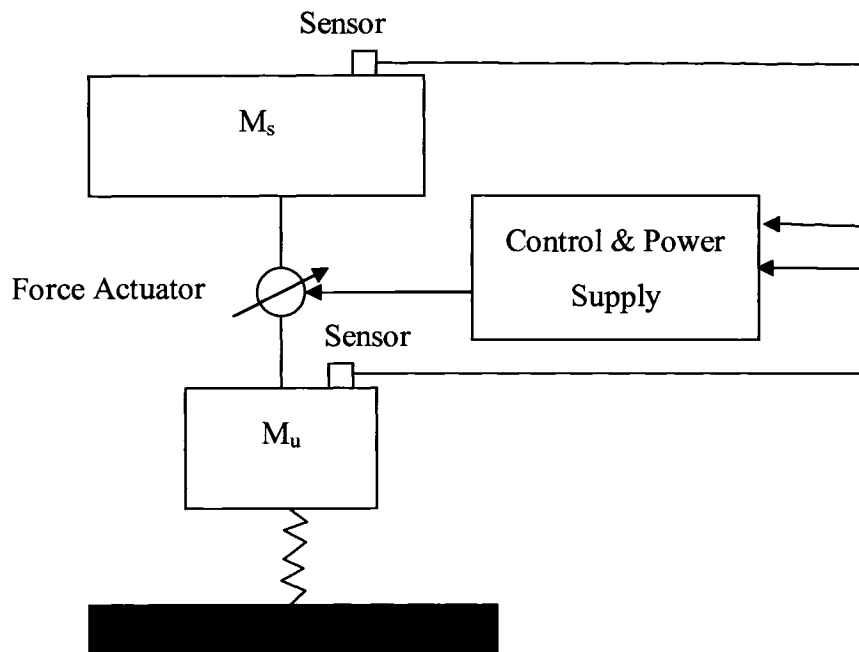


Figure 1.9 Active Suspension System (after Wong, 1993)

1.2.6.3 Semi-active

The semi-active system has been developed as a means to reduce the complexities and cost of an active system while still maintaining performance (Motta et al., 2000). Figure 1.10 illustrates a semi-active system. Similar to the passive setup, the semi-active utilizes a spring and damper. The difference is the semi-active uses a damper that can vary its dampening force according to the operating conditions. Similar to an active system, a semi-active system utilizes sensors and control strategy to alter the dampening properties of the damper. One way of modulating the dampening force is by adjusting the orifice area, thus changing the resistance to fluid flow. Another method is using a fluid called an electrorheological fluid to alter the dampening force (Petek, 1992). This special fluid is a mixture of dielectric base oil and fine semi-conducting particles. As a current is applied to the fluid it stiffens up resisting movement.

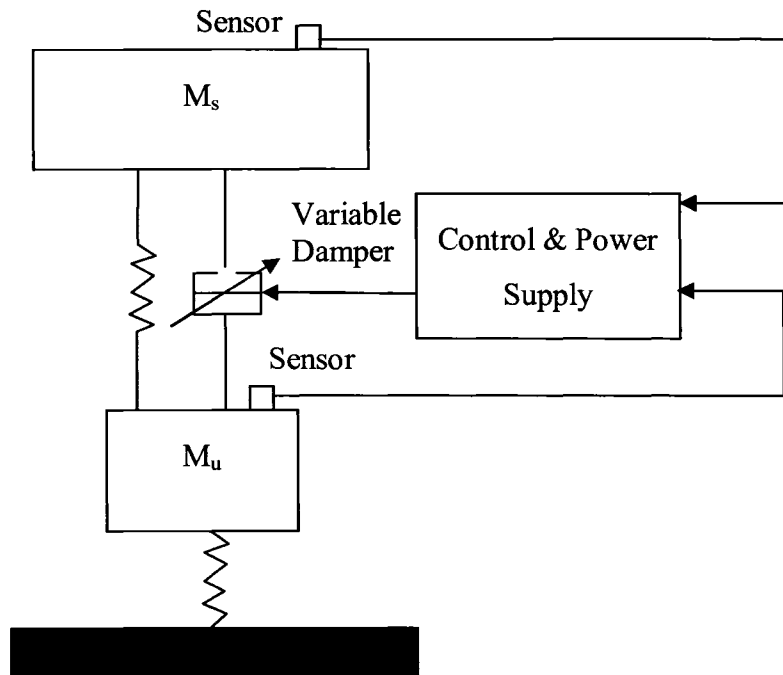


Figure 1.10 Semi-active Suspension System (after Wong, 1993)

1.3 Suspension Systems for Ultra Class Haul Trucks

The suspension system for ultra class haul trucks is basically a scaled up version of the systems used in older smaller models. For the front suspension there are a few different setups available. Each manufacturer utilizes a different concept. At the other end, the rear suspension setup for all haul trucks is similar where a solid axle type suspension is utilized. The advantage in using a solid axle type suspension is that it is more robust and has the ability to carry a heavier payload. In addition, solids axles are a relatively simple design, less expensive, and contribute to a lighter overall vehicle weight. As seen in Figure 1.11, the rear suspension setup has dual wheels mounted on both ends of a rigid beam called the axle housing. The rear axle housing functions by transmitting any movement of one wheel to the opposing wheel which causes both wheels to steer and camber together (Goodsell, 1989).

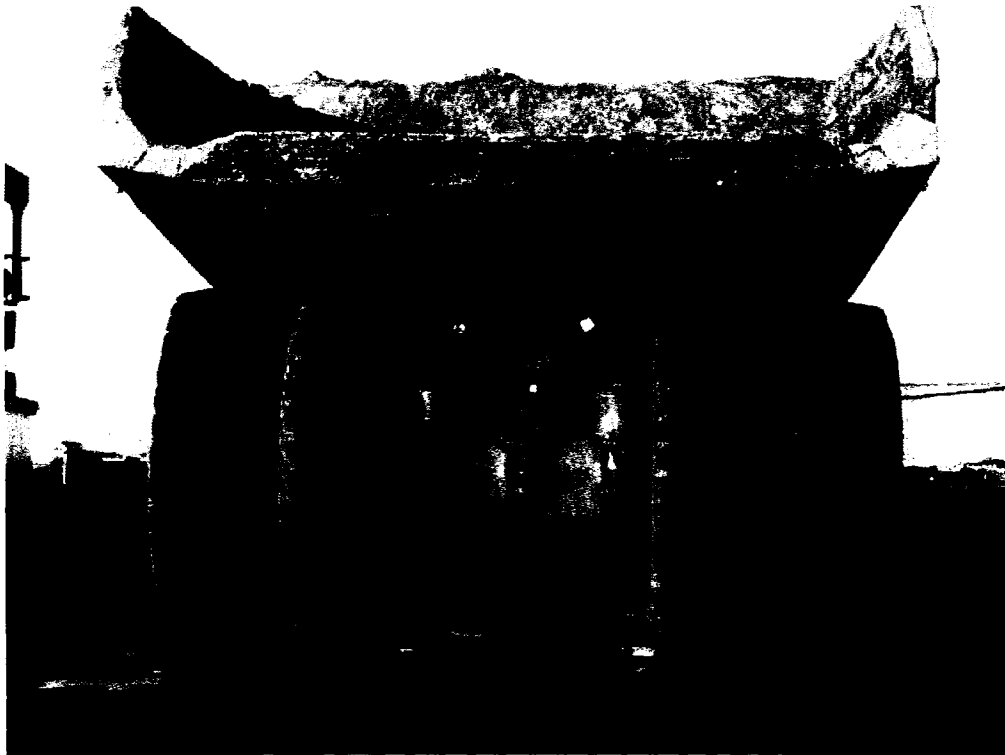


Figure 1.11 Rear Suspension Setup

1.3.1 Oil-pneumatic Suspension Cylinder

In order to provide ride isolation and handling, oil-pneumatic suspension cylinders are utilized in all haul trucks. An oil-pneumatic suspension cylinder combines both the spring and damper into one unit (Figure 1.12). The basic design is classified as a simple damper containing fixed orifices where the dampening coefficient is constant.

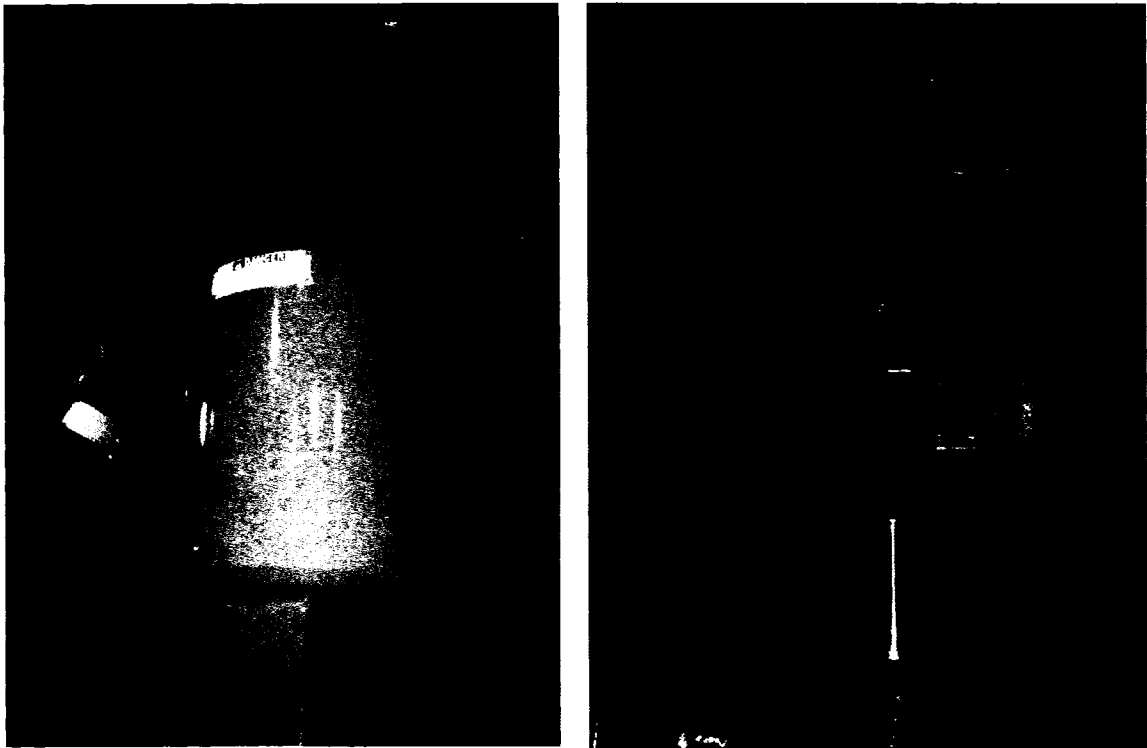


Figure 1.12 Example of the Oil-pneumatic Suspension Cylinder

The basic components of an oil-pneumatic suspension cylinder are illustrated below in Figure 1.13. The components consist of two telescopic tubes where one acts as the cylinder tube and the other functions as a piston rod. The orifice is located on the side wall of the piston. The oil-pneumatic suspension system uses a nitrogen gas

spring as opposed to a metal spring. Nitrogen is used as the gas medium due to its highly compressible and unreactive nature. The dampening fluid used is hydraulic oil.

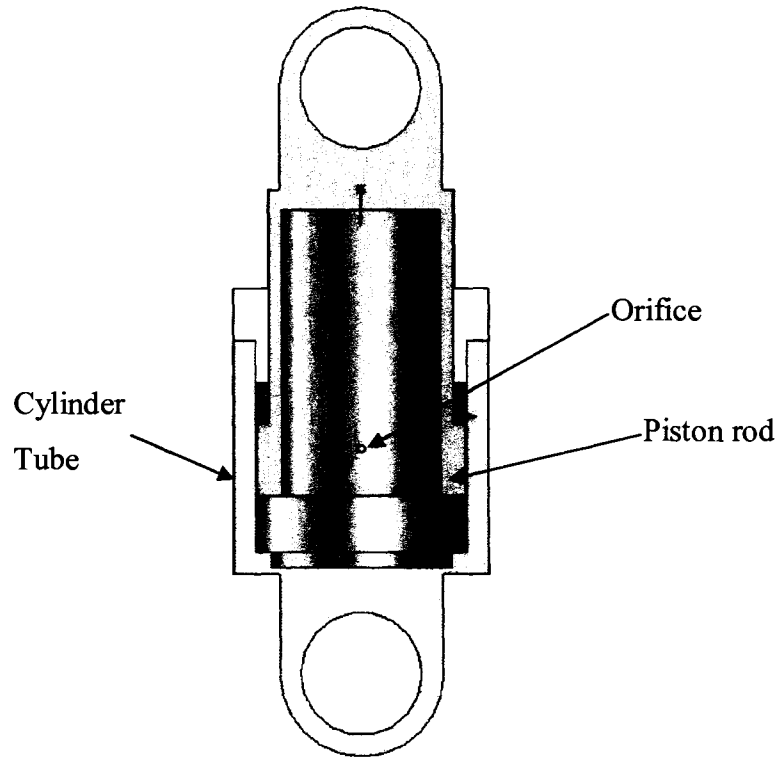


Figure 1.13 Components of an Oil-pneumatic Cylinder

The use of a gas spring in an oil-pneumatic suspension cylinder has advantages. Since the stiffness characteristic of an air spring is progressive, it is ideal for the heavy load of the truck. Also, the weight of the system is reduced since the spring is a gas. Another benefit of the oil-pneumatic suspension cylinder is that it can be used right side up or inverted, as illustrated in Figure 1.14.

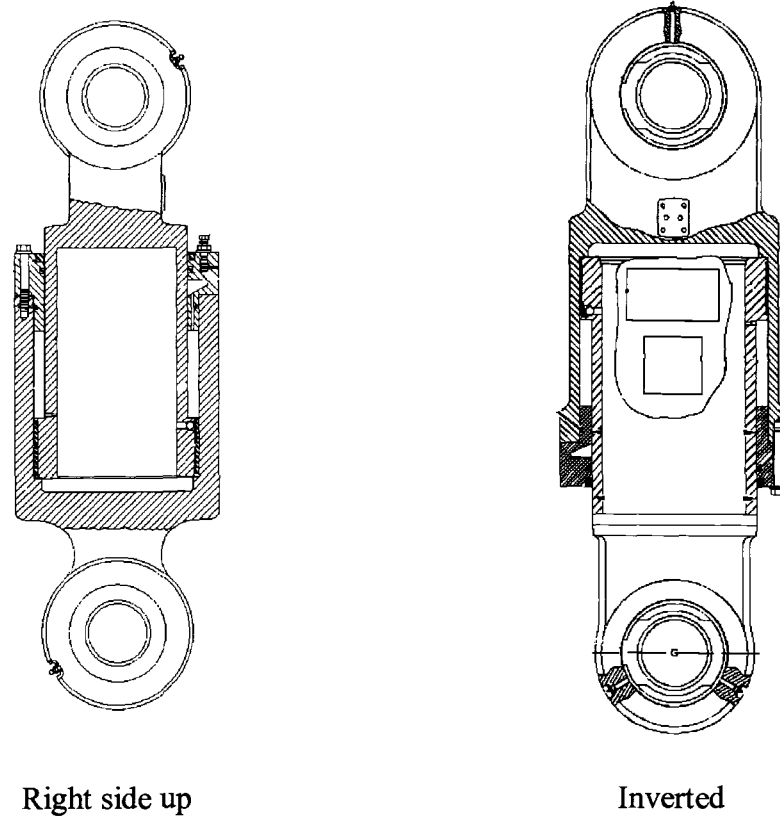


Figure 1.14 Damper Orientations (after Caterpillar, 2006)

1.3.2 Basic Operation of an Oil-pneumatic Suspension Cylinder

When a wheel rolls over a bump on the ground, it causes the oil-pneumatic suspension cylinder to compress (Fig 1.15). As the cylinder compresses, the piston (1) moves down the cylinder (2), which decreases the volume of the oil chamber (3), while increasing the volume of the cavity chamber (4). The fluid from the oil chamber is then forced to flow into the cavity via a fixed orifice (5) and ball check valve (6). The movement of the piston also reduces the overall internal volume of the suspension cylinder. As the internal volume decreases, the nitrogen gas is compressed, thus increasing the stiffness of the gas spring.

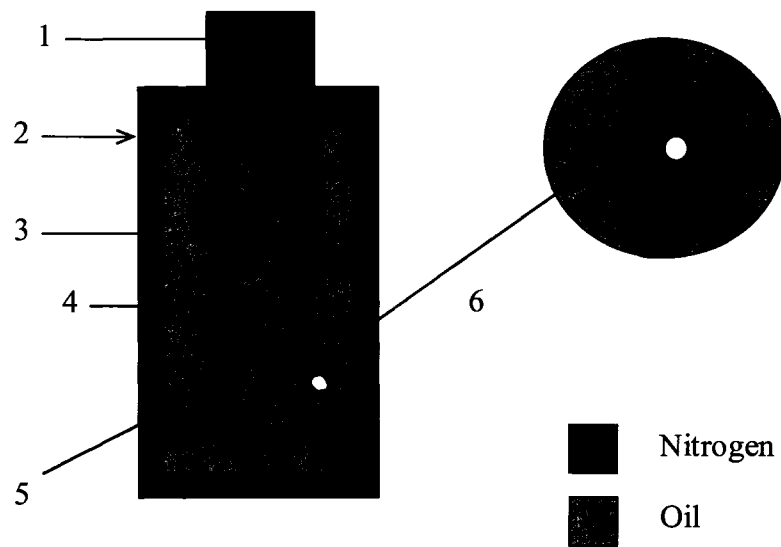


Figure 1.15 Compression (after Caterpillar, 2001)

When the gas spring has absorbed all the energy created by the bump, the rebound stroke will start. During rebound the nitrogen gas releases its stored energy by expanding. The expansion causes the piston to move up the cylinder tube, decreasing the volume in the cavity chamber and pressurizing the oil (Fig 1.16). The increased pressure of the oil causes the ball check valve to close therefore forcing the oil to flow through the fixed orifice into the oil chamber. The restriction of flow causes the rebound dampening to be greater than the compression dampening. As a result of the increased rebound dampening, the energy release by the gas spring is controlled, which keeps the truck body movement to a minimum.

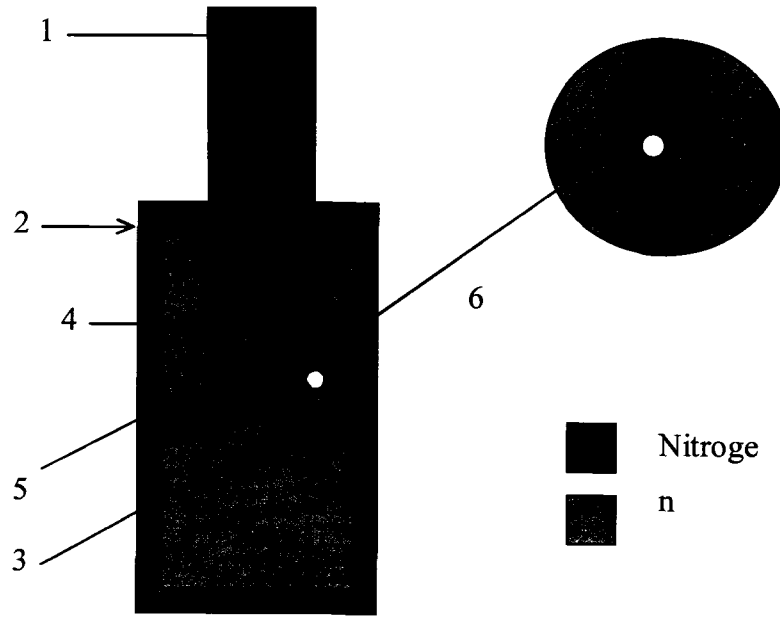


Figure 1.16 Rebound (after Caterpillar, 2001)

1.4 Measurement of Suspension Properties

The suspension system is a vital part of a vehicle in terms of safety and handling; therefore manufacturers spend a great deal of time developing and testing their suspension systems. The most common test for manufacturers is driving a test vehicle on a test track and recording various parameters. This method is mostly used for testing of a new vehicle and not for testing to improve an existing system. This section will focus more on the smaller scale testing methods that a single or small team of individuals can perform. There are many testing methods available, ranging from testing single components to the complete system.

1.4.1 Spring Rater

The stiffness of a spring can be measured with a device called a spring rater, which is illustrated in Figure 1.17. The spring rater compresses a spring and measures the displacement force of the spring. The displacement is measured with a linear variable differential transducer (LVDT) and the force is measured with a load cell. The measurements taken of the displacement and force produced during compression are used to generate a displacement-force graph, and the stiffness is calculated using Equation 1.1.

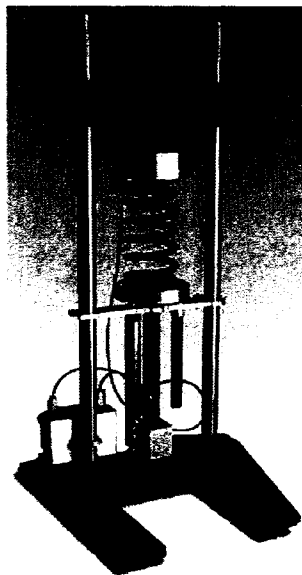


Figure 1.17 Spring Rater (after Roehrig Engineering, 2005)

1.4.2 Shock Dynamometer

A damper's performance can be determined with a shock dynamometer (Figure 1.18). The shock dynamometer compresses and extends (rebound) the damper at a known speed and measures the force produced at the particular speed. Figure 1.19 illustrates the components of a mechanical shock dynamometer. The damper is compressed and expanded via a rotating crank plate, which is activated by an electric motor via a drive belt. A linear bearing is used to connect the damper's shaft to the crank plate to ensure a vertical movement. The stroke length is dependent on the distance away from the center of the crank plate (the further from the center, the longer the stroke). More sophisticated dynamometers use an electro-magnetic actuator. The actuator replaces the crank, motor, and linear bearing. Force is measured with a load cell and the velocity with a speed sensor. From the test, force-velocity graphs are created

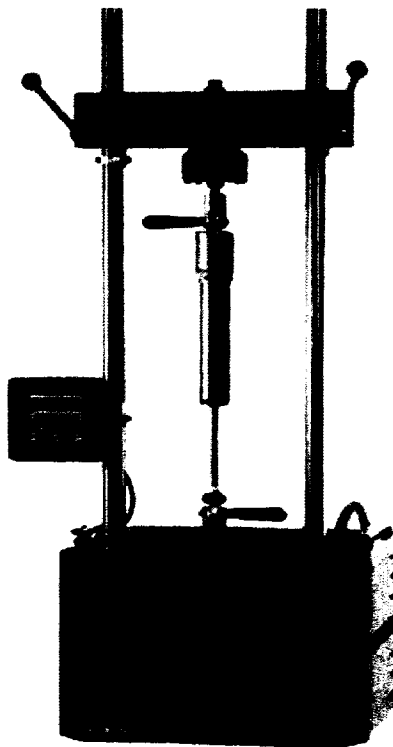


Figure 1.18 Shock Dynamometer (after Roehrig Engineering, 2005)

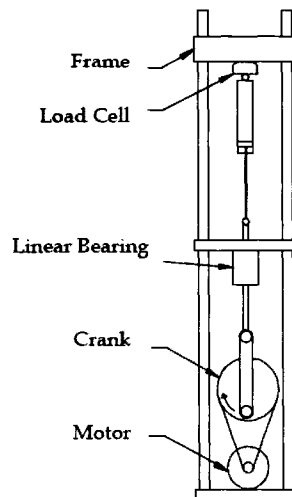


Figure 1.19 Components of a Shock Dynamometer (after Hanley, 2004)

1.4.3 Vehicle Dynamic Simulation

The newest and most valuable tool being applied in the automotive industry is vehicle dynamic simulation (Cambiaghi et al. 1998 and Miller 2002). The simulation models the road conditions in a lab with the use of a shaker rig, shown in Figure 1.20. The rig is composed of a number of platforms. Each platform is independently moved vertically with a hydraulic actuator, which simulates the road conditions. A powerful hydraulic power unit (pump) drives the actuators. Accelerators and load cells are placed at various points on the suspension system, depending on what is being measured. The advantage with this method is that the whole suspension system can be tested. Also, it takes less time to optimize and validate experimental models than to do physical testing.



Figure 1.20 Shaker Rig (Cambiaghi et al, 1998)

1.5 Fluid Mechanics Considerations

1.5.1 Gas Spring

The force generated by the gas spring is proportional to its pressure. The spring force (F_s) generated by the gas can be defined with the following equation:

$$F_s = P \times A \quad (1.6)$$

where:

P = pressure

A = effective area of the piston

As a damper is compressed, the internal volume inside it decreases. The reduction in volume causes the pressure of the nitrogen gas to increase. The relationship between volume and pressure depends on the nature of the process. For this thesis project, two assumptions were made. The first assumption was the process will be considered to follow Boyle's Law. Boyle's law states that if a gas behaves ideally, the gas pressure multiplied by its volume equals a constant value for a given temperature. Secondly, that the process is isentropic, where the entropy stays the same throughout the process. The relationship is shown in equation 1.7 below.

$$P_1 V_1^k = P_2 V_2^k$$

$$(1.7)$$

where;

k = specific heat ratio

V = volume

1.5.2 Flow across an orifice

Fluid flow rate is based on the principle of Bernoulli's equation. The equation states that the sum of all energy in a fluid flowing along an enclosed path is the same at any two points on that path. Therefore, between two points in a streamline for a steady, inviscid, incompressible fluid, the Bernoulli equation is:

$$P_1 + \frac{1}{2}\rho v_1^2 + \gamma z_1 = P_2 + \frac{1}{2}\rho v_2^2 + \gamma z_2$$

(1.8)

Where:

p = pressure

ρ = density

γ = specific weight

v = velocity

z = elevation

In the case of a suspension cylinder the change in elevation is negligible ($z_1 = z_2$). Therefore, the Bernoulli equation takes on the form:

$$P_1 + \frac{1}{2}\rho v_1^2 = P_2 + \frac{1}{2}\rho v_2^2$$

(1.9)

Because the suspension cylinder is a closed system the continuity equation applies. Thus, the mass flow rate (\dot{m}_1) going into the system is equal to the mass flow rate (\dot{m}_2) leaving the system. The continuity equation in its basic form is:

$$\dot{m}_1 = \dot{m}_2 \Rightarrow \rho_1 A_1 v_1 = \rho_2 A_2 v_2$$

(1.10)

The density of the oil in the cylinder is assumed not to change throughout the process ($\rho_1 = \rho_2$), making the above the continuity equation for incompressible flow:

$$\dot{m}_1 = \dot{m}_2 \Rightarrow A_1 v_1 = A_2 v_2 \Rightarrow Q_1 = Q_2$$

(1.10a)

where:

Q = volume flow rate

= Av

Becoming:

$$Q_1 = A_2 v_2 \quad (1.11)$$

Using both the Bernoulli (Eq. 1.8) and continuity (Eq. 1.10) equations, the theoretical flow rate can be calculated as:

$$Q = A_2 \sqrt{\frac{2(P_1 - P_2)}{\rho \left[1 - \left(\frac{A_2}{A_1} \right)^2 \right]}} \quad (1.12)$$

Where:

A_1 = area of damper tube

A_2 = area of orifices

Another method to calculate the flow rate is by using pressure differential (ΔP) and hydraulic resistance (R_t). Equation 1.13 illustrates the alternate method of calculating flow rate when turbulent flow exists.

$$R_t = \frac{\Delta P}{Q^2} = \frac{\rho \xi}{2A^2} \Rightarrow Q = A^2 \sqrt{\frac{2\Delta P}{\rho \xi}} \quad (1.13)$$

where:

ξ = resistance coefficient

The resistance coefficient is dependent on the parameters producing the pressure loss and in most cases is determined only with complicated formulae (Dulay, 1988). The equations to calculate the resistance coefficient of an orifice (ζ_{orifice}) and ball check valve ($\zeta_{\text{ballcheck}}$) are listed below.

$$\zeta_{orifice} = \left(1 - \frac{D_1^2}{D_2^2}\right)^2$$

(1.14)

$$\zeta_{ballcheck} = 2.65 - 0.8\left(\frac{h}{d_o}\right) + 0.14\left(\frac{h}{d_o}\right)^2$$

(1.15)

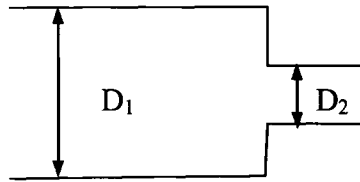


Figure 1.21 Orifice (Furesz et al. 1998)

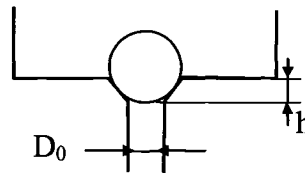


Figure 1.22 Ball Check Valve (Furesz et al. 1998)

1.5.3 Hydraulic Dampening Force

A damper produces a force called hydraulic dampening. It is the equal to the resistance for the piston to move through the oil. The idea behind dampers is that the kinetic energy produced by the gas spring is absorbed by the fluid as the piston moves through some kind of hydraulic resistance. In this case, the orifice causes the hydraulic resistnace. The hydraulic dampening force (F_{damp}) can be calculated with the following equation:

$$F_{damp} = \Delta P \times A$$

(1.16)

1.5.4 Total Dampening Force

The total dampening force (F_{total}) of an oil-pneumatic damper is a combination of the force created by the gas spring and the hydraulic dampening force, caused by the oil.

$$F_{total} = F_s + F_{damp}$$

(1.17)

1.6 Suspension System Alternatives

In a mining environment, haul trucks are consistently being subjected to high shock loading. The major contributors to this type of loading are poorly maintained road surfaces, improper loading by shovels, and the ground material itself. Due to the increase in size of haul trucks in recent years, many mines are experiencing premature failure of major components, such as the frame and drive train. The extra sprung mass of the latest units combined with the high shock loading causes more occurrences of bottoming out (El-Sayed, 2003). Repetitive exposure to bottoming out results in failure of truck components and is a hazard to the operator. As a result of the industry wide problem and safety concerns, this thesis will focus on reducing the effects of shock loading causing the bottoming out phenomenon. The method of reducing the shock loading will be to suggest an alternative to the truck's suspension. Because shock loading only occurs during compression, only compression will be examined.

Two approaches exist to reduce bottoming out on haul trucks. The first method is to completely redesign the whole suspension system, and the second approach is to change or modify an original equipment manufacturer (OEM) component of the system.

1.6.1 New Suspension System Design

The suspension system currently being used in ultra class trucks is based on old designs. It would seem the best solution would be to design a new suspension system for the ultra class truck. However, this is not completely necessary. The front suspension is less likely to bottom out than the rear suspension. This is because only ~30% of the weight, when loaded, is distributed to the front (Caterpillar, 2002). Because there is less weight on the front combined with a longer suspension travel there is less likelihood the front would bottom out. The focus of the manufacturer on the front suspension is handling and stability rather than controlling the effects of shock loading. As a result, no significant change can be made to the front to reduce the effects of shock loading, without affecting the handling of the unit.

The rear suspension is where the majority of the weight is distributed (~70% when loaded), therefore this is the more critical area (Caterpillar, 2002). A solid axle setup is common to all manufacturers because it is a simple design comprising few parts. The use of a modern independent type suspension would allow for an improvement in ride and handling; however, there are draw backs to implementing an independent system. One of the major disadvantages to the independent system are additional components. Since space under a truck is at a premium, it would be too difficult to accommodate the additional parts to run an independent system. Manufacturing parts for an independent suspension system, which would be strong enough to handle the rough duty, without adding additional weight to the system would be an additional complication. As a result of the complexity and additional parts, the independent system would also be more expensive to build.

Another possible solution to reduce the effects of shock loading would be to design a suspension setup to have a longer suspension travel. The downside to a longer travel would mean that the center of gravity of the truck will be higher. As a result of the higher center of gravity, the truck becomes more unstable generating an increased risk of rollover.

1.6.2 Changing Spring Rate

An aspect of suspension tuning is changing the spring rate. A softer spring will absorb road irregularities more readily, but is more prone to bottoming out. A firmer spring rate will deform less, therefore reducing the chances of bottoming out. For the gas spring in the oil-pneumatic suspension, the nitrogen gas can be charged to a high pressure to firm up the gas spring. The disadvantage of a stiffer spring is that because the spring will not deform easily, the spring cannot absorb the irregularities of the road. Therefore the stiffness of a spring can be altered to prevent bottoming out, but at the price of ride quality.

1.6.3 Damper Type

The damper being used in current suspension systems is a passive type. One possibility to reduce the effect of high shock loading is to replace the passive damper with a more modern type, such as an active or semi-active damper. Unfortunately, there are no dampers (active or semi-active) large enough to fit an ultra class truck on the market. The development of a new active or semi-active system for an ultra class hauler would require an enormous amount of research and development.

Another aspect of suspension tuning is tailoring the damper to achieve optimum performance. The ideal performance is accomplished by valving the damper (Gillespie, 1992). Valving involves altering the check valves, orifice, shims, etc. of a damper to obtain the desired dampening characteristics. This method altering the suspension characteristics is used extensively in motor sports.

1.6.4 Possible Solution

A possible retrofit solution for haul trucks to reduce the bottoming phenomenon is to modify the design of the oil-pneumatic suspension cylinder. As it is found in all haul trucks, it is logical to alter this variable to find an appropriate solution. The apparent solution involves modifying the current passive damper to be more reactive to operating conditions. Alterations to the current design would be made to increase the dampening ratio as the damper nears the end of its stroke. Effectively, the dampening ratio will increase to a level where it will increase the stiffness of the overall suspension. As a result of the modification, the redesigned damper would be theoretically dependent on both the velocity and stroke displacement. From this point on the thesis will refer to the oil-pneumatic suspension cylinder as the damper.

1.6.5 The Concept for an Alternative Ultra Haul Class Hauler Suspension

The concept for this thesis project originates from the design of dampers used in airplanes. Similar to haul trucks, the dampers in airplanes use a variation of the oil-pneumatic suspension cylinder. The type used by airplanes is called an oleo-

pneumatic suspension. The single primary function of an airplane damper is observed during landing. The damper's role is to absorb and dissipate the impact energy such that the forces transferred to the airframe are reduced to a safe level (Anon, 1994 and Currey, 1988). An oleo-pneumatic system is depicted in Figure 1.23. After comparing the two different damper designs found in the truck and in the airplane, it is apparent that both share similar components. The two differences between the oleo-pneumatic damper and the damper found in haul trucks are that the oleo-pneumatic suspension has a metering pin and is single-acting (Chai and Mason, 1997). Single-acting means that the damper will function either in compression or rebound, unlike an automobile damper which is double-acting.

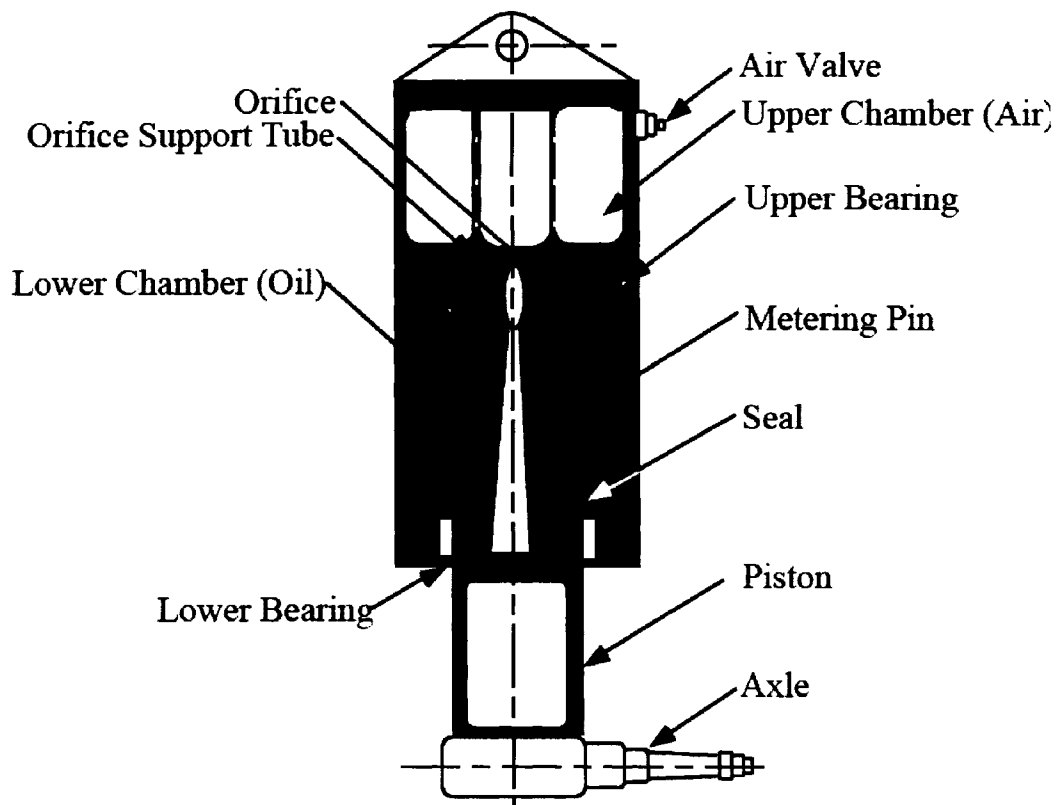


Figure 1.23 Oleo-pneumatic Damper (after Chai and Mason, 1997)

An oleo-pneumatic damper operates similar to the truck damper. As the plane is landing the damper is compressed forcing the oil through the orifice into the upper chamber. As more oil flows into the upper chamber the gas is compressed, absorbing

the energy. The metering pin comes into play by varying the orifice area as the damper is compressed. As the damper is compressed, the orifice area decreases, thus a greater dampening force is produced.

The metering pin concept provides a means to reduce the effects of shock loading and bottoming out. All that is required to apply the concept is a simple retrofit of a plate and metering pin to the existing damper. The plate would be attached on the top of the piston rod. The metering pin would be fixed at the bottom of the cylinder tube. Both pieces would effectively act as the variable orifice. Figure 1.24 is a conceptual drawing of the required modification to the original equipment manufacturer (OEM) damper. As the suspension cylinder compresses, the orifice area of the plate is reduced, therefore increasing the dampening force.

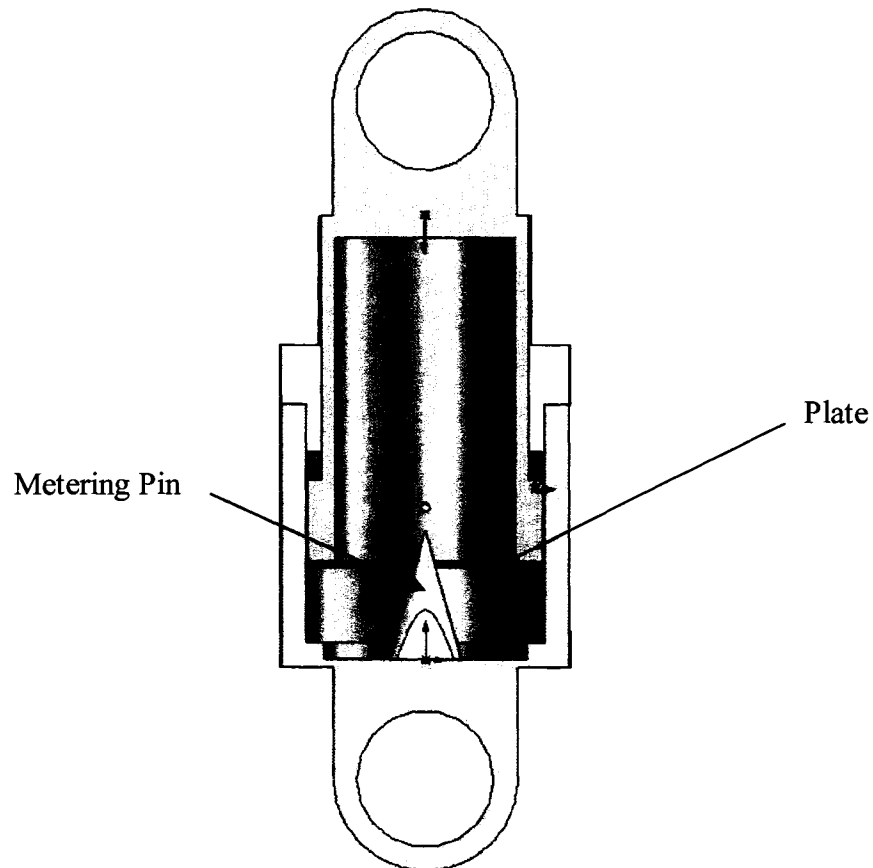


Figure 1.24 Modified Damper

CHAPTER 2 Thesis Project

2.1 Methodology

In order to evaluate the thesis concept the project was divided into two parts, an analytical and physical part. The analytical stage involved formulating a computer model, which was used to model the dampening characteristics of the damper. The second part was the physical testing of the damper where a dynamic test was performed to validate the computer model. The physical testing was done using a scaled down version of the truck damper. To further simplify and reduce the number of variables being evaluated during testing only the hydraulic dampening was observed. The effects of the gas spring were considered on an isentropic calculation basis for both analytical and physical models to allow a focus on the dampening effects of the hydraulic fluid alone.

2.1.1 Computer Modeling

A model was created using Microsoft Excel to simulate the dampening force produced by the damper. The model served three functions. The first was to show the baseline dampening characteristic of the damper. The second was as a tool to compare the performance of the OEM and conceptual modified damper. Lastly, it was determine the parameters of the metering pin and plate to provide the optimum dampening characteristics.

The model was created using the equations found in Section 1.5. Table 2.1 below lists the parameters used in the model. The only parameter that was varied during the modeling stage was velocity. The input velocity was kept constant for each simulation, keeping the model a static analysis for each iteration.

The flow chart in Figure 2.1 illustrates the sequence of calculations involved in modeling a damper. The model calculates the stroke and dampening force at 0.01 second intervals for one compression cycle (Appendix A). Results of the model analysis were plotted to illustrate the dampening characteristic of the damper (fig. 2.2).

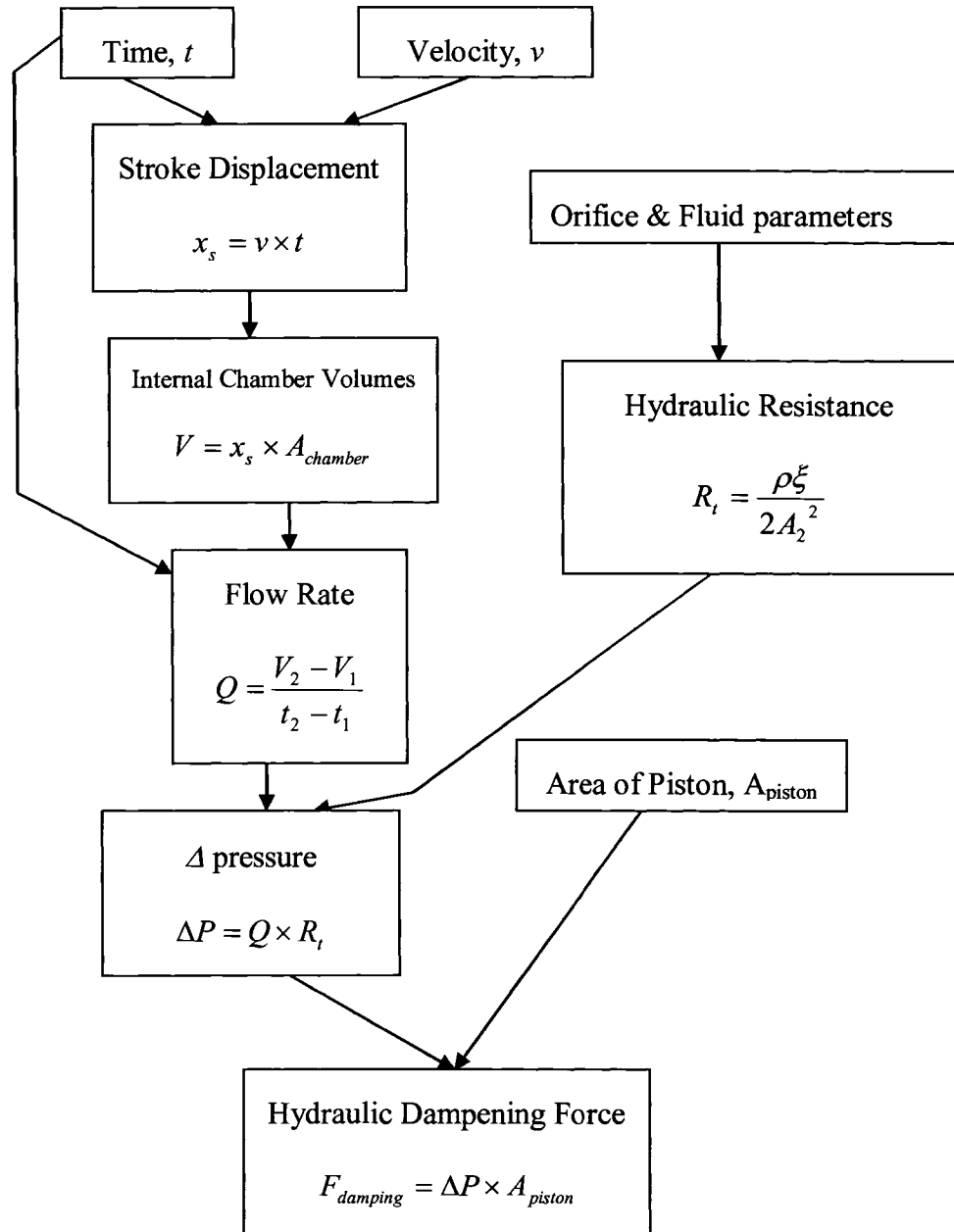


Figure 2.1 Model Flow

Damper Parameters	<ul style="list-style-type: none"> • total stroke • internal dimensions
Velocity	<ul style="list-style-type: none"> • piston speed
Orifice Parameter	<ul style="list-style-type: none"> • diameter
Fluid Properties	<ul style="list-style-type: none"> • density • viscosity

Table 2.1: Damper Parameters

Hydraulic Damping

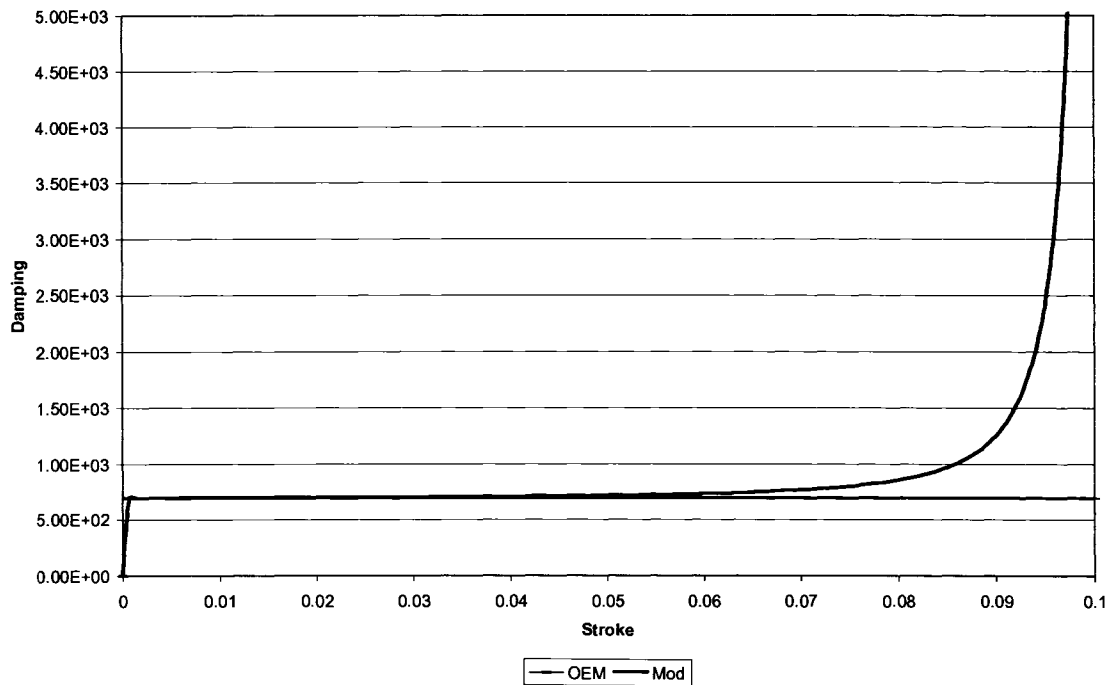


Figure 2.2 Example of Modeled Dampening Characteristic

2.1.1.2 Scaled Down Damper

For the physical testing, a scaled down version of the suspension damper was used. A common hydraulic actuator used on hydraulic powered machines was

modified to perform like an oil-pneumatic suspension damper. There are two differences between the original and scaled down damper versions. The first difference is that the scaled down damper has the same dampening ratio for both the compression and rebound, whereas the original damper has roughly a 3:1 ratio (compression: rebound). Second, the smaller version is not equipped with a gas spring. However, because the project only examines the compression stroke and hydraulic dampening force, the two shortfalls of the scaled down damper were not expected to affect the outcome of the test.

The hydraulic actuator used for the test was manufactured by “Shur-lift”. It is a double acting cylinder, which means its shaft can be extended or retracted. The hydraulic actuator is depicted in Figure 2.3 and its specifications are displayed in Table 2.2. The actuator consists of a cylinder, piston, shaft and ports. In the basic operation of the actuator, the fluid is pumped through the port and into one of the chambers. As the chamber fills up with incompressible fluid, the fluid exerts a force on the piston causing it to move up or down.

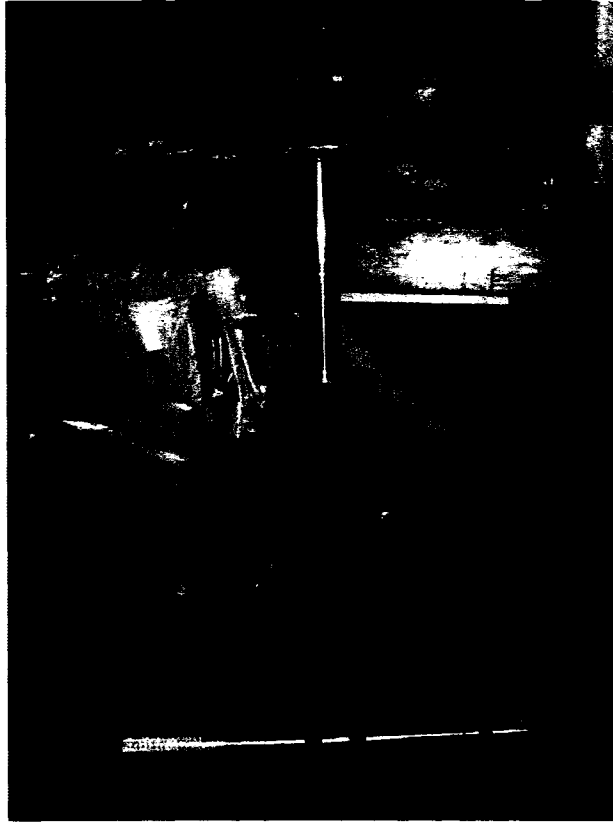


Figure 2.3 Shur-Lift Hydraulic Cylinder

Stroke	10"
Cylinder Bore	4"
Retracted Length	20.25"
Rod Diameter	1.5"
Max. Continuous Pressure	3,000 PSI
Weight	39.0 lbs
End Mounts	Clevis (1")

Table 2.2 Shur-Lift Cylinder Spec.

In order for the hydraulic actuator to function like the haul truck's oil-pneumatic damper a few modifications were made. A total of three changes were

made to make the actuator function like the truck damper. The first change was that four holes were drilled through the piston as displayed in Figure 2.4. The purpose of the holes is to effectively be the orifices, which will allow the piston to move up and down the cylinder. The second change involved reducing the amount of travel of the Shur-Lift cylinder. The original stroke of 10" was too large for the scaled down version. Therefore, the effective travel was reduced to 4" by attaching a 6" spacer to the piston. The spacer was made from a 3.5" diameter steel pipe with a wall thickness of ¼". It was threaded to the bottom of the piston as depicted in Figure 2.5. The last change involved plugging the inlet ports on the cylinder tube to have a closed system as with the original truck damper. Incorporating the three changes resulted in the Shur-Lift hydraulic actuator performing like an OEM haul truck damper. Figure 2.6 illustrates the fluid flow path of the scaled OEM damper. Table 2.3 lists all the input parameters for the scaled OEM damper.

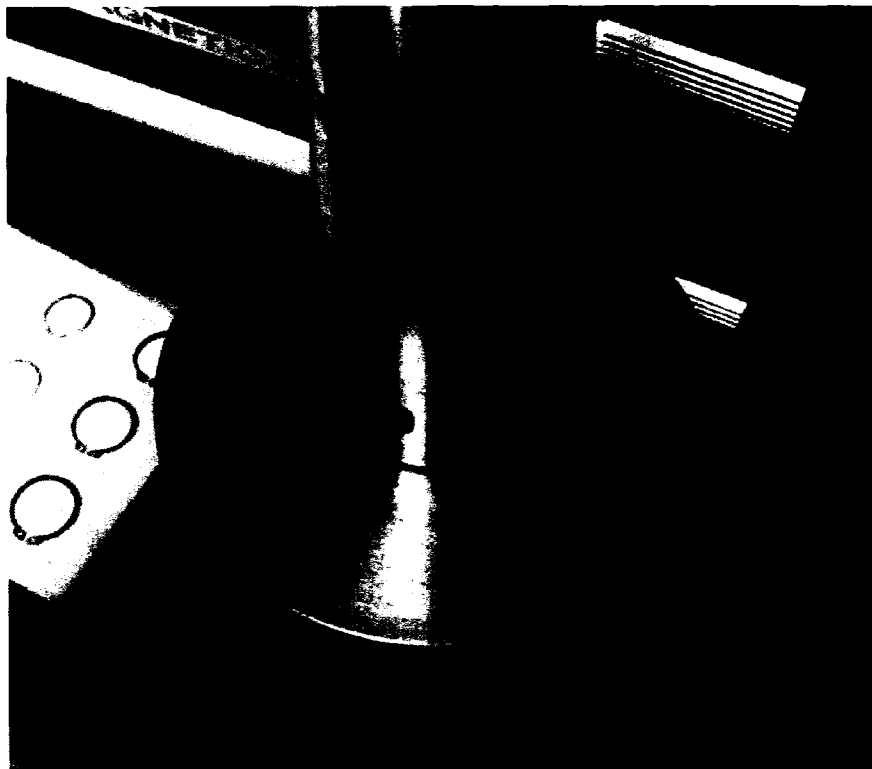


Figure 2.4 Modified Piston

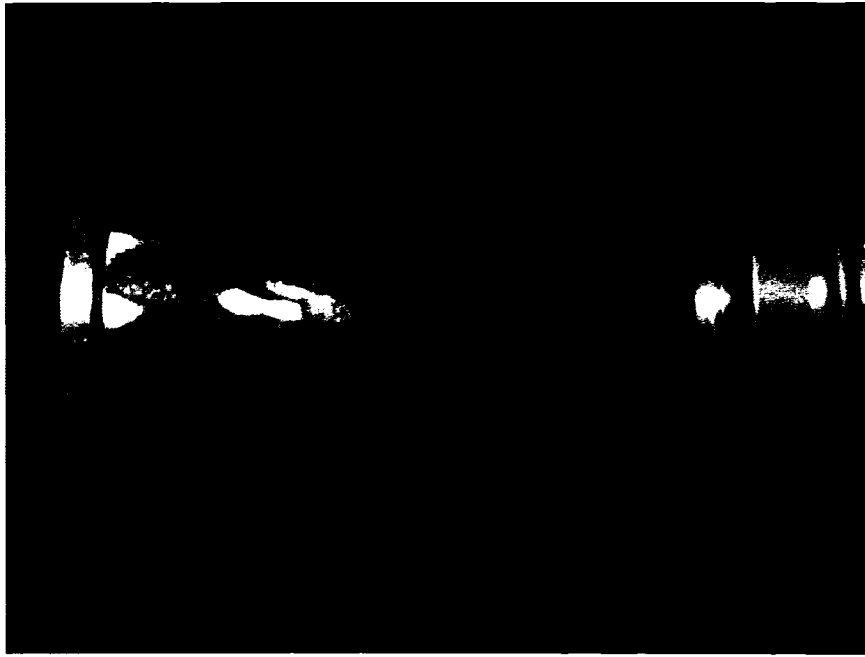


Figure 2.5 Spacer

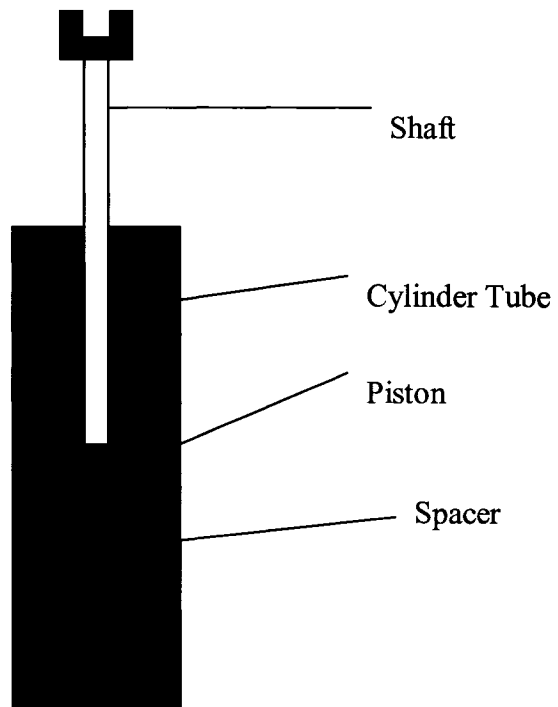


Figure 2.6 Fluid Flow of the Scaled OEM Damper

Inside piston diameter	66.9 mm
Outside piston diameter	73.0 mm
Piston diameter	101.6 mm
Inside height	139.7 mm
Shaft diameter	38.1 mm
Inner tube diameter	101.8 mm
Total stroke	101.6 mm
Orifice diameter	4.8 mm
Number of orifices	4
Fluid density	912 kg/m ³
Fluid Viscosity	4.20E-4 Ns/m ²

Table 2.3 Scaled OEM Damper Input

For the modified scaled damper a metering pin and plate was added to allow for a variable dampening ratio. The specification of the metering pin and plate were determined by the model. The pin was machined from a 3/4" steel rod. A hole was drilled at the bottom of the cylinder to bolt the metering pin in place (fig 2.7). In its scaled OEM form there is no pin present, so the hole was plugged with a bolt and nut. The second component, the plate, was machined from a solid 3.5" steel rod. It was threaded to the bottom of the spacer. Figure 2.8 depicts the internals of the scaled modified damper and Figure 2.9 illustrates the fluid flow within. Table 2.4 lists the additional input variables for the modified scaled damper.

Metering pin height	114.3 mm
Metering pin base diameter	12.7 mm
Metering Pin Angle	86.42°
Plate orifice diameter	12.9 mm

Table 2.4 Metering Pin Parameters

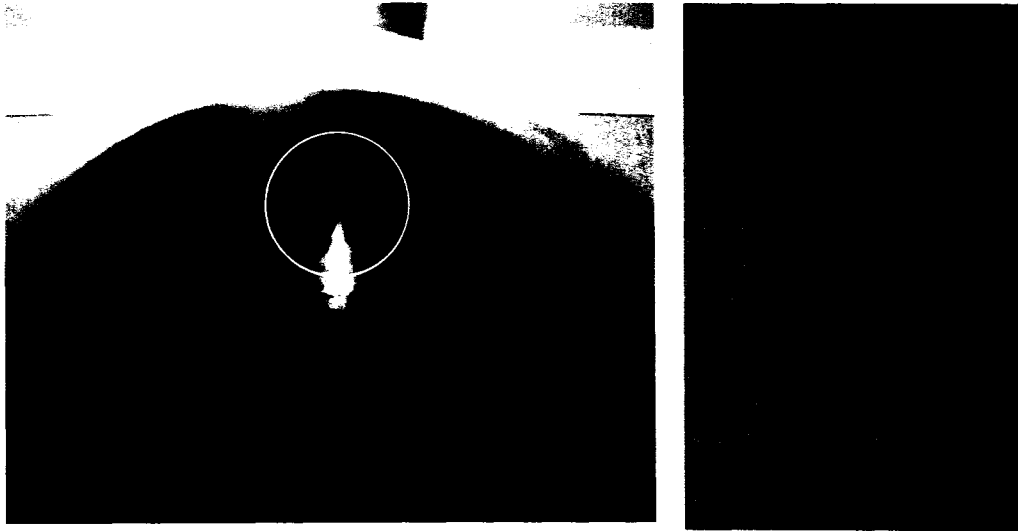


Figure 2.7 Metering Pin

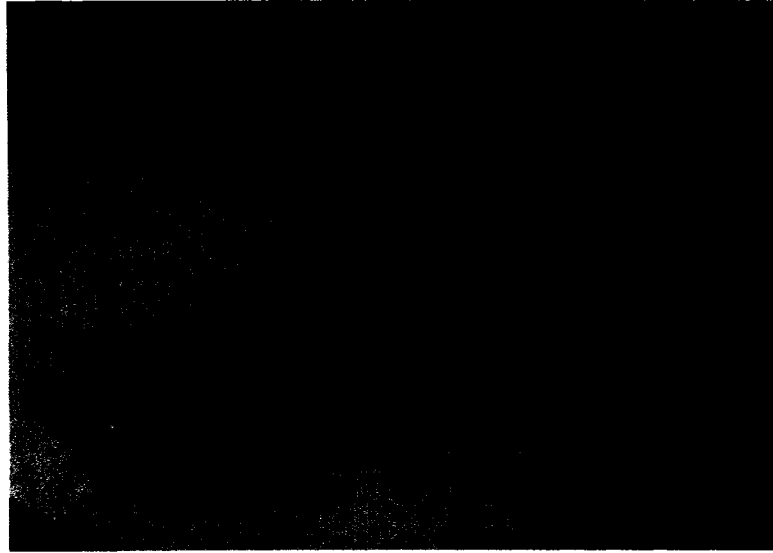


Table 2.8 Modified piston and Plate

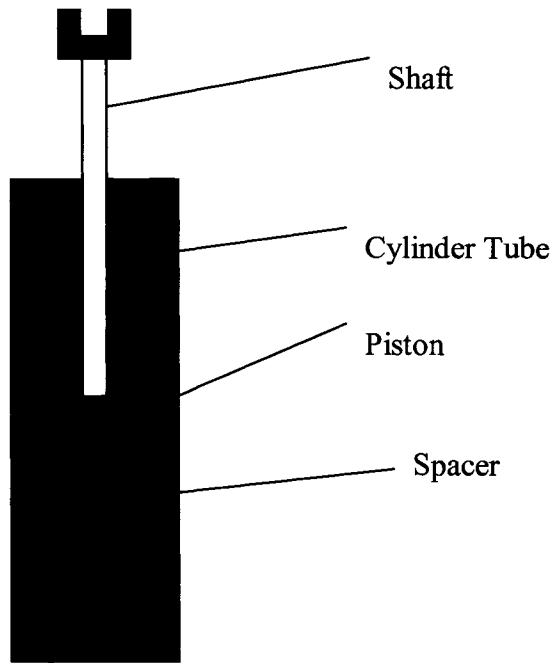


Table 2.9 Fluid Flow of the Scaled Modified Damper

2.2 Test Methodology

Testing was conducted on a test frame similar to the commercially available shock dynamometer. The test frame used hydraulic power to compress the damper. During the test three variables were collected: stroke displacement, internal pressures, and dampening force. A data acquisition system was used to collect the signals from the sensors and LabView was used to process the collected data.

2.2.1 Test Frame

The test frame was originally used for materials testing. For the goal of this thesis, the test frame was set up to function similar to a shock dynamometer. Figure 2.10 below depicts the test frame. The enormous frame structure was constructed with structural steel and was held together with bolts. Large I-beams were used as the four posts of the frame. The posts were anchored to the concrete floor and additional steel bars were used as cross members between the posts. At the end of the frame a hydraulic actuator was fixed above the test specimen.

The hydraulic actuator simulates the damper being loaded. Power to the actuators was provided by a hydraulic pump. Attached to each actuator was a servovalve, which functioned to regulate the flow of fluid to the actuator. The servovalve was governed by a digital servo controller, which was manipulated by the user.

2.2.2 Servo Controller

The cyclic loading for the test was controlled with a Kelsey Instrument K7500 digital servo controller (fig. 2.11). The controller sent signals to the servovalve, which in turn manipulated the hydraulic actuator. The K7500 provided a wide range of features for closed loop control of servo hydraulic actuators. The K7500 can be used for mechanical testing (static and dynamic) and motion control systems. It can operate in one of the two control modes: load or displacement. In load control mode, the amount of load (compression or tension) that the actuator produces is controlled

by the servo controller regardless of the actuator's position. In displacement mode, the position of the actuator is controlled by the servo controller regardless of the load produced. The K7500 is capable of operating as a single (stand alone) or multi-channel (slave or master) unit. For this test only one actuator and controller was used, therefore the controller was in stand alone operation.

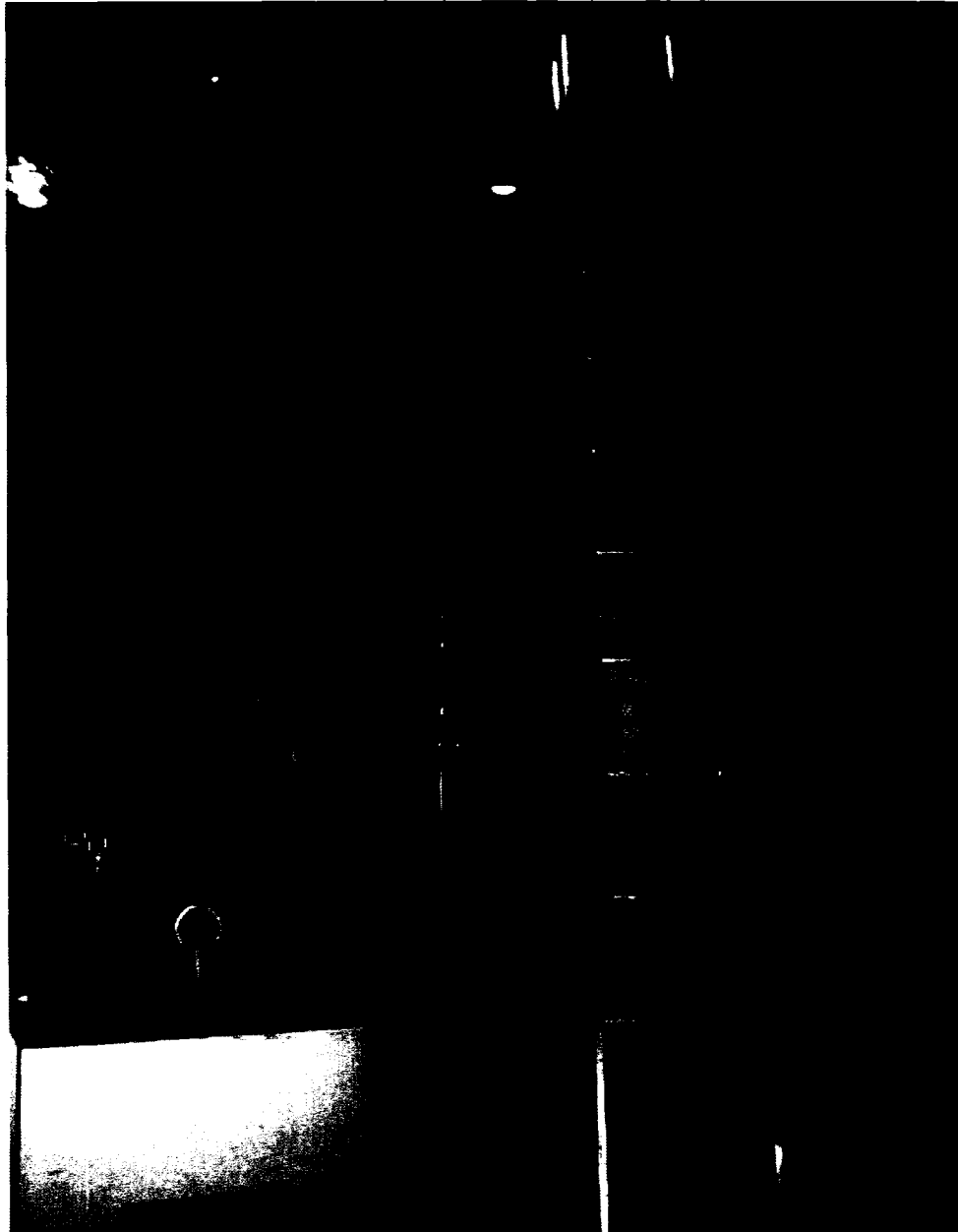


Figure 2.10 Test Frame



Figure 2.11 K7500 Servo Controller



Figure 2.12 K7500 Interface

The advantage of the K7500 was its ability to set up tests in short time periods and to save settings for future use. Figure 2.12 displays the user interface, which incorporates an alphanumeric display. The display provided two parameter readouts and test status. For the test, display #1 indicated the current position of the stroke and display #2 was the total stroke. A high resolution rotary encoder, called an adjustment control dial, was used to provide parameter selection and adjustment.

2.2.3 Sensors

During the test, three variables were collected. The variables that were recorded were the displacement of the damper (stroke), the pressure within the damper and the hydraulic dampening force created by the damper. Each variable was measured with an electronic sensor. Table 2.5 below lists the sensors used and Figure 2.13 illustrates the setup. The LVDT and the load cell were already in place as they were essential for operation of the K7500 servo controller. Pressure transducers were added to monitor the internal pressure of each chamber within the damper.

Variable	Sensor
Stroke displacement	Linear variable differential
Pressure	Pressure transducer
Hydraulic Dampening Force	Load Cell

Table 2.5 Variables and Sensors

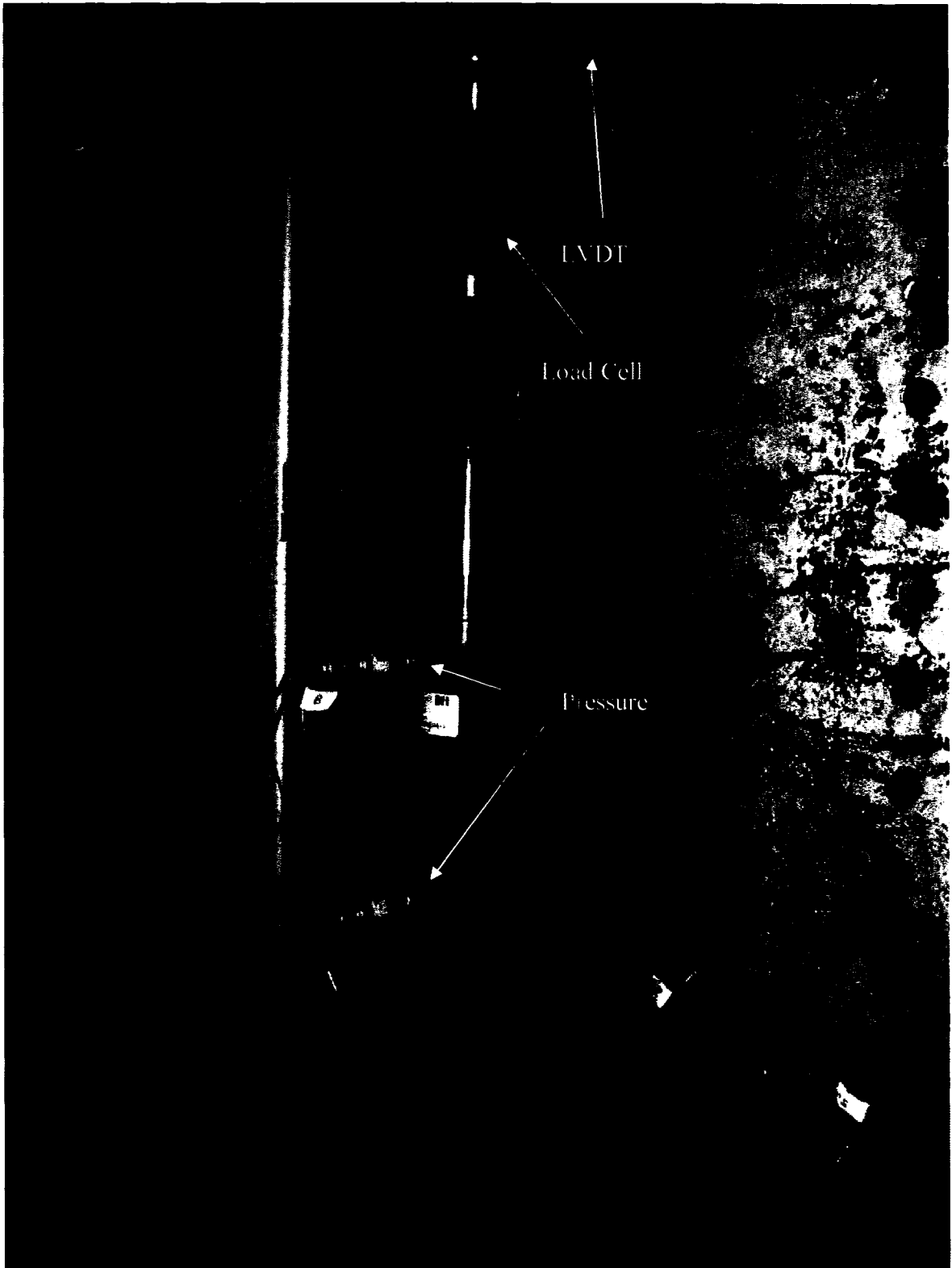


Figure 2.13 Sensor Setup

2.2.3.1 Linear variable Differential Transformer (LVDT)

The primary function of the LVDT was to monitor the displacement of the actuator. The LVDT model used in the test was manufactured by Pegasus, model #1820B. The basic parameters of the LVDT are shown below in Table 2.6. Because the displacement of the actuator is equal to the stroke displacement, the LVDT served a dual purpose. The LVDT's coil was fixed to the actuator's cylinder and the push rod was attached to the load cell as shown in Figure 2.14.

2.2.3.2 Load Cell

The load cell measured the hydraulic dampening force produced by the damper. The model of the load cell in the test was manufactured by Pegasus (model # 3129-11d). Table 2.7 shows the basic parameters of the load cell. Figure 2.15 depicts the load cell and how it was attached. The base of the load cell was threaded to the end of the actuator's shaft and the damper was attached at the other end of the load cell.

Range	170 mm
Scale Factor	8.5mm/volt
Excitation Voltage	10 Volts

Table 2.6 LVDT Parameters

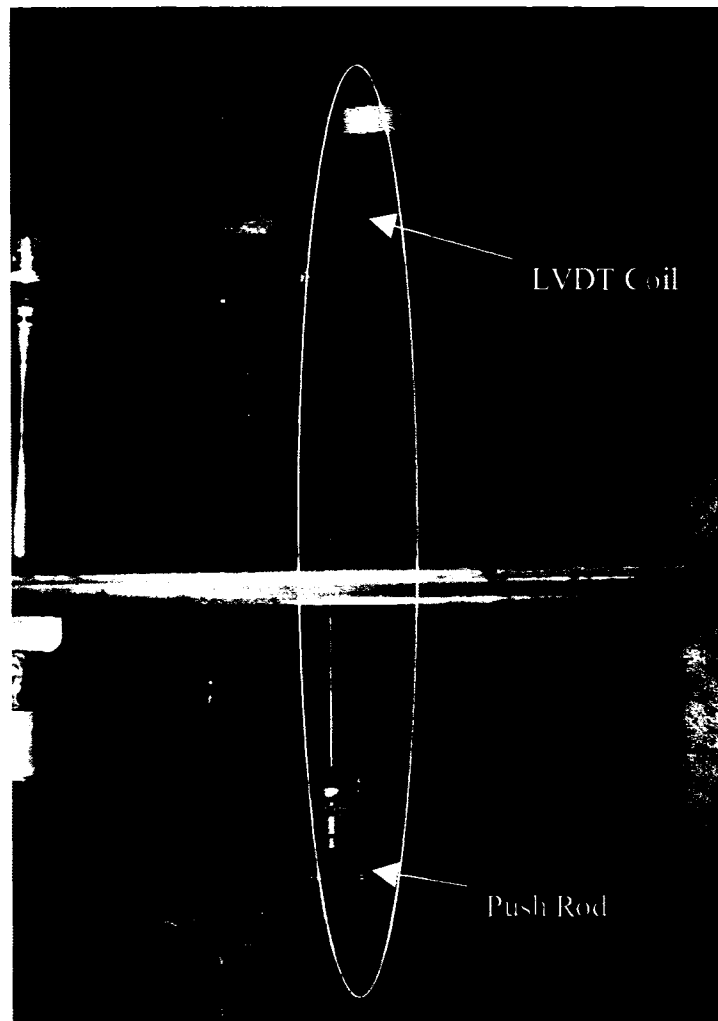


Figure 2.14 LVDT

Range	667 kN
Scale Factor	67.5 kN/volt
Excitation Voltage	10 Volts

Table 2.7 Load Cell Parameters

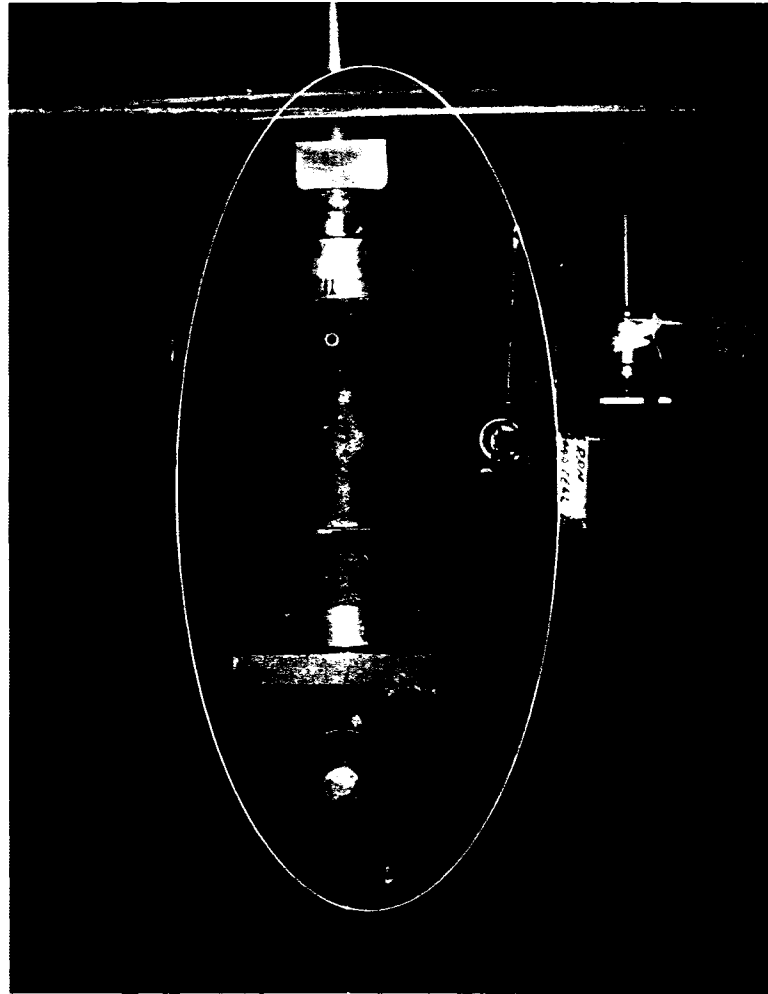


Figure 2.15 Load Cell

2.2.3.3 Pressure Transducer

Schaevitz pressure transducers were used for monitoring the pressures inside the damper cylinder. Two pressure transducers were used, one measuring the bottom chamber, A, and the second one measured the upper chamber, B (Fig. 2.16). Both transducers were attached to the existing ports on the cylinder. Table 2.8 lists the parameters of the pressure transducers.

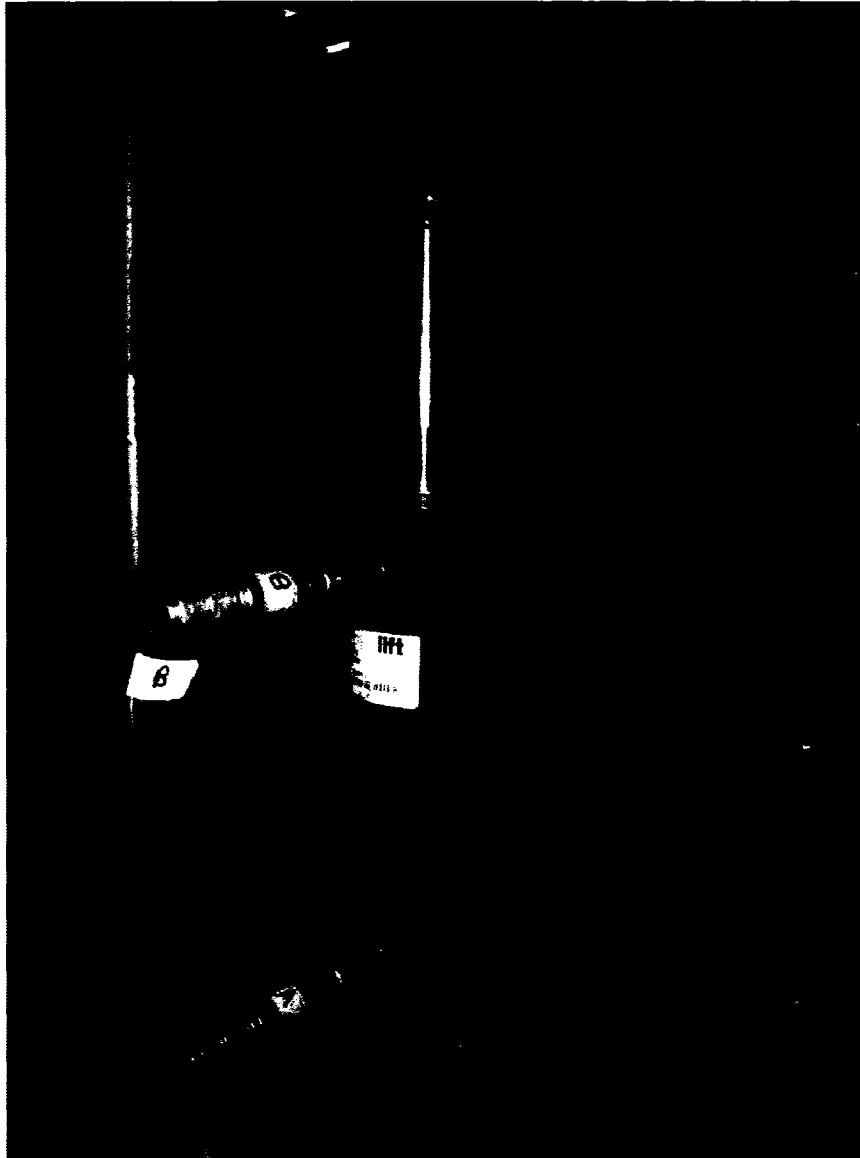


Figure 2.16 Pressure Transducer

Range	1723 kPa (250 PSI)	
Scale Factor	A: 69.26 kPa/mV	B: 68.97 kPa/mV
Excitation Voltage	10 Volts	

Table 2.8 Pressure Transducer Parameters

2.2.4 Data Acquisition System

Monitoring and recording of the data during the test was done with a data acquisition system. Table 2.9 below explains the functions of each component.

Component	Function
Sensor	A device that measures a physical phenomenon and converts it into a measurable electrical signal such as voltage.
Signal Conditioning	Some sensors generate signals too difficult to be read by the data acquisition hardware. A signal conditioning device conditions those signals to be accurately read by the data acquisition hardware. Signal conditioning also offers signal amplification, isolation, filtering, and multiplexing.
Data Acquisition Hardware	The hardware acts as the interface between the computer and the outside world. Its function is to digitize incoming signals so that a computer can interpret them.
Software	Software transforms the computer along with the data acquisition hardware into a complete data acquisition, analysis, and presentation tool. Software controls the hardware.

Table 2.9 Data Acquisition Components

The hardware used for the data acquisition system consisted of sensors (LVDT, load cell, and two pressure transducers), a signal conditioning unit, a data acquisition unit, and a desktop. Figure 2.17 displays the flow of information through the system.

The first step in data acquisition was the collection of all signals from various sensors. Both of the pressure transducers were connected directly to the National Instruments interface block. The interface block allowed for the simplification of wiring of various sensors to the signal conditioning module and provided the sensors with the excitation voltage. Both the LVDT and the load cell signals were first routed to the K7500 servo controller. The K7500 needs the LVDT and load cell signal for its various mode controls. After the K7500 has read the LVDT and load cell signals, the signals are then output via a cable to the connection interface. The signals were then sent through a ribbon cable to a signal conditioning module.

The SCXI-1100 32 channel analog input module was used for signal conditioning and was housed in a SCXI-1001 chassis. Both the SCXI-1100 module and the SCXI-1001 chassis were manufactured by National Instruments. The primary purpose of the SCXI-1001 was to connect all the modules to the data acquisition hardware. The signal from the SCXI-1100 was then digitized by an E series multifunction data acquisition card, also made by National Instrument. The signal must be digitized in order to make the signal readable by computer software. The software controlled the data acquisition system and turned the signal into readable data.

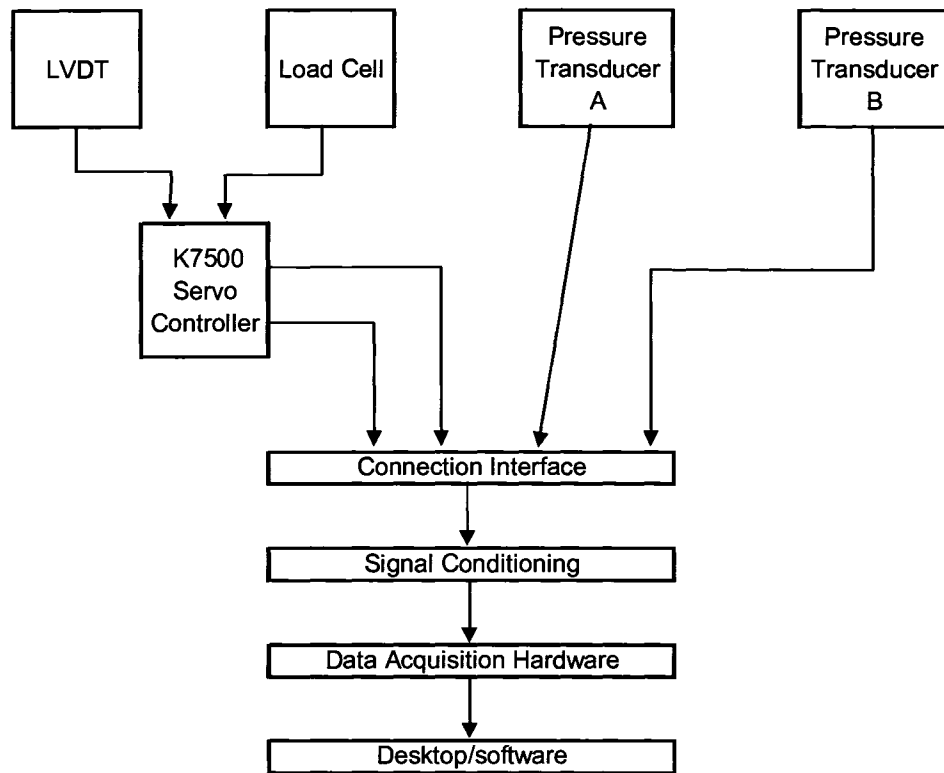


Figure 2.17 Flow of Information

2.2.5 Software

The software used to process the signal coming from the data acquisition hardware was National Instrument's LabView, a graphical development environment for designing tests, measurements, and control systems. The graphical environment made it easier to create a project. Due to the nature of the test, a high speed sampling rate was required. The data acquisition system setup was capable of handle high sampling rates, but there was no LabView program readily available to acquire data at high speed. A program, *damper.vi*, was created specifically for this application. The algorithm wiring diagram for the program is found in Appendix B. The program was designed to monitor each of the four sensors in real time and was set up to sample 100 Hz.

A key feature of LabView is its visualization capabilities. The program was setup to graphically monitor each sensor during testing, shown in Figure 2.18. The

graphs made it easy to visually see the changes in each sensor when a test parameter was varied. Each of four plots corresponded to a sensor. Table 2.10 lists the corresponding channel and chart of each sensor.

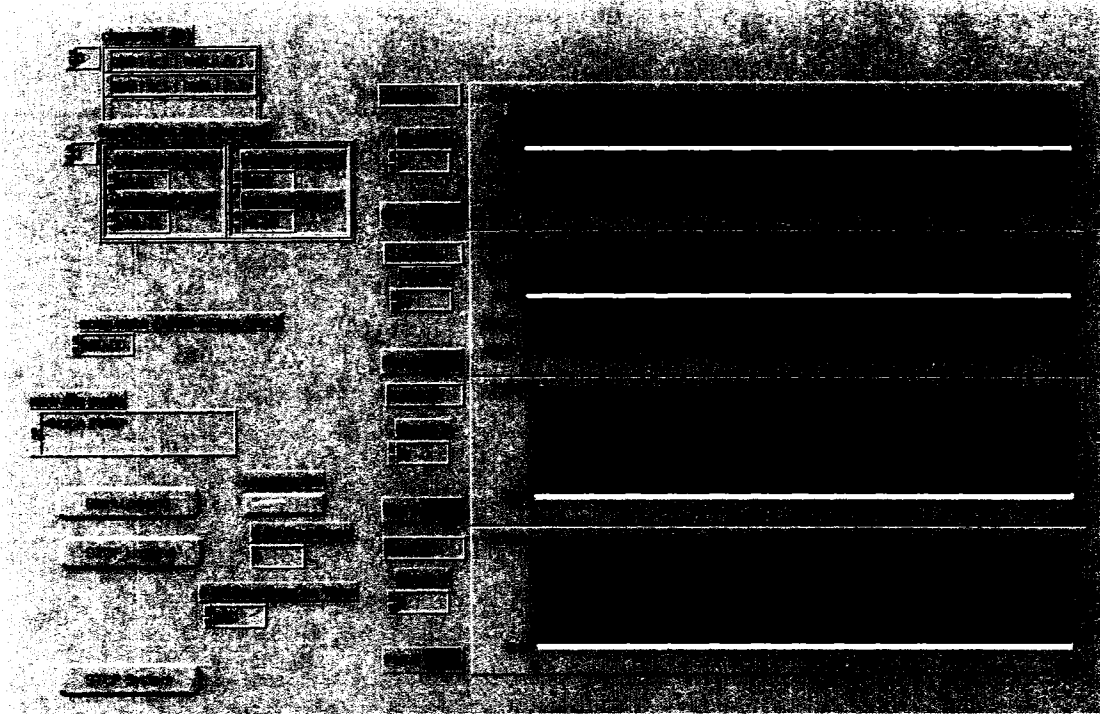


Figure 2.18 LabView Interface

Channel	Chart #	Sensor
0	1	Load Cell
1	2	LVDT
2	3	Pressure Transducer A
3	4	Pressure Transducer B

Table 2.10: Channels

Another advantage of the program was that it allowed the user to record a set of data at any time during the test. Recording begins and ends by clicking on the “start logging” and “end logging” buttons respectively. The program records readings from each of the four sensors and stores it into files. The recorded data is saved into a text (.txt) format file, where each time the “start logging” button is selected, the data is saved into a new file.

2.3 Testing

Testing of the damper was done at the University of Alberta Structure Lab. The damper was set up in the testing rig and cycled up and down as a cyclic test. During the test the dampening force, the displacement and the pressures were recorded. Section 2.2 contains further details with regards to the equipment, hardware, and software involved in the testing.

2.3.1 Set up

The testing frame was originally used for material testing, which required a high loading and low displacement rate. The velocities that the hydraulic actuator was capable of producing were unknown. Therefore, a few tests were done to ensure that the testing rig could produce a high enough velocity. For safety reasons, the setup run was done without the damper in the testing frame.

The type of test being performed on the damper was a cyclic test. The first step was to set up the K7500 controller for a test, thus the controller was set to displacement mode. The displacement mode's controlling parameter is the displacement of the hydraulic actuator. After setting up the controller, the type of wave function was selected. The K7500 controller had the option of 4 wave functions (sine, square, triangle, and sawtooth). A triangle wave function closely simulated the suspension cylinder on a heavy haul truck hitting a bump or loading, so it was chosen as the ideal wave function for the test being performed. Next, the frequency range of the test was set from 0.0001 to 2 Hz, and a frequency of 0.01 Hz as the starting point.

During the test, the span and the frequency on the controller were varied. By altering the span, the total stroke could be varied. Equation 2.1 shows how the span is related to the total stroke.

$$span(\%) = \frac{x_t}{x_{actuator}} \quad (2.1)$$

Where:

x_t = total stroke

x_{actuator} = total stroke of the hydraulic actuator

The actuator in the test frame had a maximum stroke displacement of 160 mm, while the damper has a total travel of 101.6 mm; therefore a span of 63.5% was used. However, in order to prevent the damper from bottoming out and topping out (full extension of the damper), the span was lowered to approximately 56%. As a result, the damper's total travel was reduced to 90 mm.

Next, the frequency of the cycle was altered. By changing the frequency, the velocity of the damper's shaft also changed. The maximum velocity of the damper was calculated using Equation 2.2.

$$v \approx (fq) \times (x_t) \tag{2.2}$$

Where:

fq = frequency

The modeling done in Excel showed that a velocity greater or equal to 40 mm/s was required in order to show the differences in the dampening force between the OEM and modified damper. In order for the hydraulic actuator to have a velocity of 40 mm/s, the required frequency for the cycle was calculated to be 0.22 Hz.

After the K7500 controller was set up, the hydraulic pump was turned on to power the actuator. The hydraulic oil heats up because the actuator cycles fairly rapidly. To prevent the pump from overheating, chilled water was circulated throughout the pumping system. Although the servo controller was set to stop, the hydraulic accumulator moved up and down erratically upon start up. The erratic motion was caused by the gain being set too high, thus making the controller overly sensitive. In order to overcome the overly sensitive controller, the gain parameters were lowered until the erratic movement stopped.

With the controller and actuator stable, the first preliminary run was started. The span was slowly increased to 56%, which increased the stroke accordingly. Next, the frequency was increased to the calculated 0.22 Hz, at which point the test was stable and running well. Because the test was stable, it was concluded that the test rig was capable of producing a suitable velocity. The frequency was then increased to determine the maximum velocity attainable. The frequency was increased to up 0.9 Hz, at which point the oil began to heat up. Therefore, the maximum frequency for the test was set to 0.7 Hz to prevent the system from over heating and becoming damaged.

2.3.2 Test Run

For the first test run with the damper in the test rig, the data acquisition was not turned on. The only thing that was monitored was frequency of the cycle and pressures in the damper. Using the Excel model, the pressures generated inside of the cylinder were calculated to be under 950 kPa at 0.7 Hz. Even though the pressure transducers available for the test had an operating range of 0 – 1723 kPa, the Excel model was not verified with known results. Therefore there was a risk that the pressures inside the damper could exceed the pressure calculated. In order to avoid damaging the pressure transducers, a set of mechanical pressure gauges connected directly to the cylinder ports were used to monitor the pressure. The set of pressure gauges had an operating range of 0-1379 kPa, which provided a method to verify that the pressure in the cylinder would not exceed the operating pressure range of the pressure transducers.

The testing frame was set up so that it cycled up (+) and down (-) equal distance from a datum point. This meant that the damper had to be positioned in the middle of its stroke when placing it in the test frame. With the damper in mid stroke, the bottom clevis of the cylinder was first pinned, and then the actuator adjusted, via the K7500 controller, until it lined up with the top clevis. With the damper at mid stroke, the datum point of the test was set.

The cyclic testing was initiated after the OEM damper and pressure gauges were in place. The first step was to increase the span. Once the correct span was reached, the frequency was then slowly increased. As the frequency increased, the pressure generated inside the cylinder also increased. At 0.7 Hz, the pressure gauges were reading within the range that was calculated in the model. Next, the same test was applied to the modified damper, where the same procedure was followed. Again the pressure gauges were found to be within the range of the model. Because both runs were within the range of the pressure transducers, it was concluded that the pressure transducers were safe to use in the test.

2.3.3 Test Procedure

The test consisted of two runs each for the scaled OEM and the modified damper. During the two tests, the load, position, and pressure were all monitored. For each run the frequency was increased to three different settings as follows: 0.15 Hz (27 mm/s), 0.35 Hz (63 mm/s), and 0.7 Hz (126 mm/s). The second run was done to verify the consistency of the data and also served as back up data. The following procedure was followed for each run.

1. Turn the pump on.
2. Place the damper in the test rig.
3. Press the “start” button on the K7500 controller.
4. Increase the span until it reaches 56% to give a total stroke of 90mm.
5. Once the % span is reached, increase the frequency to 0.15 Hz.
6. When 0.15 Hz is reached, click on the “start logging” button in LabView to start recording the data. After a few cycles click on the “end logging” to end recording.
7. Repeat steps 5 and 6 for the other two frequency settings (0.35 and 0.7 Hz).
8. Reduce both the span and frequency and turn off the pump.

The next step of testing was to run the modified damper. The damper was removed from the testing frame and disassembled in order to add the metering pin and plate.

Once both of the components were in place, the modified scaled damper was mounted back in the testing frame and the above steps were repeated.

CHAPTER 3 Results and Discussion

3.1 Results and Raw Trends

A total of twelve raw data sets were collected during testing of the scaled damper. The twelve data sets include three sets of data of each the OEM damper and the modified damper at the different cycle frequencies. The remaining six data sets were collected as back up data. The sampling rate for each run was set at 100 Hz. Each data file contained dampening force (load), stroke displacement, pressure A and B, and a time stamp for each data point recorded.

The raw data was imported into Microsoft Excel to produce three types of plots. The first type was a displacement-time plot. Both the OEM and modified data for each cycle frequency were plotted on the same graph, resulting in a total of three graphs showing displacement as a function of time. The remaining two plots displayed dampening force as a function of time and pressures “A” and “B” in relation to time. A total of twelve plots were created, where each one was based on three different cycle frequencies. All the plots are given in Appendix C.

Each of the plots displayed a definite cyclic pattern, which verified that the raw data were satisfactory and reproducible. Compression and rebound were both observed in the graphs. However, because the scaled damper was not set up correctly for the rebound stroke, the test results for the rebound did not accurately represent what happens in reality. Thus, the rebound will be ignored in the analysis.

3.1.1 Displacement-Time Plot

Based on the displacement plots, it is concluded that for a given cycle frequency, both the OEM and the modified data move at the same rate as displayed in Figure 3.1. The figure illustrates that during compression, the profile of the graph is a downward sloping linear line, where as an upward linear line reflects the rebound period. As a result, a triangular waveform results from the pattern of the compression and rebound. The triangular waveform corresponds to the triangular waveform selected on the K7500 Servo Digital Controller during testing. Furthermore, it was

observed that as the cycle frequency increased, the cycle times decreased. The cycle time for each cycle frequency is shown in Table 3.1.

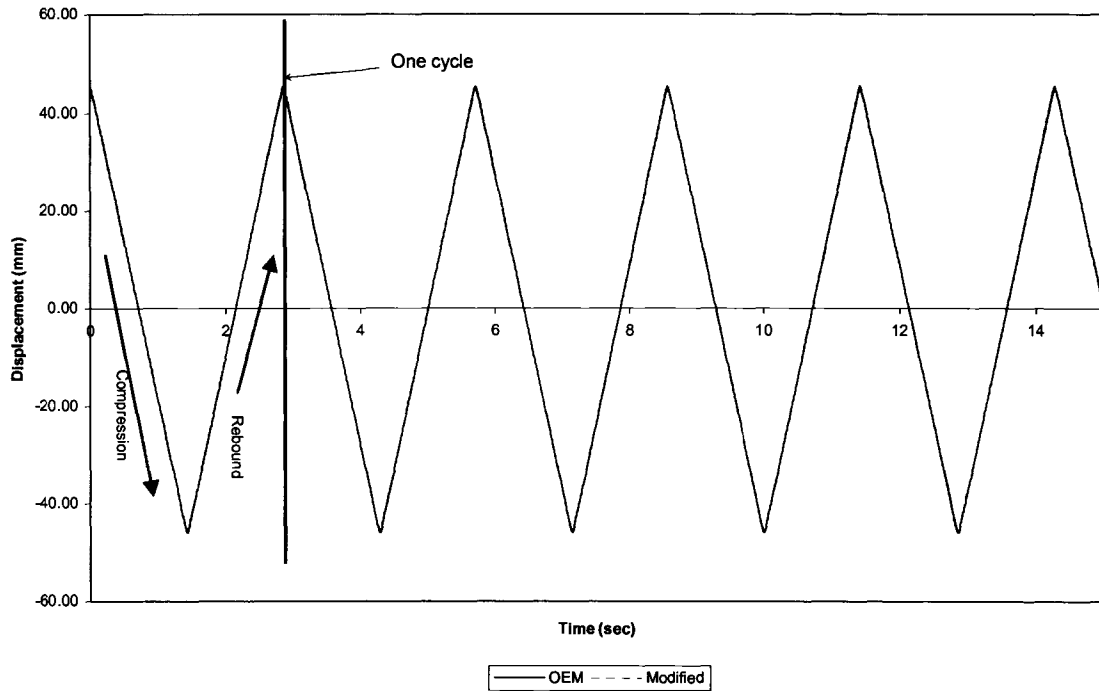


Figure 3.1 Example of Displacement-Time Plot

Frequency	Cycle Time
0.15	6.75 sec
0.35	3 sec
0.70	1.5 sec

Table 3.1 Cycle Time

3.1.2 Hydraulic Dampening Force Plot

A plot of the hydraulic dampening force is displayed in Figures 3.2. It is apparent from the graph that there is a direct relationship between the cycle frequency and the dampening force. The data shows that at a slow cycle frequency of 0.15, both the OEM and modified damper produced almost the same amount of dampening force. At higher cycle frequencies (0.35 and 0.7 Hz), the OEM damper dampening force increased linearly until reaching the midpoint of its stroke, and then it began to level off (Fig. 3.3). The greater the cycle frequency the greater the dampening force level reached.

In comparison to the OEM damper, the modified damper achieved a greater dampening force for a given cycle frequency. The modified damper continued to peak rather than level off at the mid stroke (Fig. 3.4). Table 3.2 summarizes the result of the dampening force approaching the end of the compression stroke.

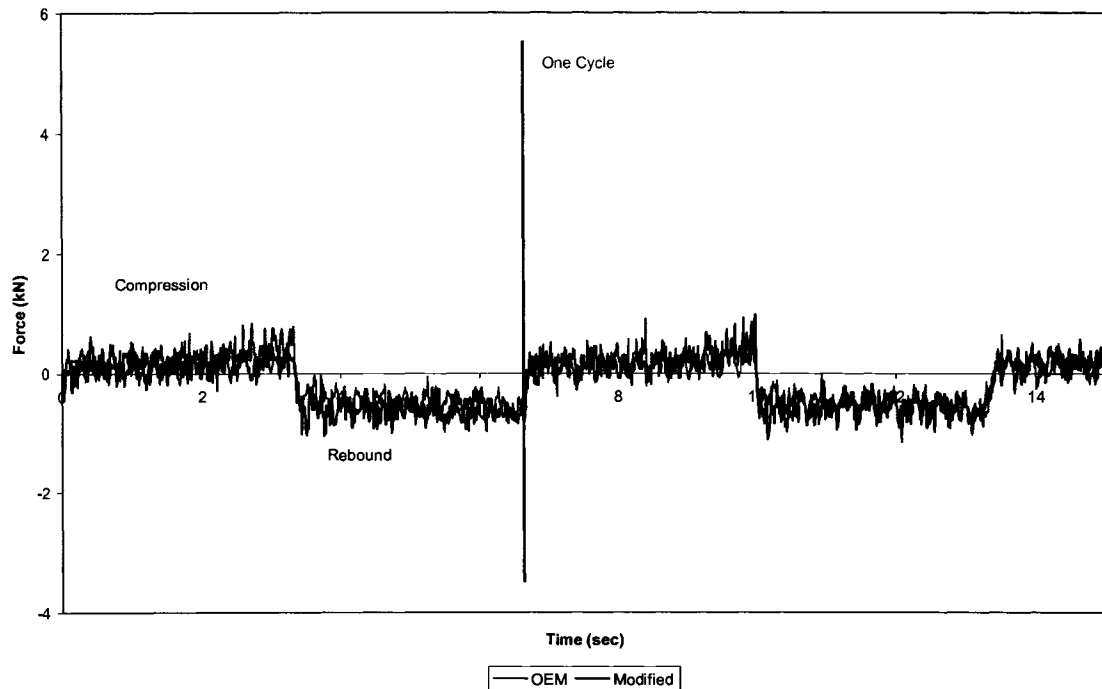


Figure 3.2 Hydraulic Dampening Force at 0.15 Hz

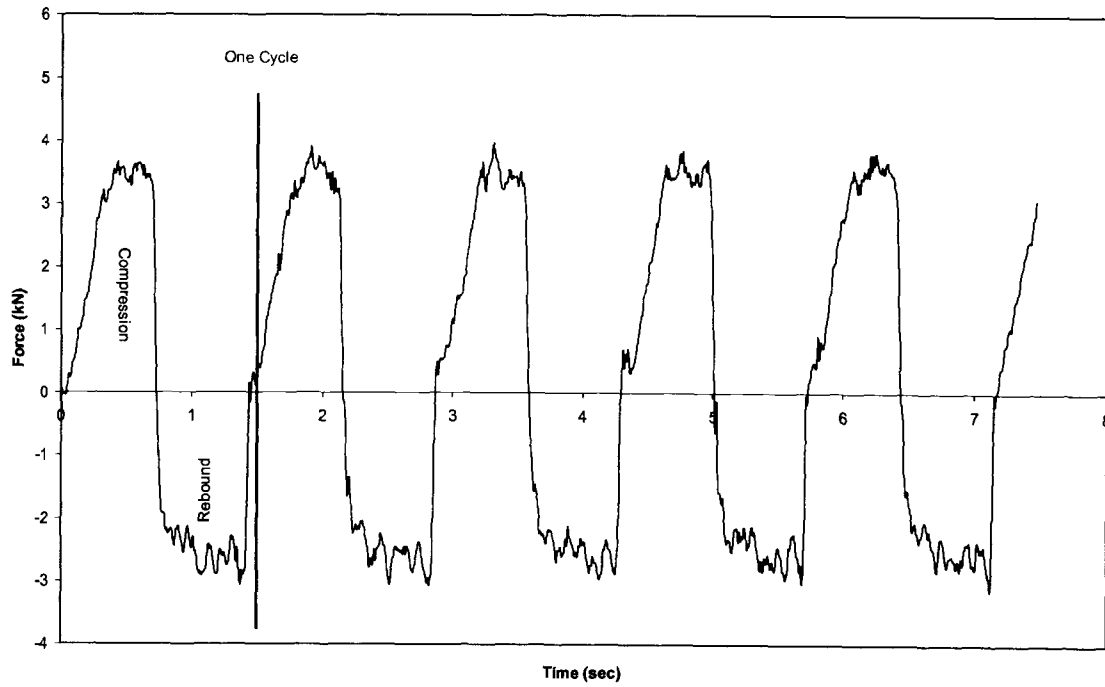


Figure 3.3 Hydraulic Dampening Force at 0.7 Hz (OEM)

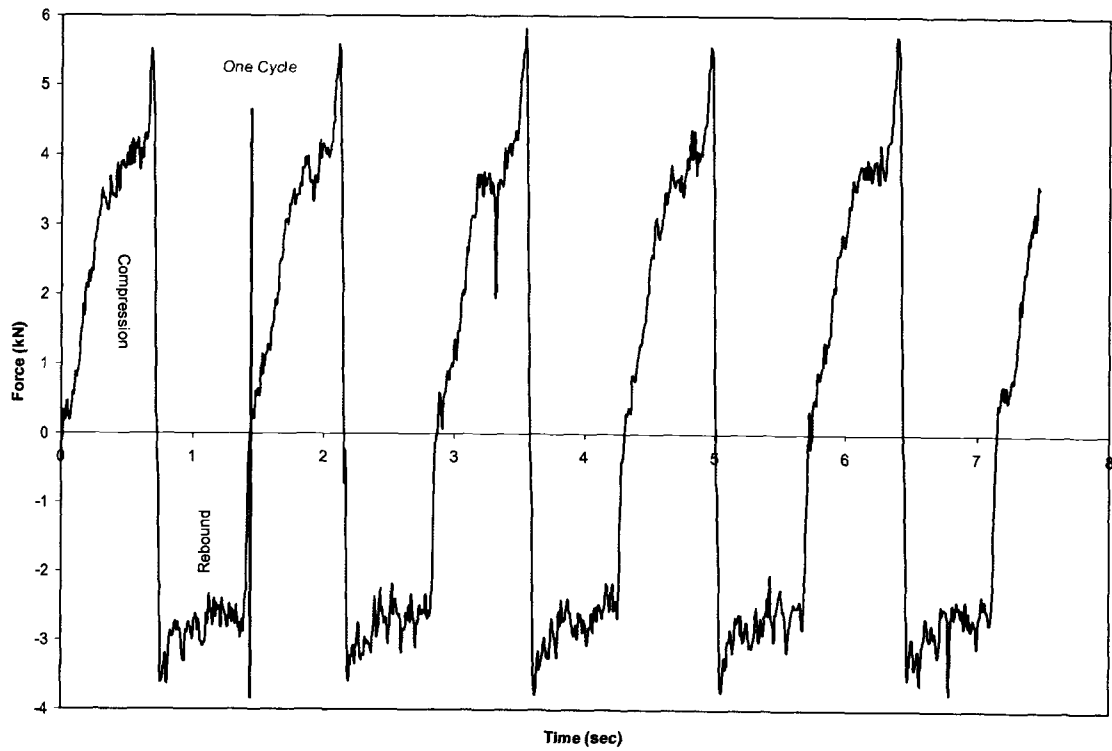


Figure 3.4 Hydraulic Dampening Force at 0.7 Hz (Modified)

Cycle Frequency	OEM	Modified
0.15	0.175 kN	0.175 kN
0.35	0.75 kN	1.5 kN
0.70	3.5 kN	5.25 kN

Table 3.2 Hydraulic Dampening Force Attained For Each Frequency Cycle

3.1.3 Pressure Plot

At each of the different cycle frequencies, the pressure plots all produced a similar trend for both the OEM and the modified damper (Fig. 3.5). Similar to the dampening force plots, pressure A and B both increased as the cycle frequency increased. A characteristic shared by all of the pressure plots was that during compression, pressure A was greater than pressure B. Fluids flow from high pressure to low pressure. Since pressure A was greater than pressure B, the oil moved from the lower chamber to the upper chamber. A summary of the achievable pressures for each test run is displayed in Table 3.3.

Cycle Frequency	OEM	Modified
0.15	125 kPa	190 kPa
0.35	160 kPa	275 kPa
0.70	450 kPa	750 kPa

Table 3.3 Pressure Attained For Each Cycle Rate

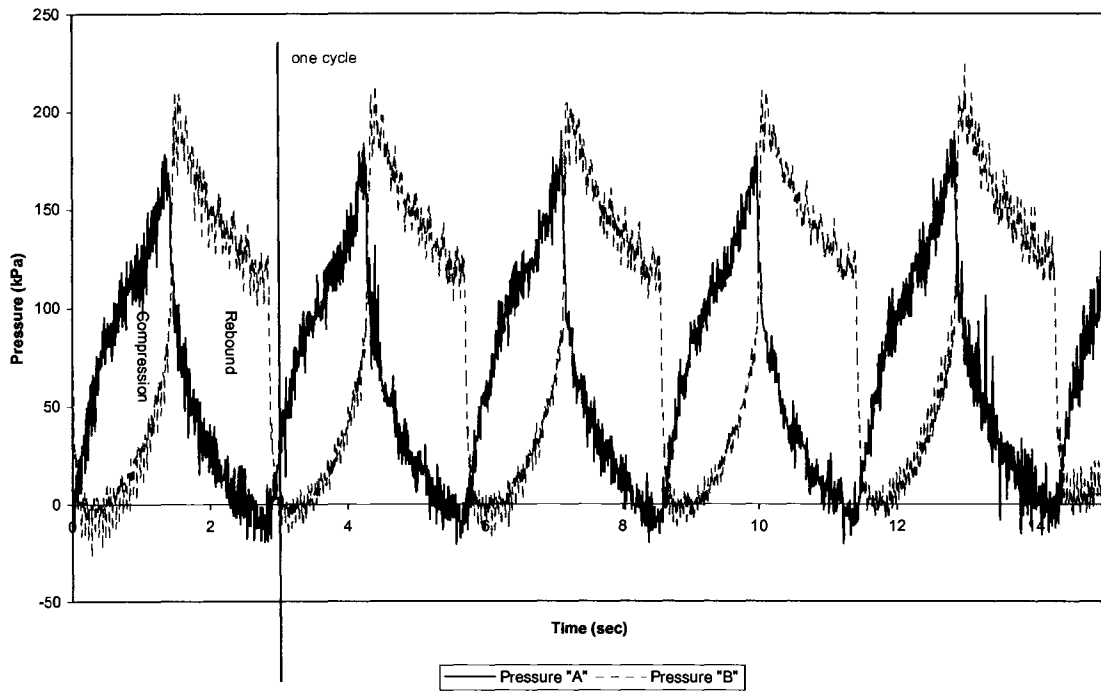


Figure 3.5 Example of Pressure Plot

3.2 Analysis

In order to evaluate the effectiveness of the modified scaled damper, both the OEM and the modified damper test data were analyzed. The next step of the analysis was to compare both OEM and modified data sets with their computer numerical model.

3.2.1 Stroke and Velocity Parameters

In order to complete a full analysis, two additional parameters were added to the original five that were recorded during testing (dampening force, displacement, pressure A and B, and time). The first parameter added was stroke (x_s), which is also a measurement of displacement. The difference between stroke and the recorded displacement is where the datum point was referenced from. The datum point of the displacement data was located at mid stroke. For stroke, the datum point was when the damper was at full extension (start of the compression). As the damper is compressed, the stroke increases. The stroke helped to line up the two sets of data being compared and is calculated via Equation 11.1. The second parameter which was added was the vertical velocity of the damper rod. Equation 11.2 was used to calculate the velocity.

$$x_s = x_t - x \quad (3.1)$$

$$v = \frac{x_s}{t} \quad (3.2)$$

where:

t = time

3.2.2 Analysis Plots

In order to determine the trends and the effectiveness of the modified damper, a series of plots were created, for one compression cycle. Data for the plots were taken from the middle of each data set, ensuring that the shaft of the damper was up to speed for a given test run. All plots can be found in Appendix D.

3.2.2.1 Force - Velocity Plot

A plot displaying the hydraulic dampening force as a function of the shaft velocity was created, as shown in Figure 3.6. The graph made it possible to reveal the modified damper's effectiveness while illustrating how the dampening force is affected by the velocity. This plot is widely used in the automotive world to characterize damper perform. By plotting both the OEM and the modified data on the same graph for a given cycle frequency, a comparison could be easily made.

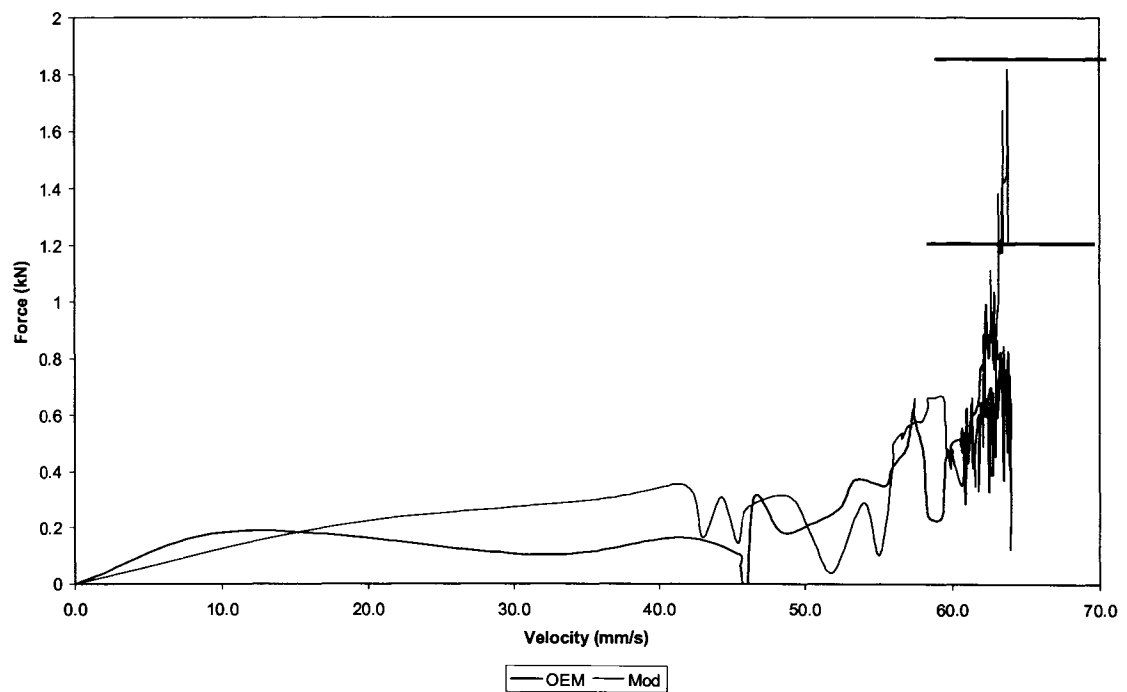


Figure 3.6 Sample of a Force -Velocity Plot

3.2.2.2 Force – Stroke Plot

The idea behind the modified damper is that it is dependent on stroke. A plot was created to illustrate the hydraulic dampening force as a function of stroke (Fig. 3.7). Similar to the previous force-velocity plots, the load-stroke plots also revealed the effectiveness of the modified damper.

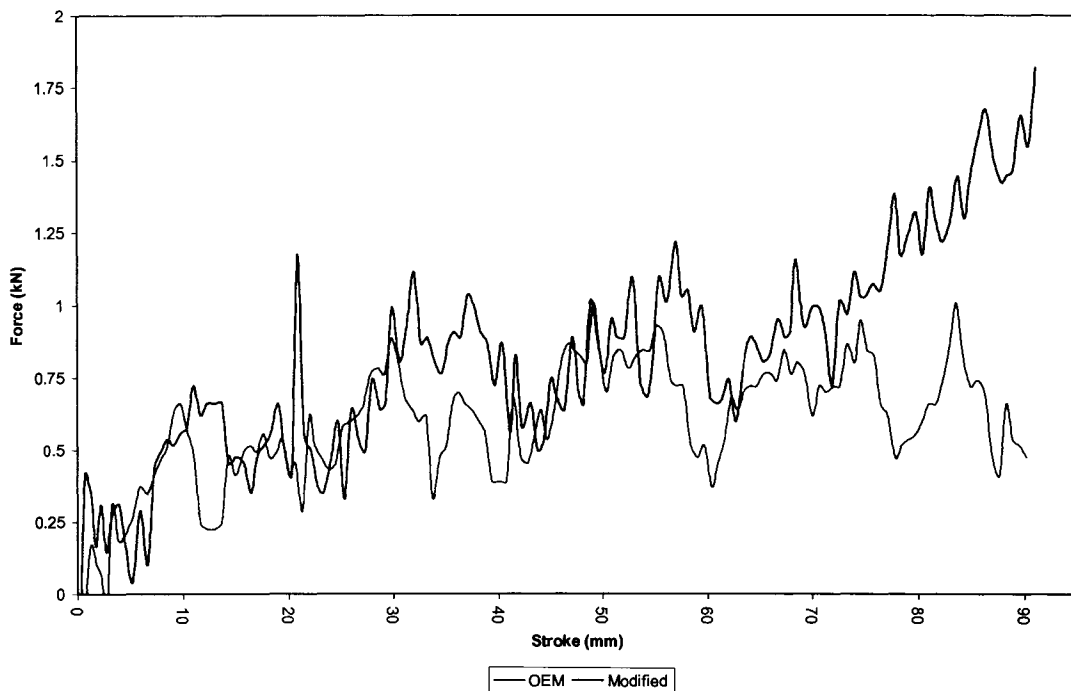


Figure 3.7 Sample of a Force-Stroke Plot

3.2.2.3 Pressure Differential

The dampening force calculated in the model was based on pressure differential (Eq. 1.16). In order to examine the relationship between the two a pressure-stroke plot was created. Both pressure A and B were plotted together on the same plot as illustrated in Figure 3.8. The distance between the two pressure curves represented the pressure differential. This analysis determined if dampening force is related to pressure differential.

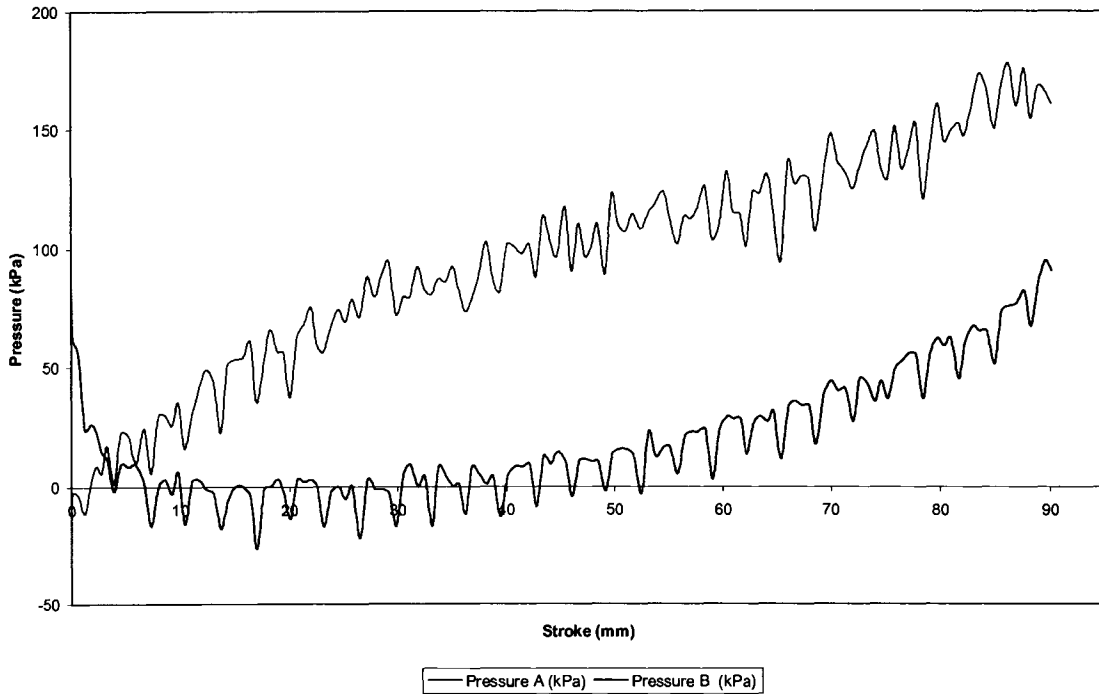


Figure 3.8 Example of Pressure Differential Plot

3.2.2.4 Model versus Test

A comparison of the numerical modeled data and the test results was done in order to determine the validity of the created dampening model. Because the model was a static analysis and the test was cyclic, a true comparison could not be made. In order for the model to be a cyclic type, the velocity had to be varied throughout its stroke, just as in testing where it accelerated to a maximum velocity. Instead of calculating the stroke in the model, the actual stroke data recorded from testing was input into the model, effectively making the model cyclic. The comparison of the test and modeled results are observed through force-stroke plots as shown in Figure 3.9.

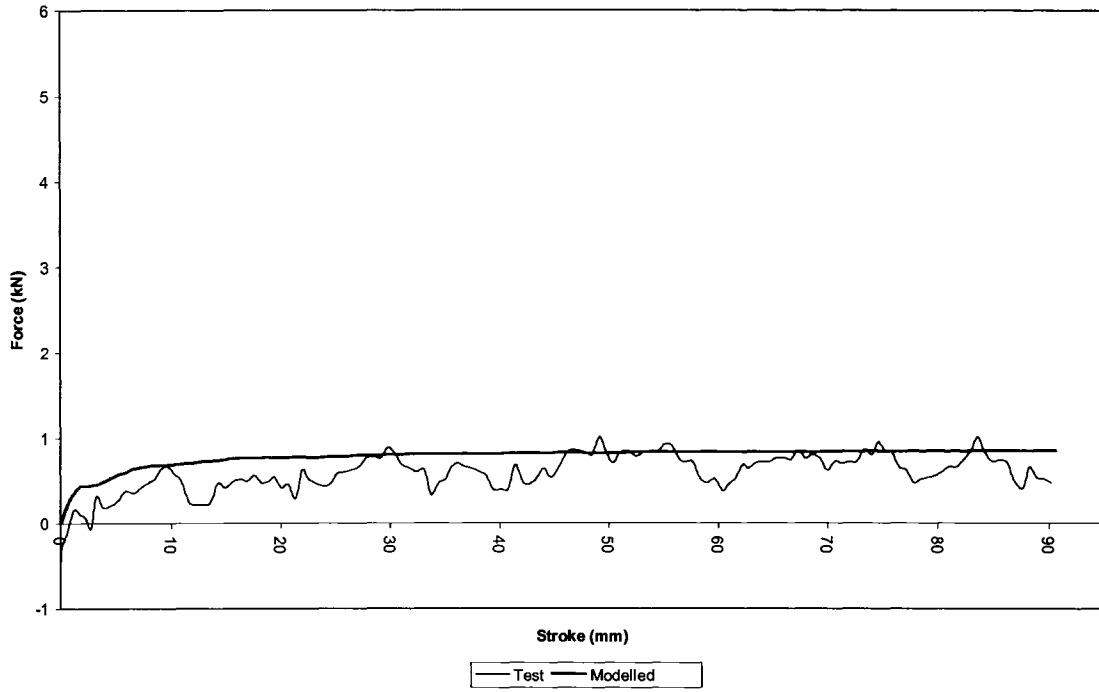


Figure 3.9 Example of Modeled versus Test

3.3 Discussion

Using the method described in the Section 3.2 to analyze and compare the data, an evaluation of the modified damper's performance was completed. The validity of the model was also evaluated analysis. The results and the success of the modified damper's ability to produce a greater dampening force are discussed below. Possible explanations for any divergence that was encountered during modeling and testing are also highlighted.

3.3.1 Force versus Velocity

Based on the analysis of the force-velocity plots, it was determined that the dampening force is dependent on the damper shaft velocity. It was observed that a greater shaft velocity results in a greater dampening force created by the damper. At a cycle frequency of 0.15 Hz, both the OEM and the modified damper approached the same amount of force throughout the stroke (Fig. 3.10). For cycles of 0.35 Hz and 0.70 Hz, both dampers produced similar forces until near the end of their stroke. At the end of the stroke, the modified damper spiked to a higher dampening force while the OEM damper remained constant (Fig.3.11). The difference between the characteristics of the dampening forces at the end of the stroke indicated that an additional factor affected the modified damper. The difference between the OEM and the modified dampening values, increased as the frequency cycle increased. For a cycle frequency of 0.35 Hz, a difference of 1 kN and at 0.7 Hz there was a difference of 2 kN between OEM and modified, respectively.

Figure 3.12 illustrates all three OEM curves for the different cycle frequencies. In the plot, the extension of the curves with each increase in frequency reflects the damper's shaft velocity increasing with an increase in cycle frequency. It is observed in the graph that the curves generated at 0.30 Hz and 0.70 Hz both overlapped and extended past the 0.15 Hz curve. At 0.15 Hz the maximum speed reached was 27 mm/s and generated a constant dampening force. Therefore, it is concluded that the dampening force is not affected by lower velocities. The shaft's velocity must be travelling at 45 mm/s or greater to really affect the dampening force, as shown by

the 0.35 Hz curve. The curve generated at 0.7 Hz did not exhibit an effect on the dampening force until a velocity of 90 mm/s. Ideally, the 0.7 Hz curve should follow and extend off of the 0.35 Hz curve. The difference from when the velocity began to affect the dampening force was attributed to an inadequate sampling rate during testing. At 0.35 Hz it took about 0.25 seconds to accelerate to 60 mm/s, whereas for a cycle frequency of 0.7 Hz it only took 0.02 second. For 0.35 Hz, twenty-five readings were taken for 0 to 60 mm/s, whereas for 0.7 Hz only two readings were recorded for the same interval. Because the 0.7 Hz curve was created from only two points, there is obviously a lower accuracy. In addition, since the change between 0-60 mm/s happened nearly instantaneously, the load cell was not sensitive enough to detect the changes in that time. Hence, the 0.7 Hz curve has a zero slope at the beginning.

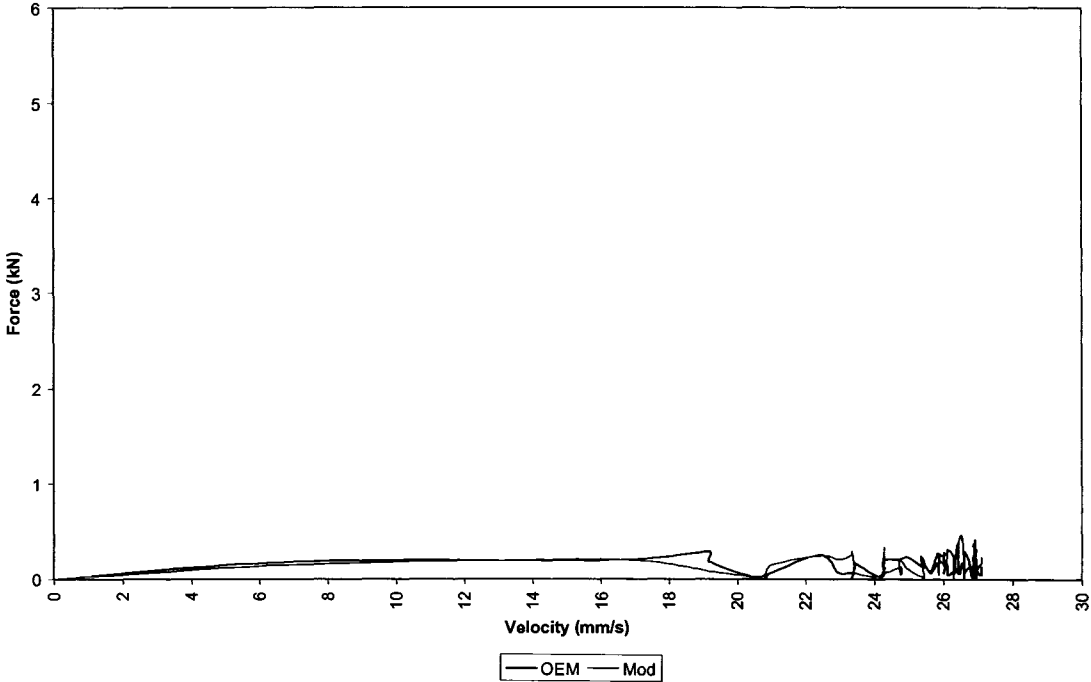


Figure 3.10 Dampening Force at 0.15 Hz

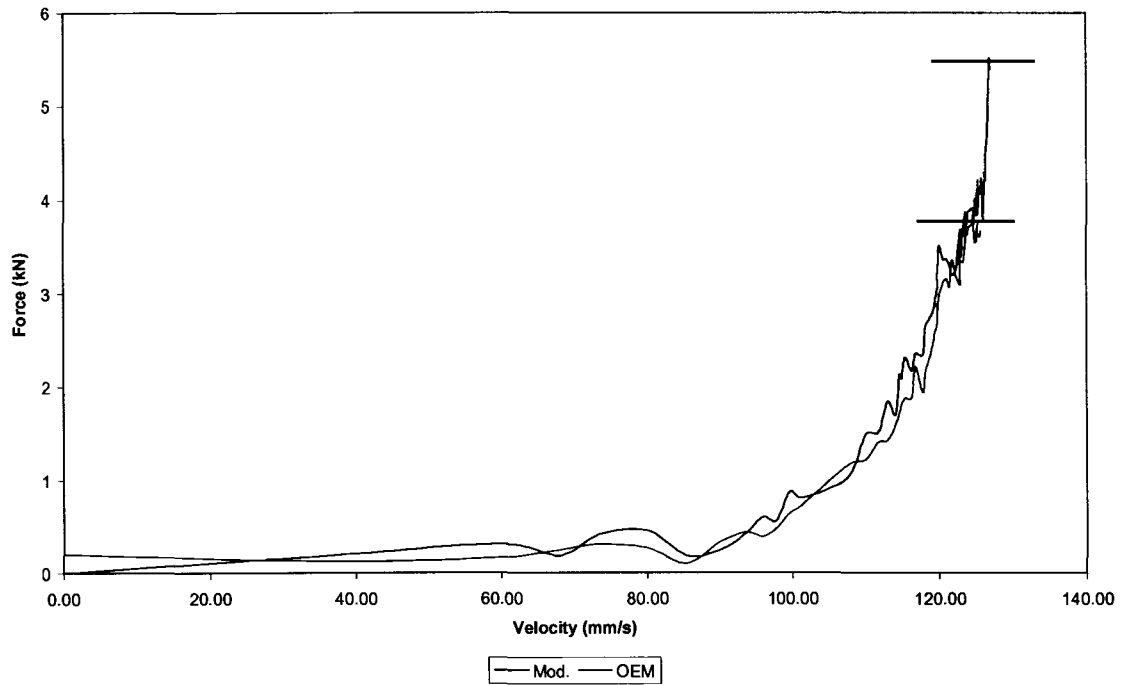


Figure 3.11 Dampening Force at a High Velocity at 0.7 Hz

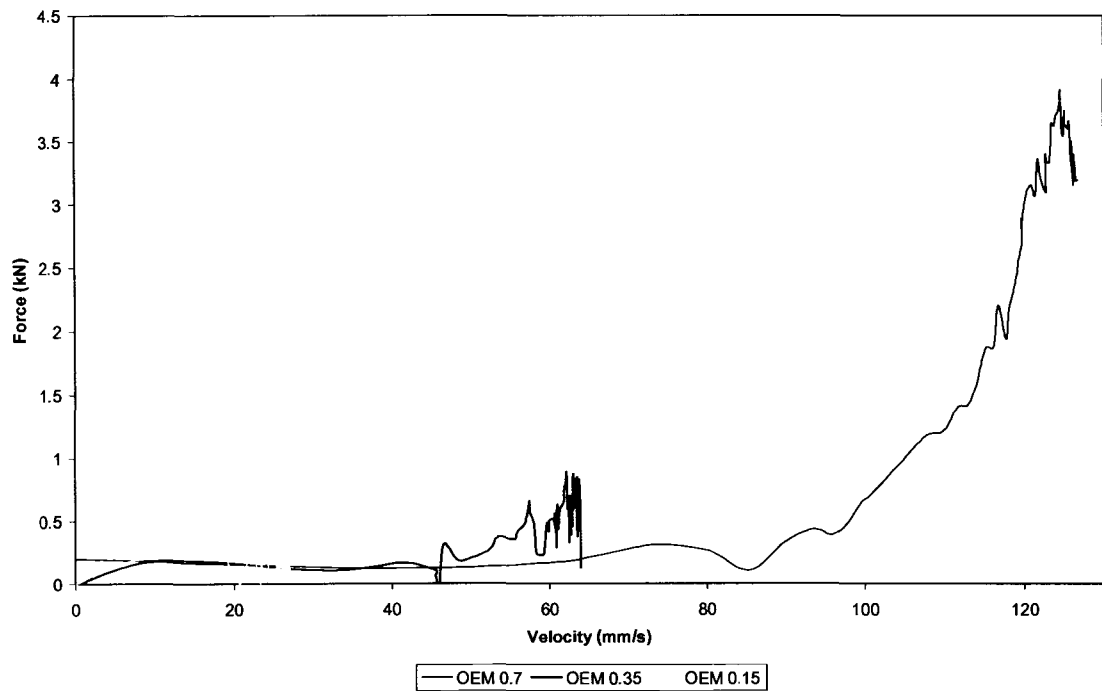


Figure 3.12 OEM Force vs. Velocity Curves

3.3.2 Force versus Stroke

The analysis of the force-stroke plots shows that the OEM and the modified design curves follow a similar trend to the force-velocity plots. Again, a slow cyclic frequency of 0.15 Hz resulted in little difference between the OEM and modified units (Fig. 3.13). Velocities, less than 45 mm/s, were too slow to effect dampening regardless of the stroke position.

For the OEM damper, the dampening force increased at the start of the stroke and then remained constant for the remainder of the stroke (Fig. 3.14 and 3.15). Because the orifice area was constant throughout the stroke, the OEM damper was not dependent on the stroke. It can be observed in figure 3.16 that it took about 20 mm and 40 mm of stroke to reach maximum velocity for 0.35 Hz and 0.7 Hz, respectively. The maximum dampening force is also reached at 10 mm and 35 mm of stroke displacement for 0.35 and 0.7 Hz, respectively. Therefore, the shape of the OEM curve was only influenced by the velocity of the damper's shaft.

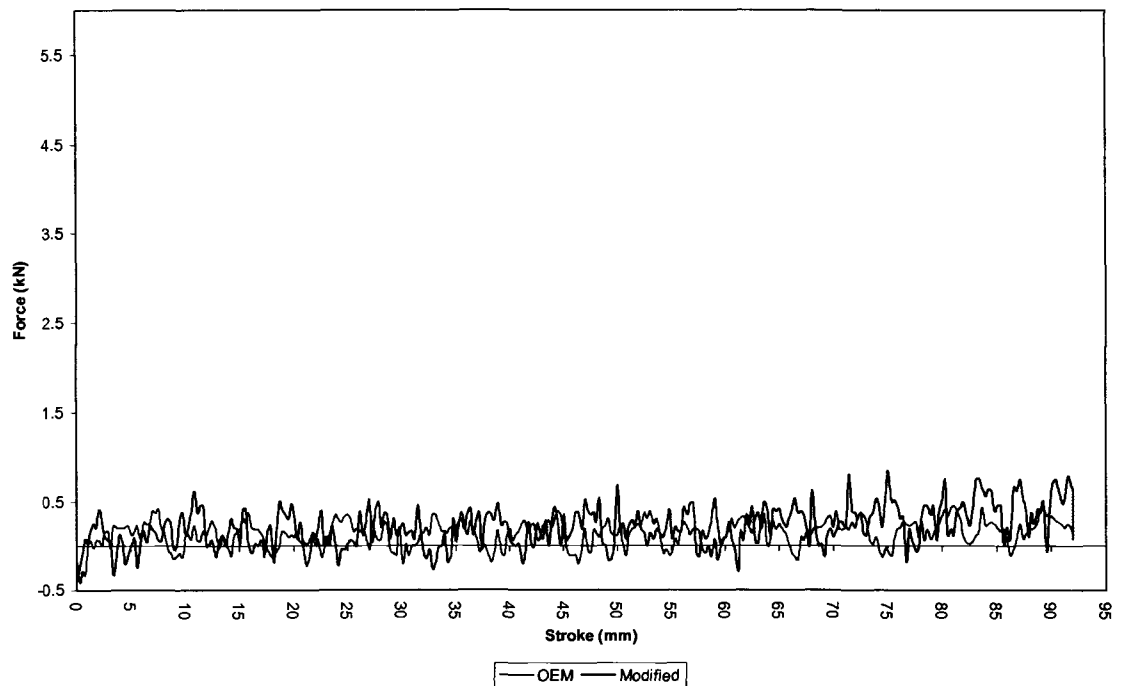


Figure 3.13 Dampening Force at 0.15 Hz

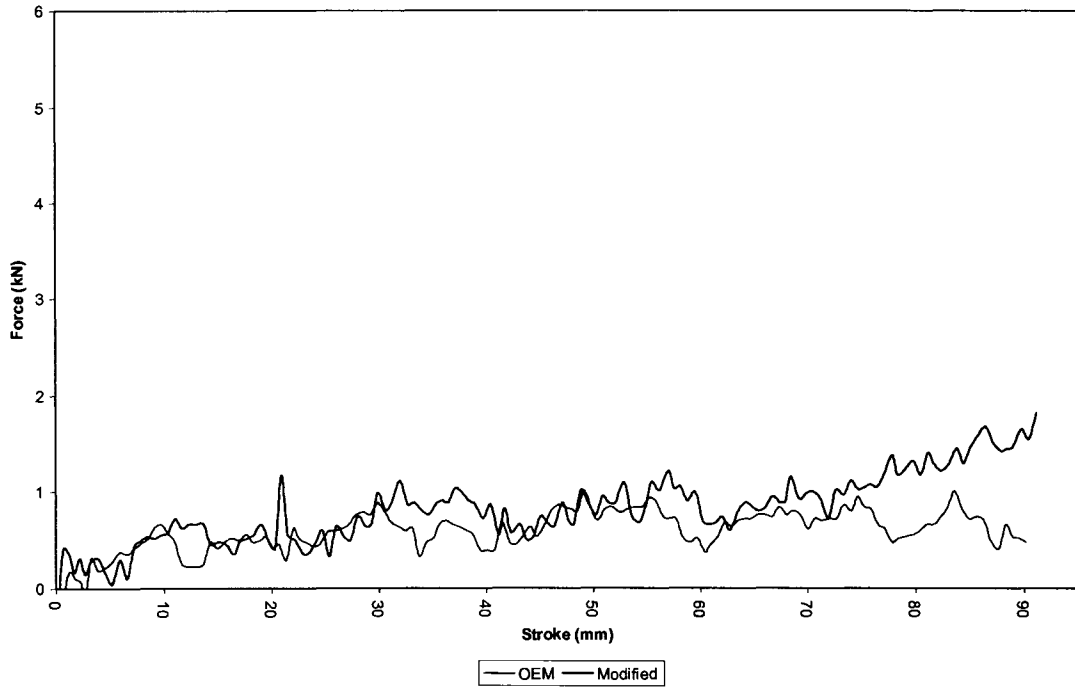


Figure 3.14 Dampening Force at 0.35 HZ

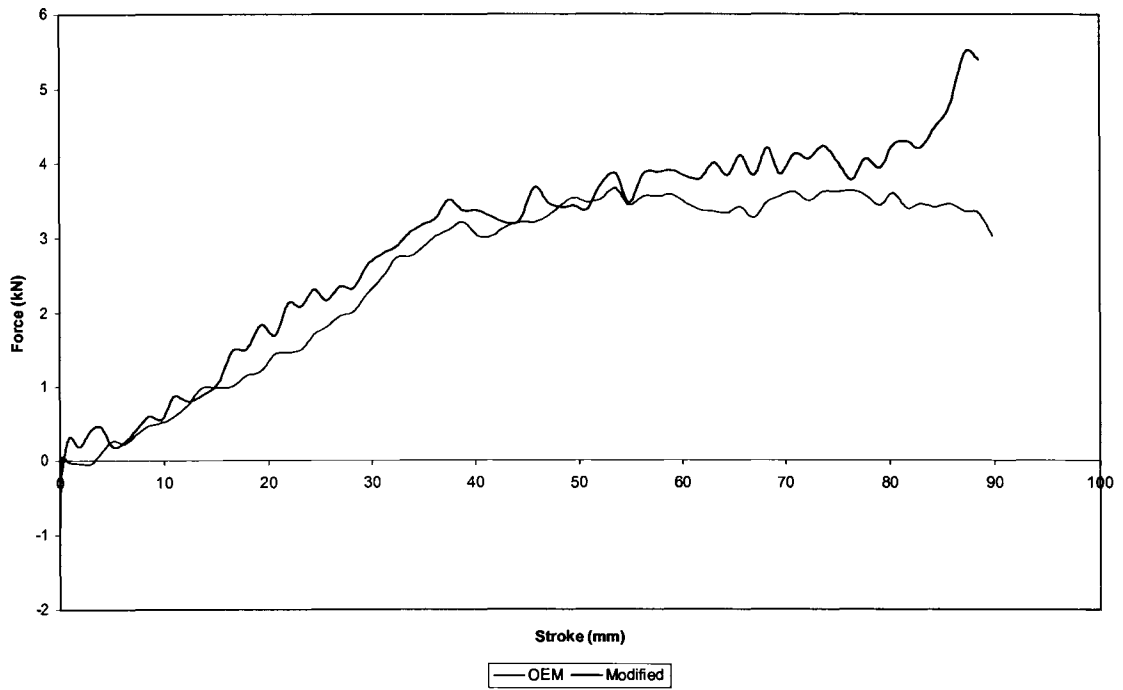


Figure 3.15 Dampening Force at 0.7 Hz

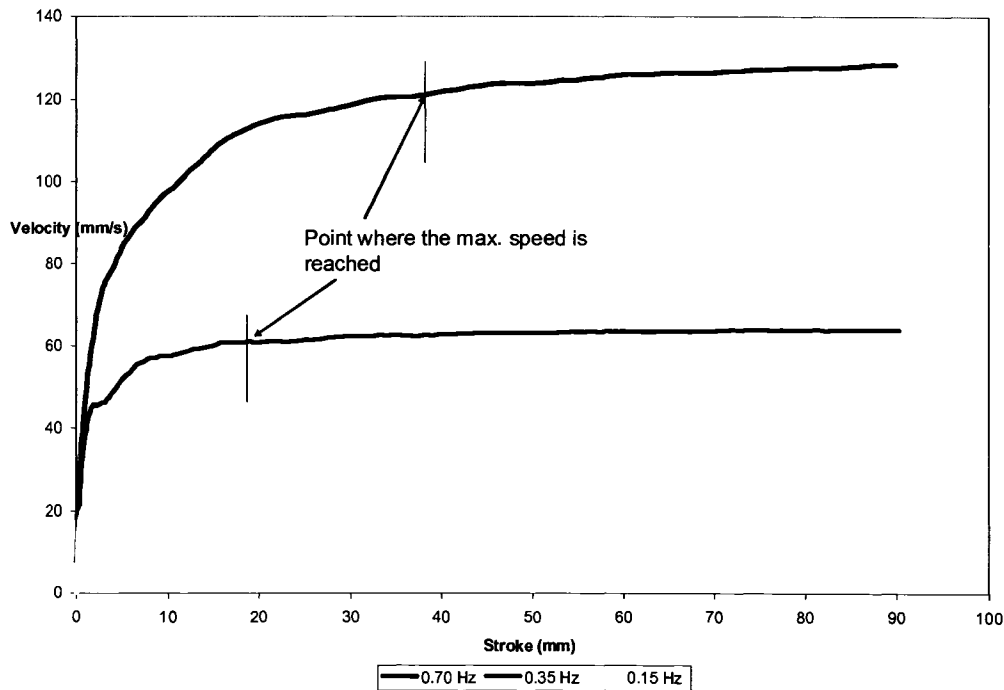


Figure 3.16 Velocity Versus Stroke Plots

For the modified damper a similar trend to the OEM was followed, except for the last 1/6th of the stroke length. During the last part of stroke length, the dampening force suddenly increased even though the velocity was constant as shown in Figures 3.14 and 3.15. Therefore, it was concluded that the modified damper was dependent not only the velocity, but also the stroke position. The variable orifice area was responsible for the modified damper's dependency on the stroke. Figure 3.17 displays the relationship between the orifice area and stroke. As the damper is compressed, the stroke displacement increases and the orifice area is reduced. The variable orifice area of the modified damper matches the orifice area of the OEM damper at about 75 mm of stroke. This is the point where modified damper curve starts to diverge from the OEM curve. The reason behind the similarity of the OEM and the modified damper curves when the stroke less than 75 mm is that the OEM orifice area is smaller than the modified damper's variable orifice. Therefore, the dampening force is more influenced by the original OEM orifice. When the stroke is greater than 75mm, the modified damper's variable orifice area is less than the OEM orifice area. The smaller orifice area restricts the movement of fluid, which causes the dampening force to

increase. As the damper shaft velocity increased, the divergence between the OEM and modified curve also increased.

The area under the curve in the force-stroke (Figs. 3.13 to 3.15) curves represents the energy absorbed by the damper. The modified damper produced a larger area than the OEM damper for both 0.35 and 0.7 Hz. Therefore, the modified damper is able to absorb and dissipate more energy. As a result, the modified damper has a greater ability to handle higher levels of shock loading.

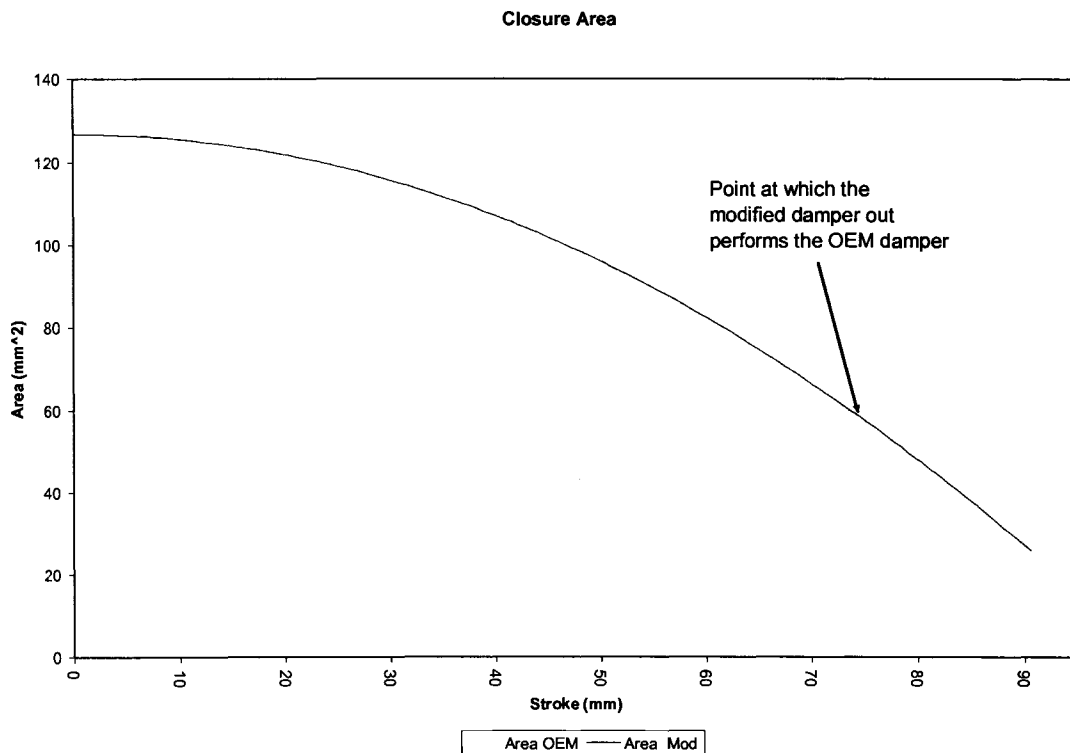


Figure 3.17 Orifice Opening Vs. Stroke

3.3.3 Pressure Differential versus Stroke

The analysis of the pressure differential-stroke plot showed that the overall pressure differential is greater as the cycle frequency is increased. When comparing the OEM to modified, it was observed that the modified had a greater pressure differential, except at low cycle frequencies. At 0.15 Hz, there a small pressure

differential value for both the OEM and modified. For the OEM damper at 0.35 and 0.7 Hz, the pressure differential remains constant once a constant velocity has been reached (Fig.3.18). For the modified damper, a large increase in pressure differential occurs just after 75 mm of stroke (Fig.3.19). Overall, the results of the pressure-stroke analysis coincide with the results from the force-displacement analysis. Therefore, it is concluded that the dampening force is dependent on the pressure differential created within the damper.

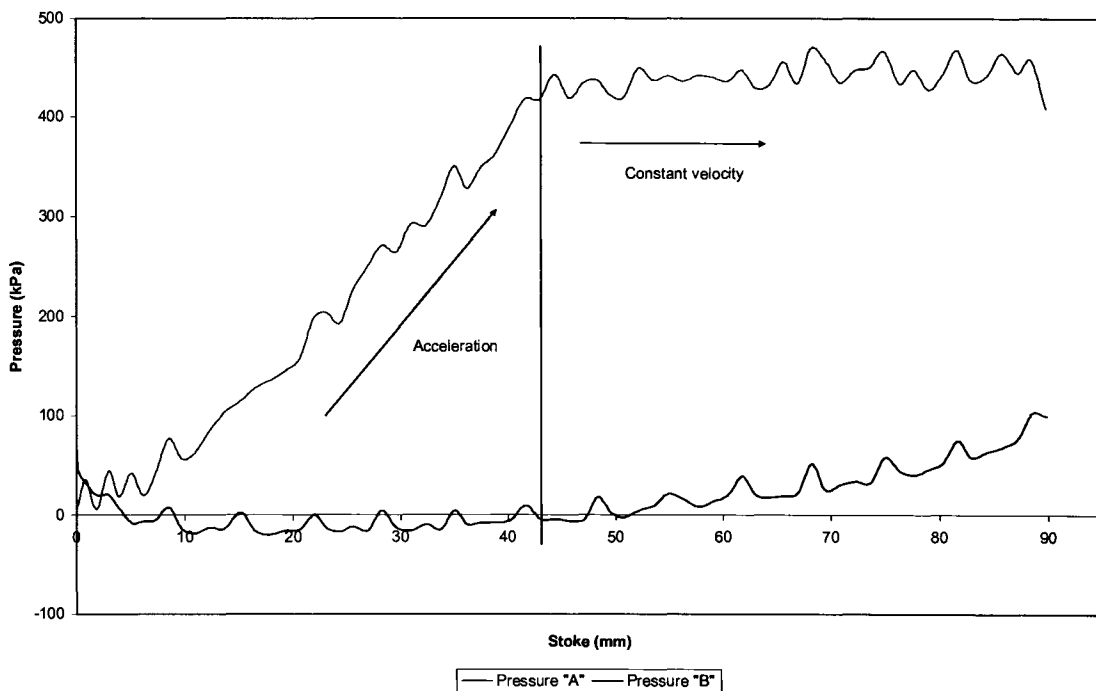


Figure 3.18 Pressure Differential at 0.7 Hz (OEM)

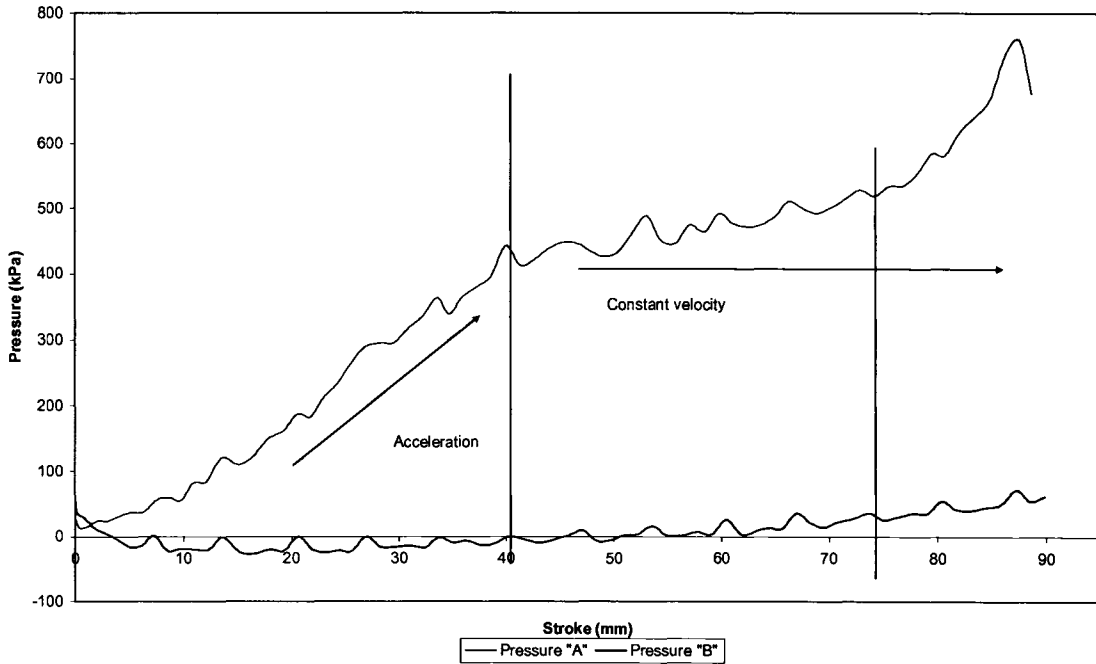


Figure 3.19 Pressure Differential at 0.7Hz (Modified)

3.3.4 Model versus Test data

The damper design was based on the modeled results, thus both the modeled and test results follow a similar trend for a given cycle. Examining the plots for the three different cycle frequencies led to the conclusion that the greater the cycle frequency the more the model and test values correlated. At 0.15 Hz the both test and the modeled were constants (Fig. 3.20). However, the test results values were greater than the model. At 0.35 and 0.7 Hz, both the modeled and the test curves had similar trends, except for the start of the stroke (Fig. 3.21).

Using the force-stroke data for both modeled and test, a regression analysis was performed to determine the coefficient of regression, R^2 . The plots of the regression analysis are found in Appendix E. Table 3.4 summarizes the R^2 values obtained from the regression analysis. It can be concluded based on the results from the regression analysis that the model appears only valid at higher frequency cycles when the R^2 value is greater than 0.85. At lower frequency cycles the model is not

representative of the physical testing, but does show the trend of the modified damper.

	OEM Damper	Modified Damper
0.15 Hz	0.0709	0.0803
0.35 Hz	0.565	0.7602
0.70 Hz	0.828	0.8921

Table 3.4 Regression Analysis Results – R² Values

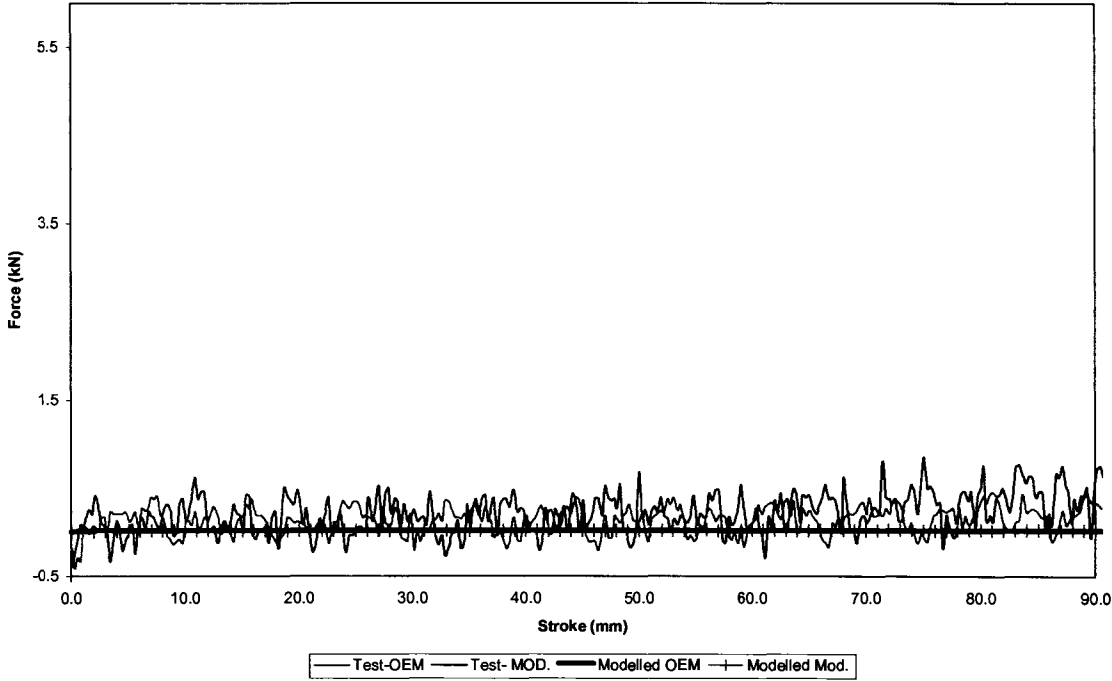


Figure 3.20 Modeled versus Test Data at 0.15 Hz

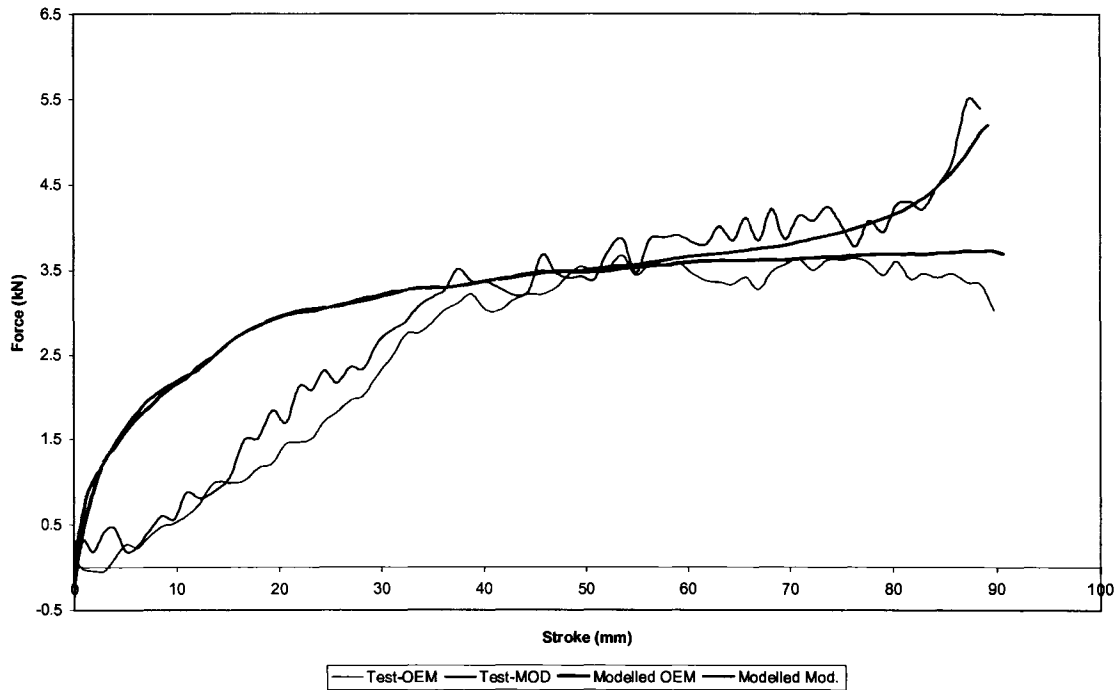


Figure 3.21 Modeled versus Test Data at 0.7 Hz

3.3.5 Full Scale Prediction

A Caterpillar 789B rear suspension damper was selected to be modeled. Prediction of a full scale truck damper was done with the computer model. In order to illustrate the true effectiveness of the metering pin concept, the computer model was slightly altered to calculate the g force acting on the damper and to incorporate the effects of the gas spring (Appendix F). G force is a comparative measurement of the acceleration applied to a body with respect to gravity. It is calculated by the following equation:

$$g \text{ force} = \frac{F_{total}}{w_{truck}} \quad (3.3)$$

Where:

w_{truck} = the effective weight of the truck resting on a damper

In order to predict the dampening characteristics, the truck's damper parameters were input into the computer model. Table 3.5 summarizes Caterpillar's 789B suspension damper parameters. Detailed design drawings of the damper can be found in Appendix G.

Inner shaft diameter	275 mm
Piston diameter	360 mm
Inside Height of shaft	476 mm
Outer shaft diameter	318 mm
Inner tube diameter	361 mm
Total stroke	165 mm
Orifice diameter	7 mm
Ball check valve diameter	12.5 mm
Fluid density	912 kg/m ³
Fluid Viscosity	4.20E-4 Ns/m ²
Initial Pressure	1275 kPa

Table 3.5 789B Suspension Damper Parameters

The g force value was calculated at a point where the damper was almost fully compressed for a given velocity. The calculation of the g force at almost full compression results in the maximum force that the damper can be exposed to without bottoming out. The g force was calculated over a range of velocities (0-1 m/s). Figure 12.4 compares the threshold g force values at the various velocities. For a full scale OEM damper, dampening is dependent solely on velocity. As the plot shows, the g force threshold increased as the velocity increased. The small change in g force signifies that the OEM damper will easily bottom out at moderate to fast speeds. For the modified damper, both the velocity and the stroke affected the dampening characteristics of the damper. As a result, the g force threshold is greater for the modified damper as in Figure 3.22. This increase will reduce the occurrence of the bottoming out.

Analysis has proven the effectiveness of the metering pin and plate concept in reducing the occurrence of bottoming out. From the model, the full scale modified damper is shown to handle up to 16% more loading before bottoming out than the OEM, which is dependent on the velocity and position in the stroke (Fig. 3.23).

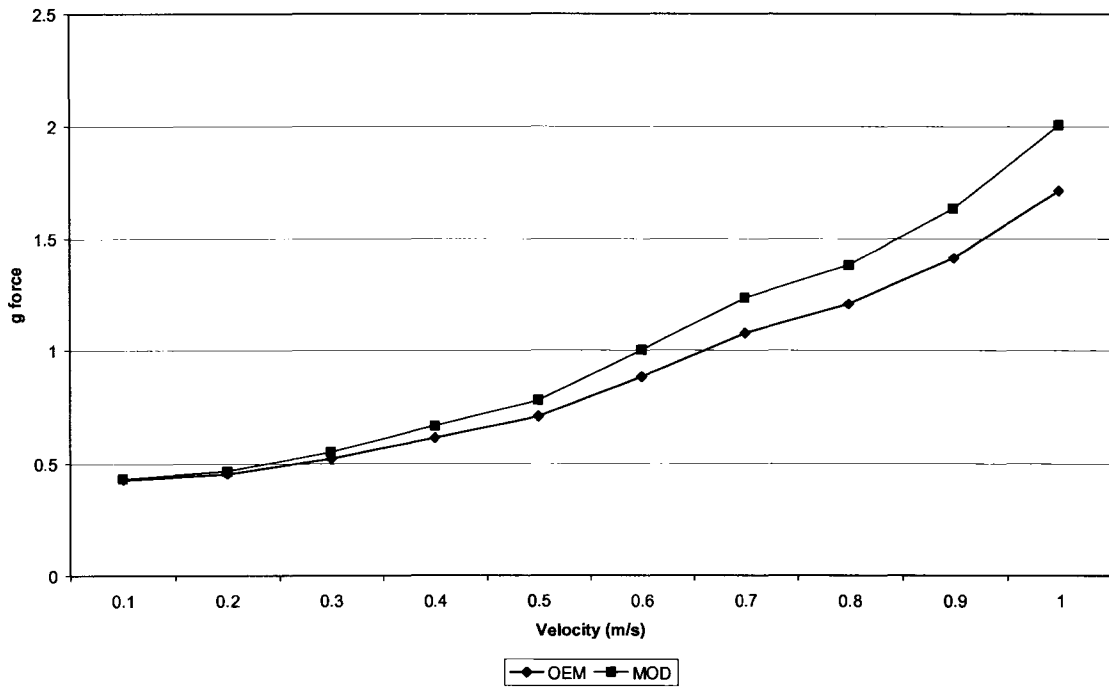


Figure 12.13 Threshold g-force Values

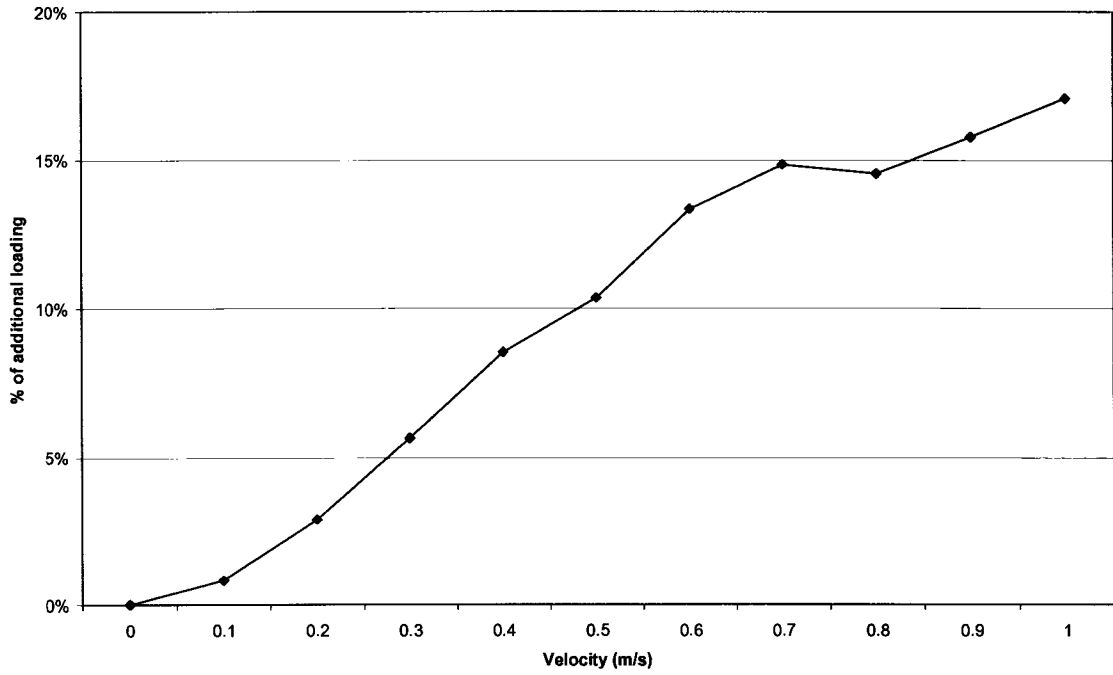


Figure 12.14 Modified Damper Improved Performance

CHAPTER 4 Conclusions and Recommendations

It has been shown from previous field observation and work that the bottoming out phenomenon occurs numerous times during a typical cycle. The repeated shock loading due to bottoming out reduces the life of the truck's components resulting in down time and lost productivity. Another problem caused by bottoming out is the vibration experienced by operators, which can result in spinal injury. It was determined in the above research work that the dampening effect was the weak link in the current OEM system causing bottoming out. Current dampers for ultra class trucks have the same design as those used in haulers for over 50 years, classified as "simple" dampers, which have merely increased in geometric size with increase in hauler payload capacity. It was apparent that the simple dampers were an out-dated design that did not provide adequate performance for present day sized units. A modification was proposed to improve the damper's dampening characteristics so that it was able to handle the greater loading, especially in adverse mining conditions where the compounding motion effects from haul road profiles lead to multiple g increases in the effective load on the suspension units. Through the literature research it was found that the simplest and most cost effective way to improve the damper was to control the flow of fluid within it. The conceptual idea was to change the existing damper with a metering pin and plate arrangement that was mechanically simple enough to be introduced as a retrofit in the field rather than a complete design change that would require the OEM to re-tool in the manufacturing process. The new arrangement would create a variable orifice to control the flow causing the dampening force to increase.

The project was separated into two parts. The first half involved creating a computer model to determine the baseline performance of a scaled down version of the OEM damper. Several iterations of the model were then completed to determine the parameters of the scaled modified damper. The second part of the project involved performing a cyclic test to both scaled OEM and modified dampers. The test was done using a testing frame arrangement similar to a shock dynamometer. The results

of both the computer model and the physical test were then analyzed. The findings of which are listed below:

- The concept of the metering pin and plate did increase the dampening force to reduce the effects of shock loading.
- The OEM damper was only dependent on the vertical velocity of the damper's shaft. As the velocity increased the dampening force also increased. The exception to this relationship is at low velocities. It was determined that the velocity had to be greater than 45 mm/s to affect the dampening force.
- The modified damper is dependent on both the velocity and the stroke. At 75mm of stroke, the area of the variable orifice is equal to the area of the equivalent OEM orifice. Also, 75mm of stroke was the point where the performance of the modified damper improved over the OEM damper, as should be expected. The increase in dampening force is a result of the restriction of fluid flow.
- The area under the curve in the force-stroke curves represents the energy absorbed by the damper.
- The differential pressure within the damper is proportionally related to the dampening force produced.
- The regression analysis showed that only at higher velocities was the computer model valid.

Overall the project was successful in showing that a modification to an existing OEM damper can reduce the occurrence of the bottoming out and reduce the level of high adverse g loading. The significance to the mining industry is the cost savings in applying a retrofit approach to the suspension system, rather than opting for an expensive new system. With less occurrence of bottoming out, the truck's components should not fail prematurely due to shock loading, which would result in less down time and less maintenance cost. Also, the operator would be less likely to suffer exposure to dangerous levels of shock vibration.

Although this project has accomplished its goals, further testing is required in order to fully implement the modification to an ultra class truck. Before doing a full scale test, it is recommended that computational fluid dynamics (CFD) software be used to accurately model the damper. The new model should include the rebound stroke, which will determine if the new modification will present a problem during the rebound phase. The model should also model the various ground conditions. For full scale testing, it is recommended that additional sensors be placed to monitor the dampers, rather than just rely on the truck's existing on-board monitoring system for information. The sensors should measure the stroke displacement and velocity of the damper; therefore giving a better picture of what the suspension is doing during a cycle. One final suggestion is to monitor the ride quality of the truck with modified dampers.

REFERENCES

- Anon. 1994. FAR Part 25 Airworthiness Standards: Transport Category Airplanes. Federal Aviation Administration, Washington, DC.
- Bastow, D. 1980. *Car Suspension and Handling*. Pentech Press, London.
- Cambiaghi, D., Gadola, M., and Vetturi, D. 1998. *Suspension System Testing and Tuning with the Use of a Four-post Rig*. SAE Technical Paper Series 983023.
- Caterpillar, 2001, Systems Operation 789 Truck Suspension Cylinder. Caterpillar Inc., SEN3436.
- Caterpillar, 2002, *Caterpillar Performance Handbook*. 2nd ed., Caterpillar Inc., Peoria, Illinois.
- Caterpillar 2006. *797B Off-Highway Truck*. Caterpillar Inc., SEBP4221-87.
- Chai, S.T. 1996. *Landing Gear Integration in Aircraft Conceptual Design*. Virginia Polytechnic Institute and State University Blacksburg, Virginia, 24061-0203.
- Chalasani, R.M. 1986. *Proceedings, Symposium on Simulation and Control of Ground Vehicles and Transportation System*. AMD-Vol.80, DSC-Vol.2, American Society of Mechanical Engineers, pp.187-204.
- Chalasani, R.M. 1986. *Ride Performance Potential of Active Suspension Systems-PartIII: Comprehensive Analysis Based a Full-Car Model*. Proceedings, Symposium on Simulation and Control of Ground Vehicles and Transportation System. AMD-Vol.80, DSC-Vol.2, American Society of Mechanical Engineers, pp.205-226.
- Curry, N.S. 1998. *Aircraft Landing Gear Design: Principles and Practices*. AIAA Education Series, Washington.
- El-Sayed, M. 2003. *Suspension Systems in Large Mining Trucks*. M.Eng. Thesis, University of Alberta, Edmonton.
- Furesz, F., Harkay, G., Lucas, J. 1988. *Fundamentals of Hydraulic Power Transmission*. (I.K. Dulay Ed.) Elsevier Science Pub. Co., New York New.
- Garrett, T.K., Newton, K., and Steeds, W. 1996. *The Motor Vehicle*. 2nd ed. Butterworth-Heinemann, Jordan Hill, Oxford.
- Gillespie, T.D. 1992. *Fundamentals of Vehicle Dynamics*. Society of Automotive Engineers Inc, Warrendale, PA.
- Goodsell, D. 1989. *Dictionary of Automotive Engineering*. Butterworths, London.

- Hanley, P. 2004. *What is a Shock Dynamometer?* Retrieved Sept. 5, 2005 from <http://www.roehrigengineering.com/cart/techinfo/techpgdynos.htm>.
- Pettitt, J. 1999. *High Performance Honda Builder's Handbook*. Cartech, Inc., North Branch, MN.
- Miller, A. 2002. Testing a Formula SAE Racecar on a Seven-Poster Vehicle Dynamics Simulator. SAE Technical Paper Series 2002-01-3309.
- Motta, D.S., Zampieri, D.E., and Pereira, A.K. 2000. *Optimization of a Vehicle Suspension Using a Semi-Active Damper*. SAE Technical Paper Series 2000-01-3304.
- Roehrig Engineering, 2005. Retrieved Dec. 20, 2006 from <http://www.roehrigengineering.com/cart/home.php?cat=1>.
- Petek, N.K. 1992. Shock Absorber Uses Electrorheological Fluid. *Automotive Engineering*.
- Thede, P. 1996, *High-speed vs. Low-speed*. Retrieved July 7, 2005, from http://www.sportrider.com/tech/146_9612_tech/.
- Thede, P. 2005. *Beyond Nuts and Bolts*. Retrieved July 7, 2005, from http://www.sportrider.com/tech/146_9602_tech/.
- Wong, J.Y. 1993. *Theory of Ground Vehicles*. 2nd ed, John Wiley & Sons Inc., New York, NY.
- Young, D.F., Munson B.R., and Okiishi, T.H. 1997. *A Brief Introduction to Fluid Mechanics*. John Wiley & Sons, Inc., New York, NY.

APPENDICES

APPENDIX A
Computer Model

Input

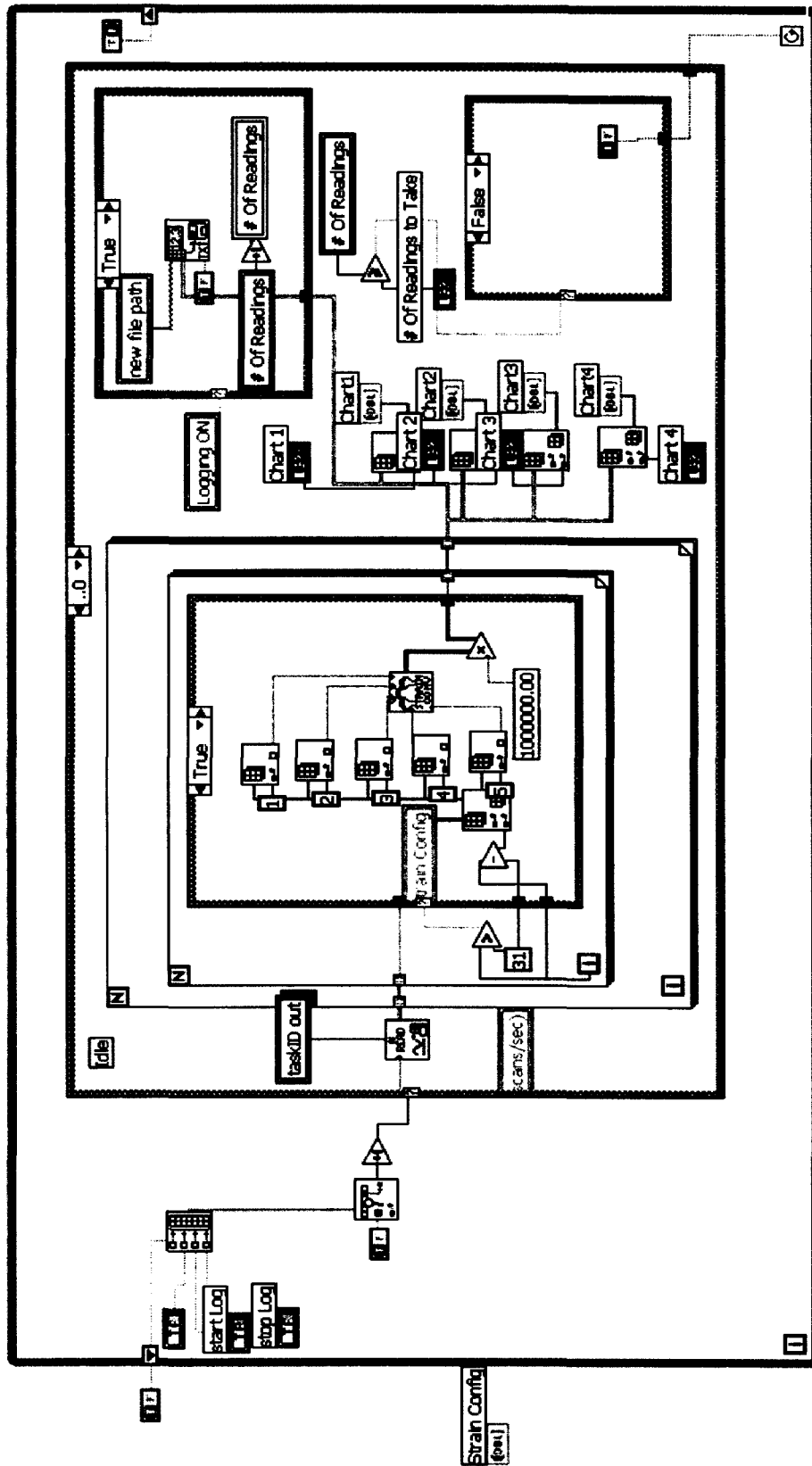
Internal Dimension	
Inner shaft diameter	0.0381 m
Inside height	0.1397 m
Piston diameter	0.1014 m
Cylinder diameter	0.1016 m
Orifice diameter	0.004 m
Total stroke	0.1016 m
Fluid Parameter	
Density	912 kg/m ³
Viscosity	0.042 Ns/m ²
Velocity (m/s)	

Time	Stroke (m)	V ₂	Vol.total	V ₁	1/R _t	Q	ΔP	Hydraulic Damping
0	0	0	0.001956	0.001956	0	0	0	0
0.01	0.006	4.18E-05	0.001949	0.001908	7.18E-13	1.75E-05	6083878	48883.57929
0.02	0.012	8.36E-05	0.001943	0.001859	7.18E-13	1.75E-05	6083878	48883.57929
0.03	0.018	0.000125	0.001936	0.00181	7.18E-13	1.75E-05	6083878	48883.57929
0.04	0.024	0.000167	0.001929	0.001762	7.18E-13	1.75E-05	6083878	48883.57929
0.05	0.03	0.000209	0.001922	0.001713	7.18E-13	1.75E-05	6083878	48883.57929
0.06	0.036	0.000251	0.001915	0.001664	7.18E-13	1.75E-05	6083878	48883.57929
0.07	0.042	0.000293	0.001908	0.001616	7.18E-13	1.75E-05	6083878	48883.57929
0.08	0.048	0.000334	0.001902	0.001567	7.18E-13	1.75E-05	6083878	48883.57929
0.09	0.054	0.000376	0.001895	0.001519	7.18E-13	1.75E-05	6083878	48883.57929
0.1	0.06	0.000418	0.001888	0.00147	7.18E-13	1.75E-05	6083878	48883.57929
0.11	0.066	0.00046	0.001881	0.001421	7.18E-13	1.75E-05	6083878	48883.57929
0.12	0.072	0.000502	0.001874	0.001373	7.18E-13	1.75E-05	6083878	48883.57929
0.13	0.078	0.000543	0.001867	0.001324	7.18E-13	1.75E-05	6083878	48883.57929
0.14	0.084	0.000585	0.001861	0.001275	7.18E-13	1.75E-05	6083878	48883.57929
0.15	0.09	0.000627	0.001854	0.001227	7.18E-13	1.75E-05	6083878	48883.57929
0.16	0.096	0.000669	0.001847	0.001178	7.18E-13	1.75E-05	6083878	48883.57929
0.17	0.102	0.000711	0.00184	0.001129	7.18E-13	1.75E-05	6083878	48883.57929
0.18	0.108	0.000752	0.001833	0.001081	7.18E-13	1.75E-05	6083878	48883.57929

Modeling of the Scaled Version of the Damper

APPENDIX B

LabView Algorithm Wiring Diagram

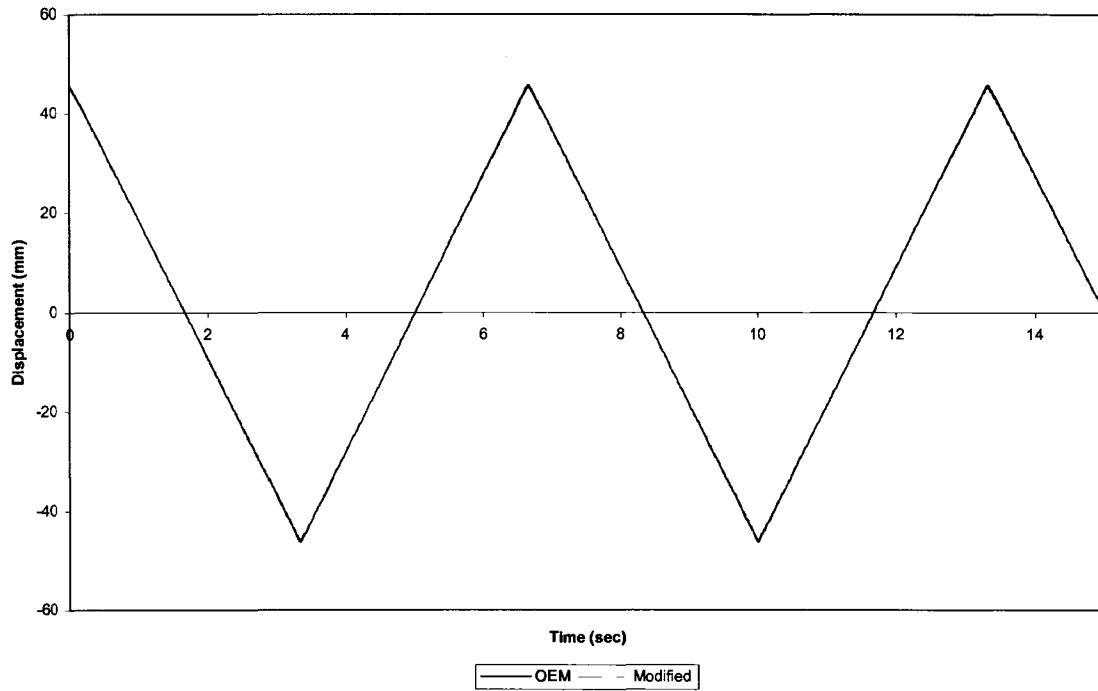


APPENDIX C

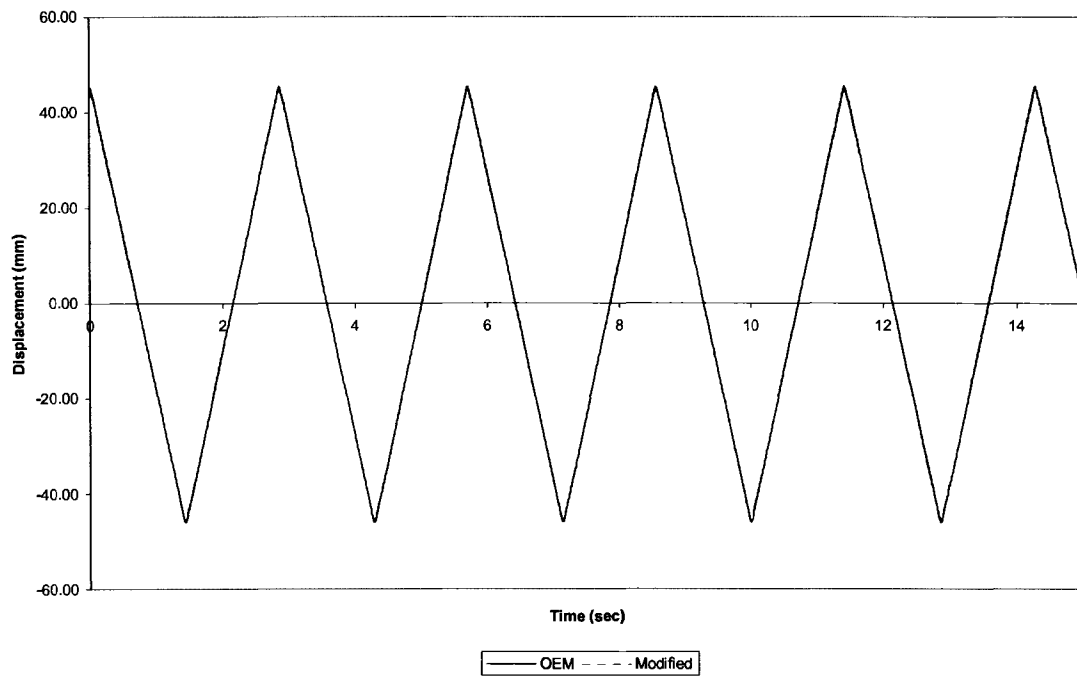
Raw Data Plots

Displacement Plots

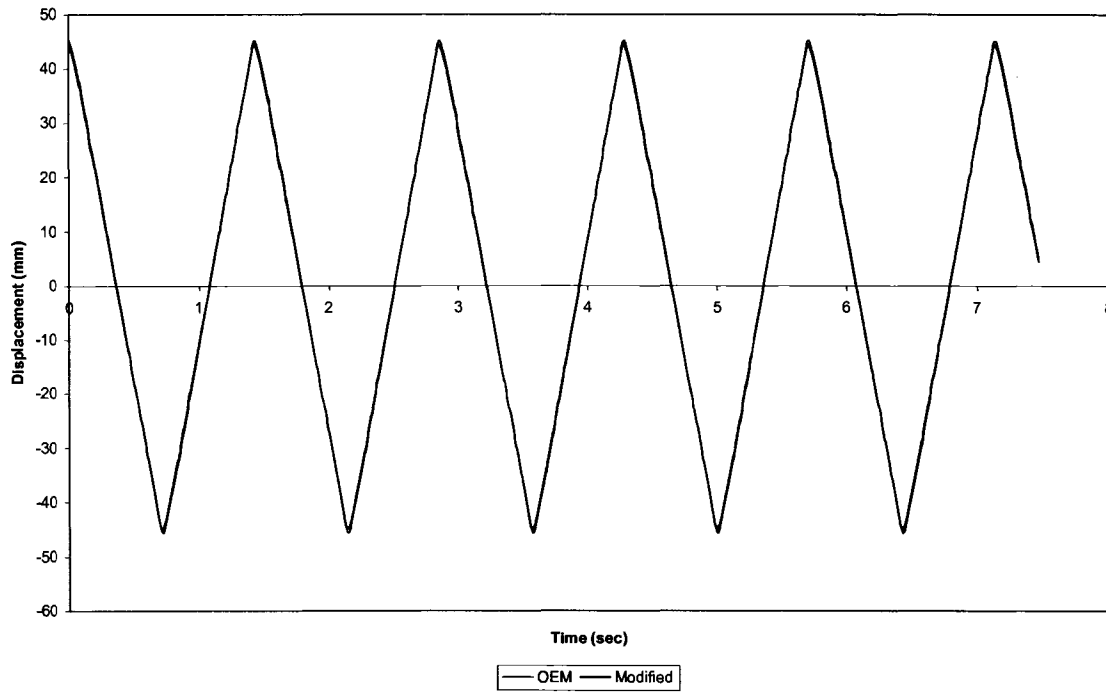
Shaft Displacement @ fq 0.15



Shaft Displacement @ fq 0.35

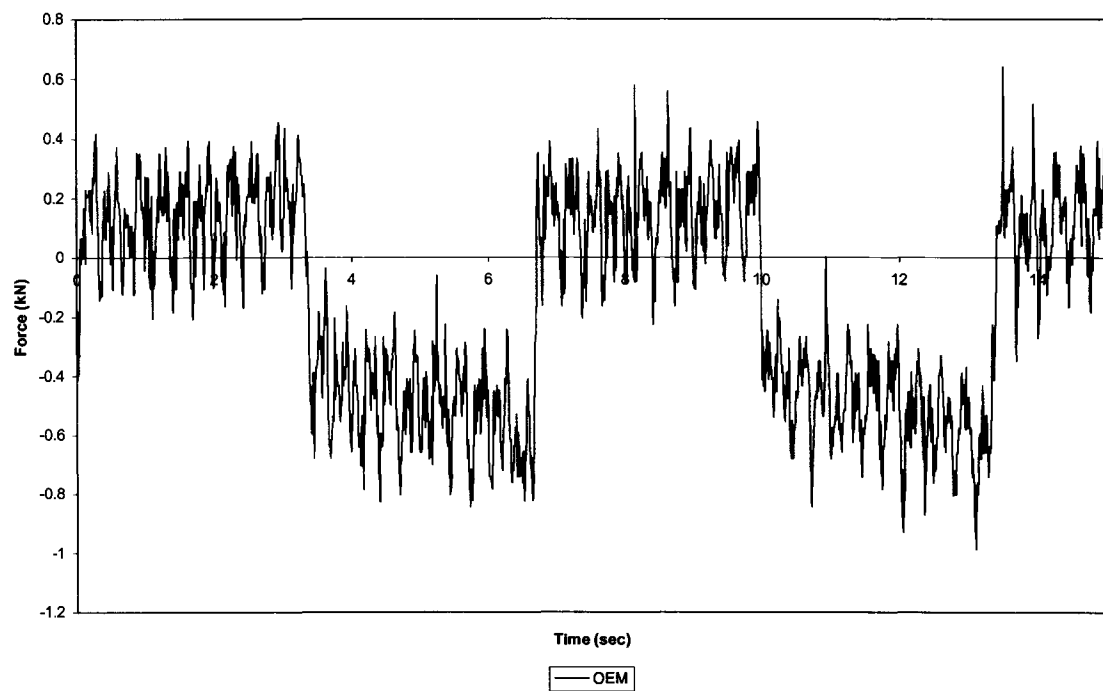


Displacement @ fq 0.7

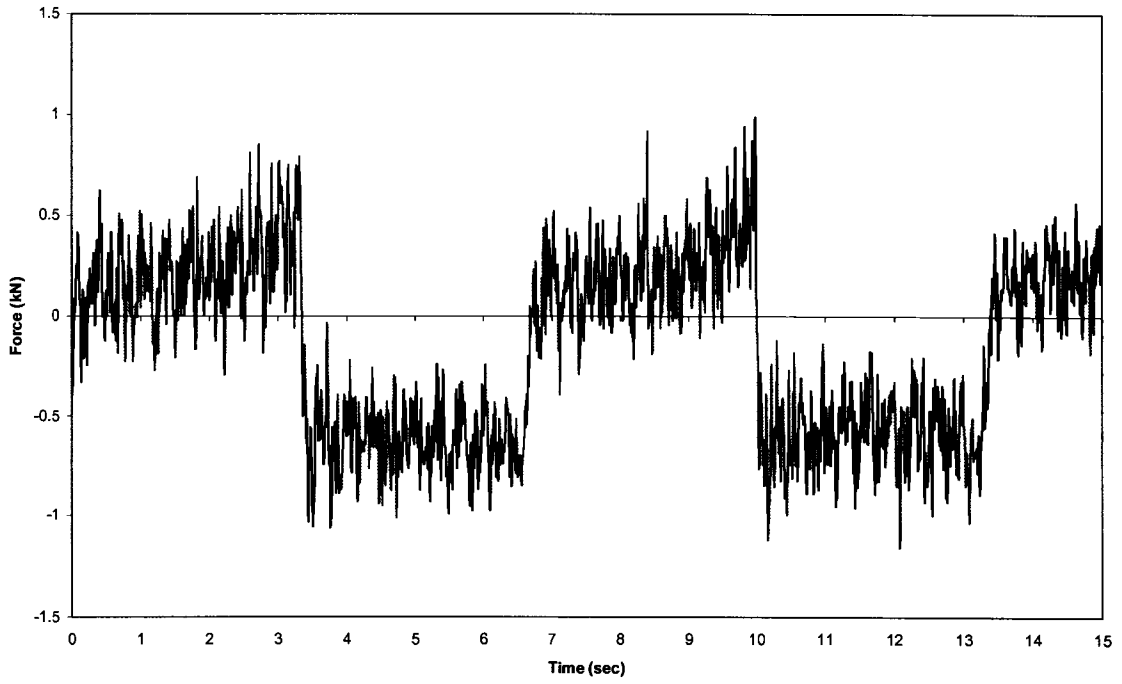


Hydraulic Dampening Plots

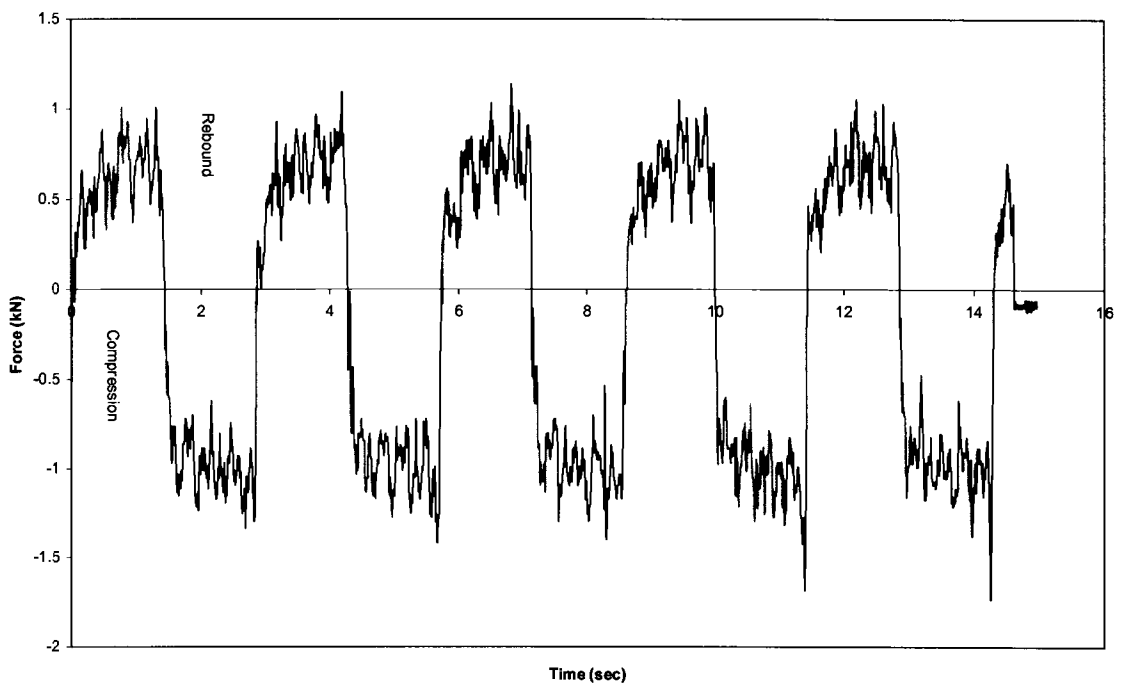
Hydraulic Damping Force @ fq 0.15 (OEM)



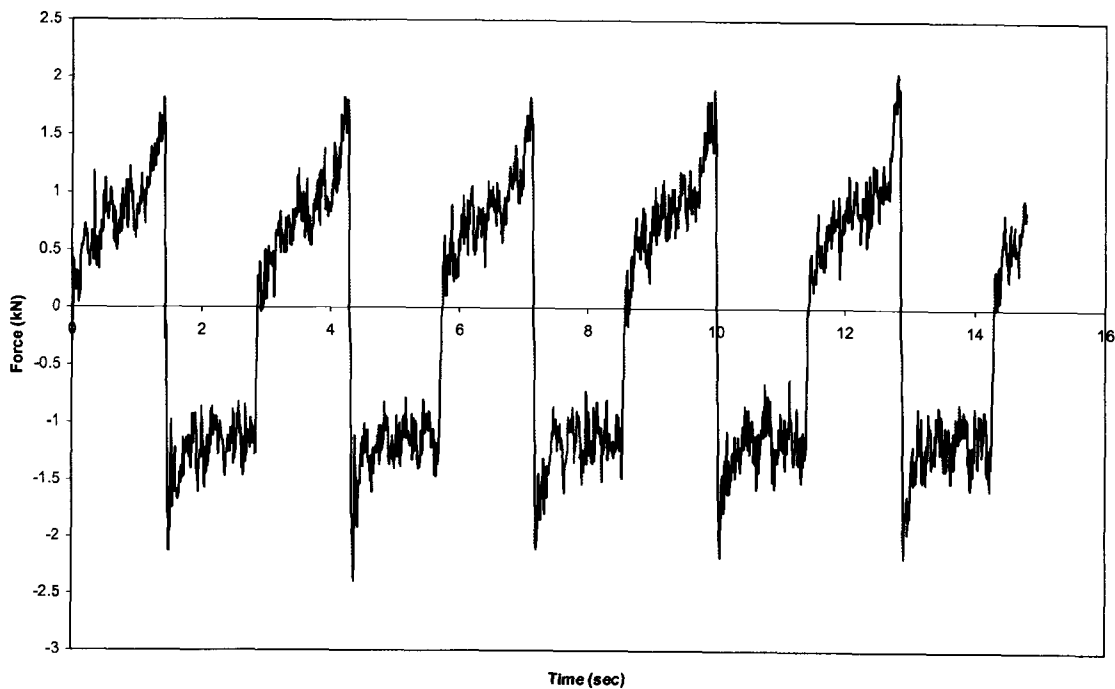
Hydraulic Damping Force @ fq 0.15 (Modified)



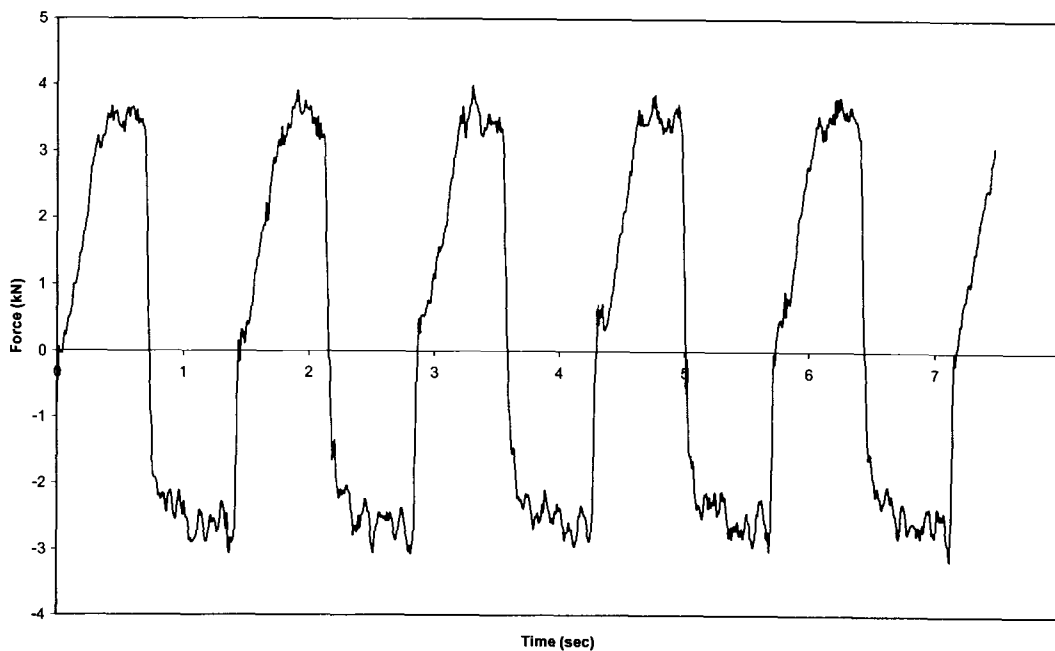
Hydraulic Damping Force @ fq 0.35 (OEM)



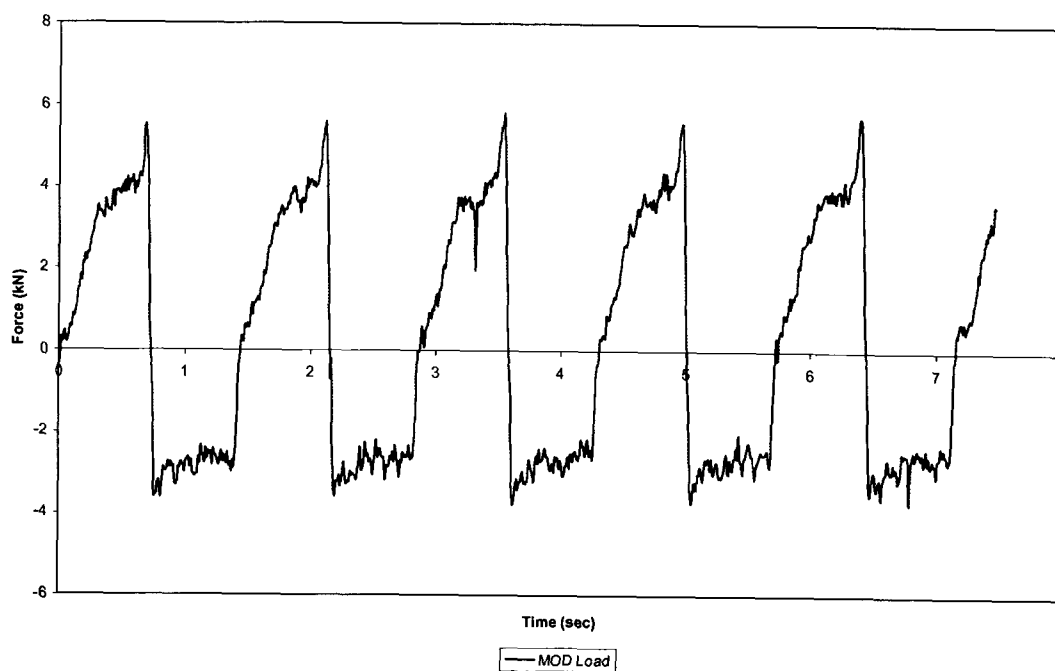
Hydraulic Damping Force @ fq 0.35 (Modified)



Damping Force @ fq 0.7(OEM)

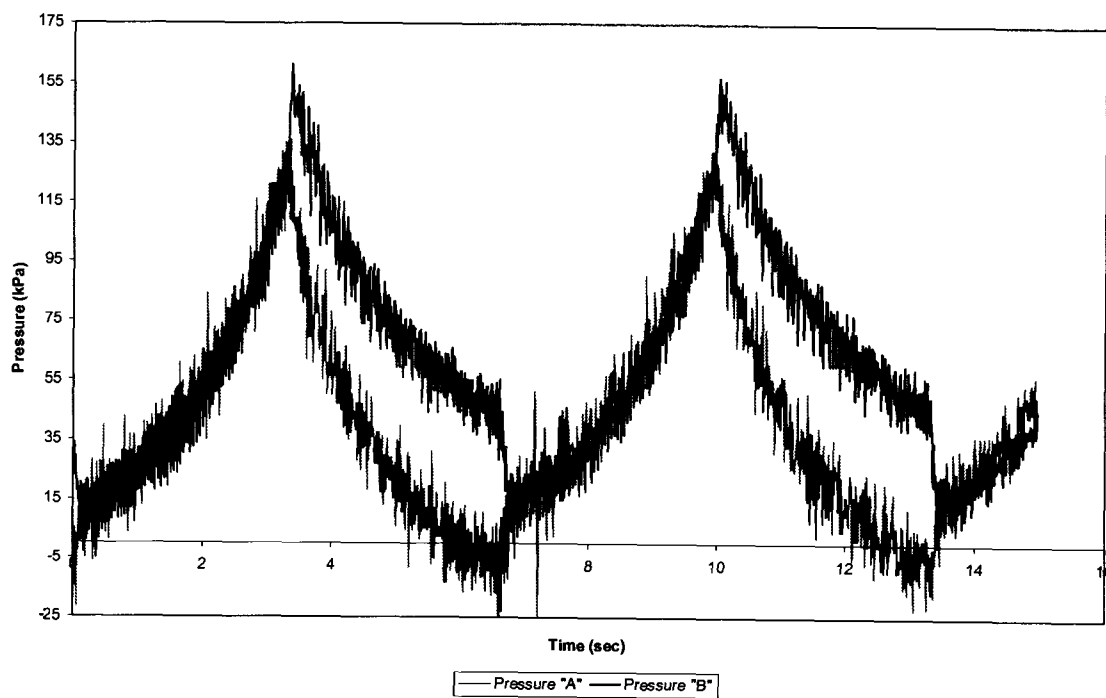


Damping Force @ fq 0.7 (Modified)

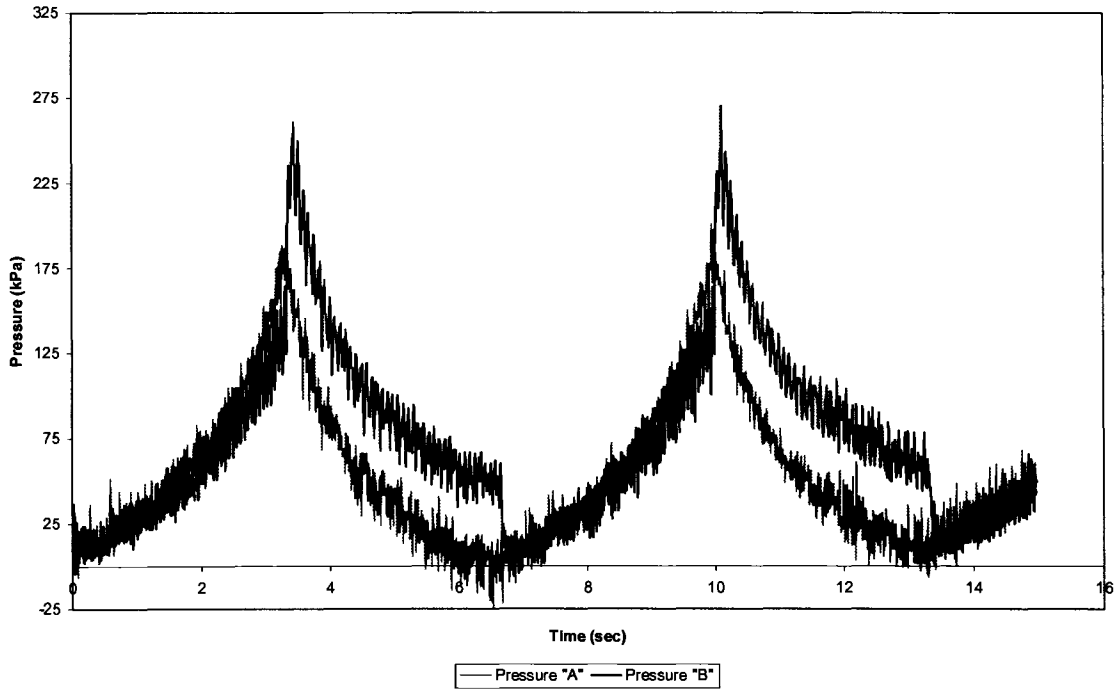


Pressure Plots

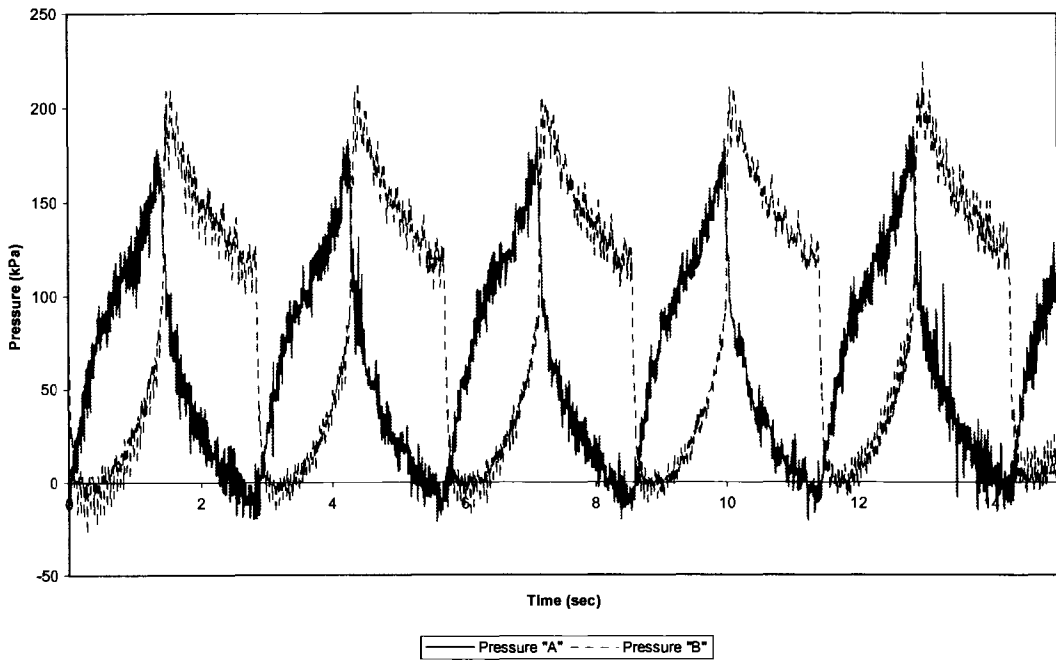
Pressure @ fq0.15 (OEM)



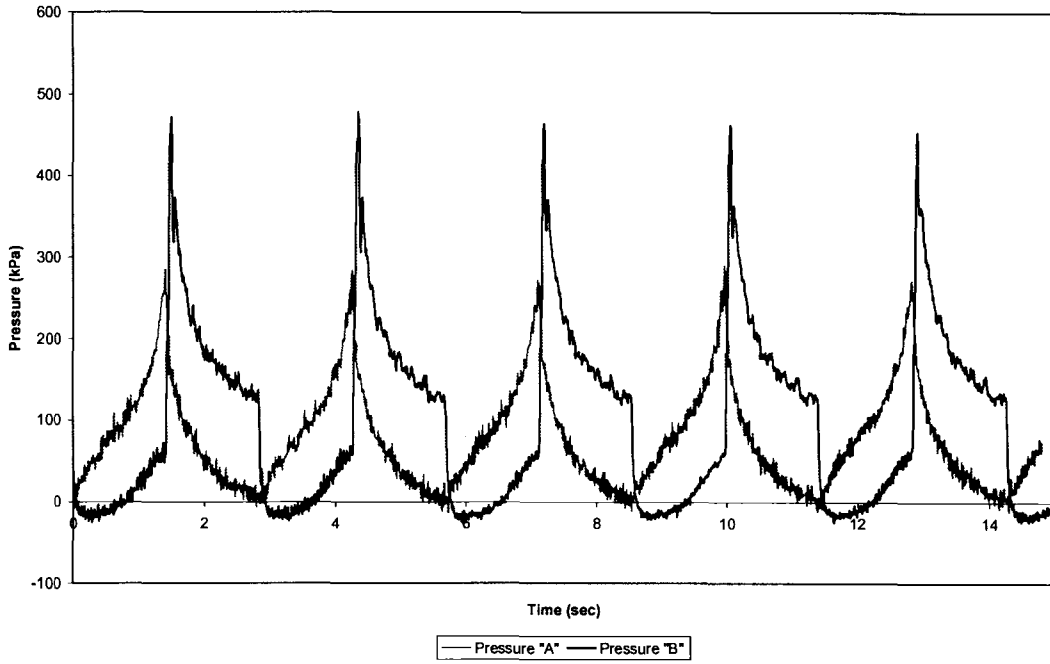
Pressure @ fq0.15 (Modified)



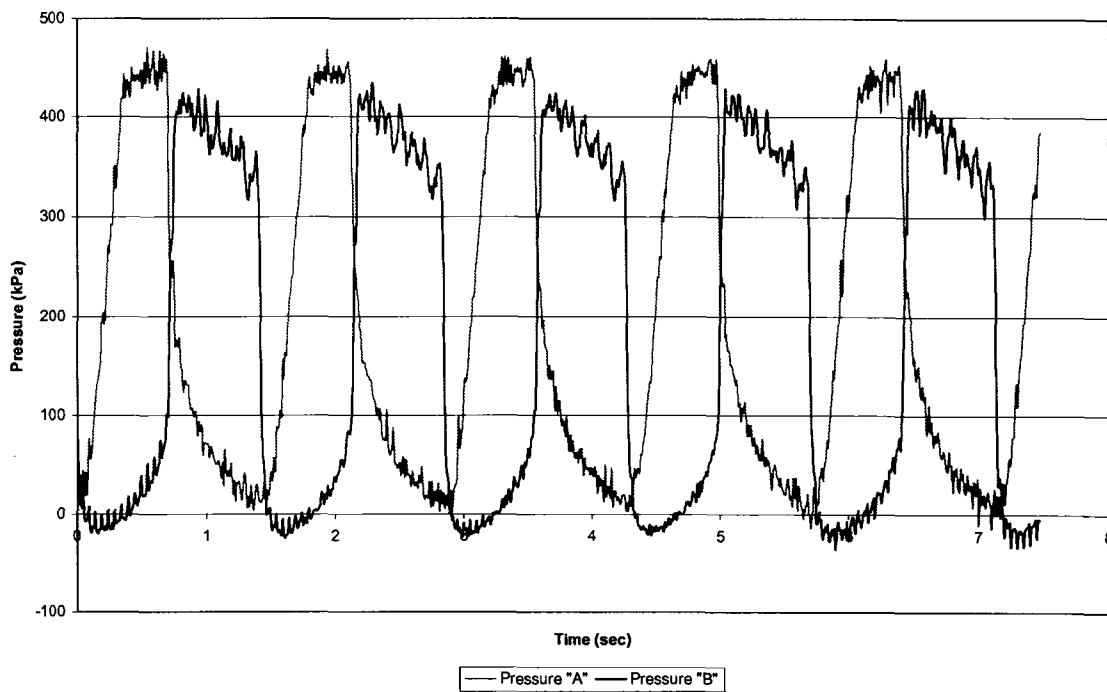
Pressure at fq 0.35 (OEM)



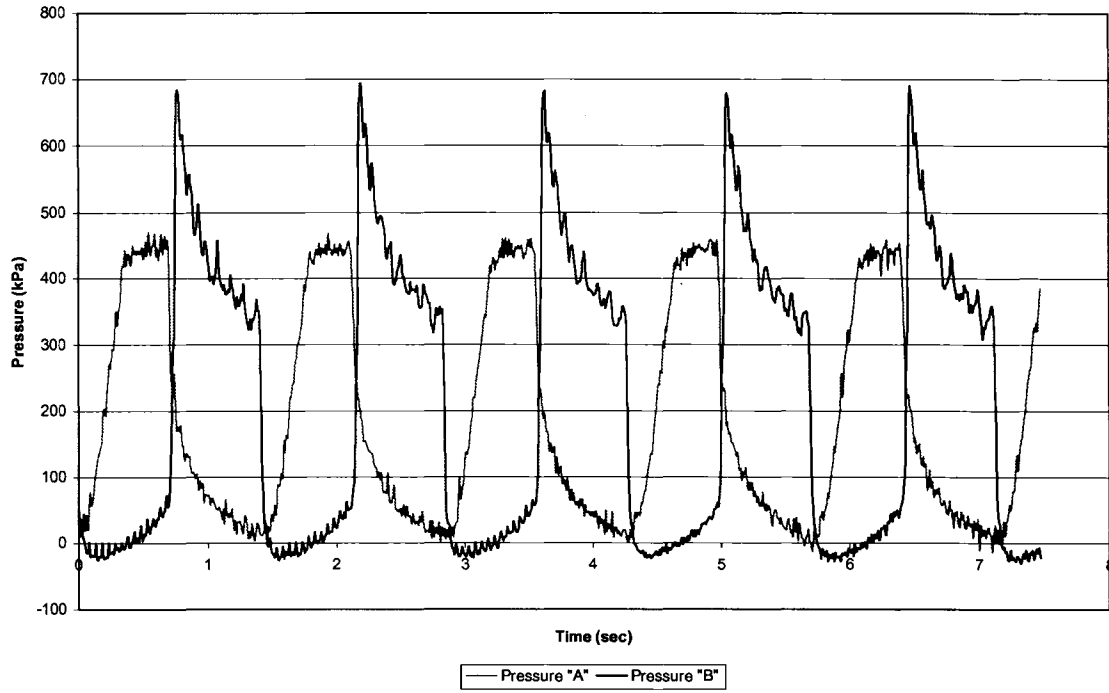
Damper Pressure @ fq 0.35 (Modified)



Pressure @ fq 0.7 (OEM)



Pressure @ fq 0.7 (Modified)

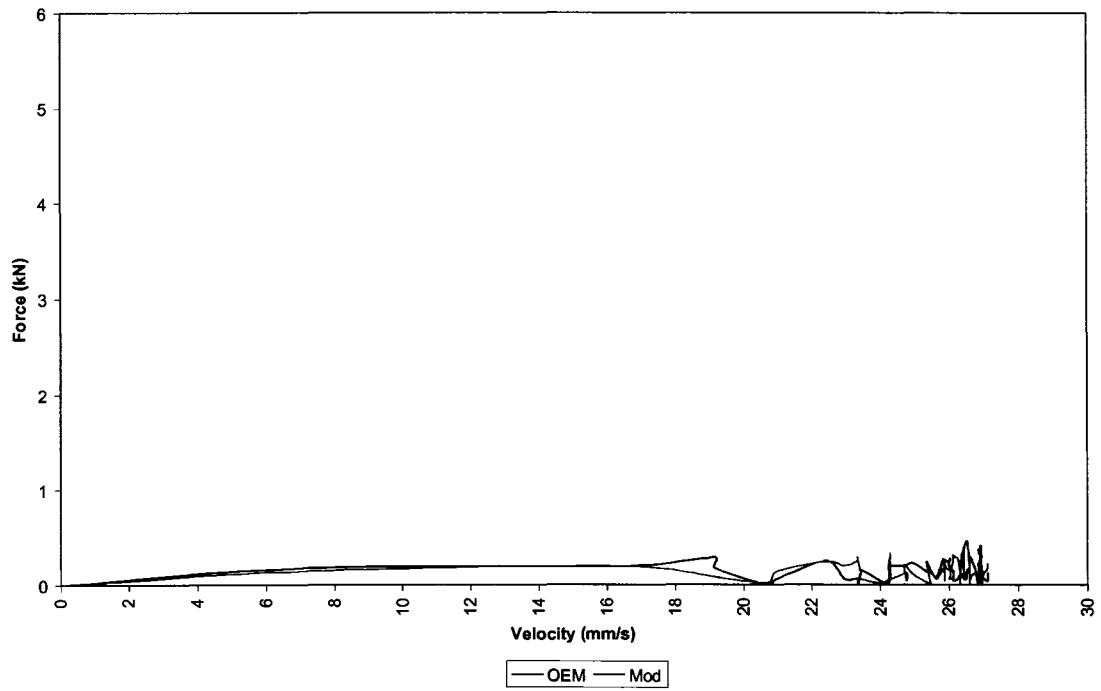


APPENDIX D

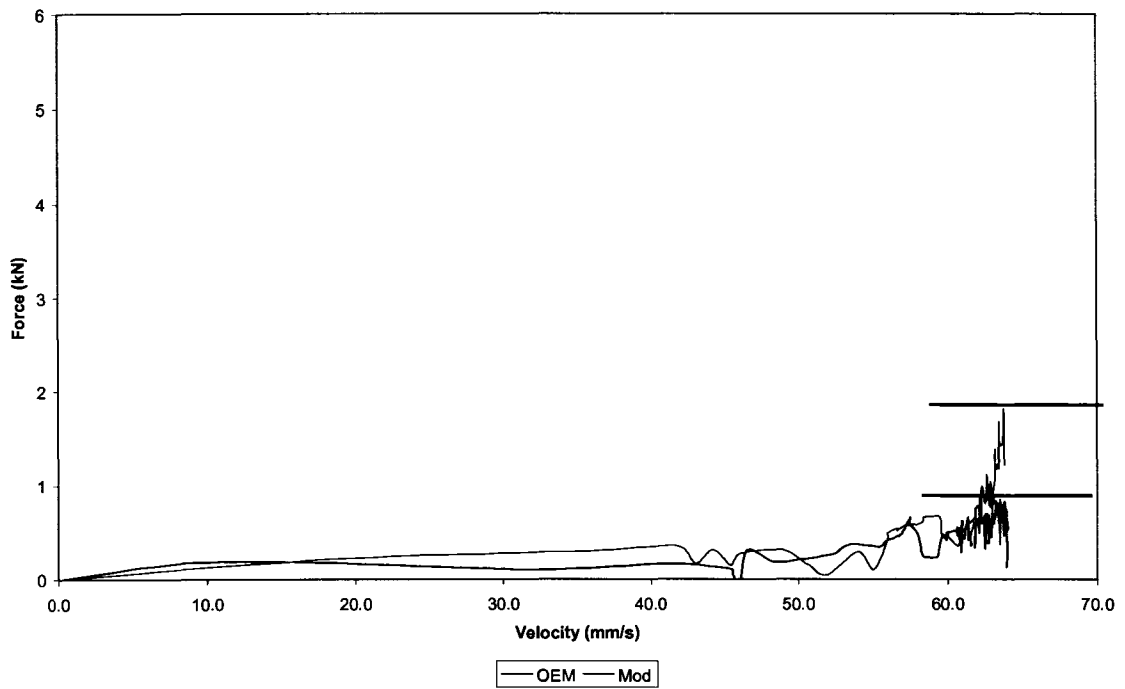
Analysis Plots

Dampening Force vs Velocity

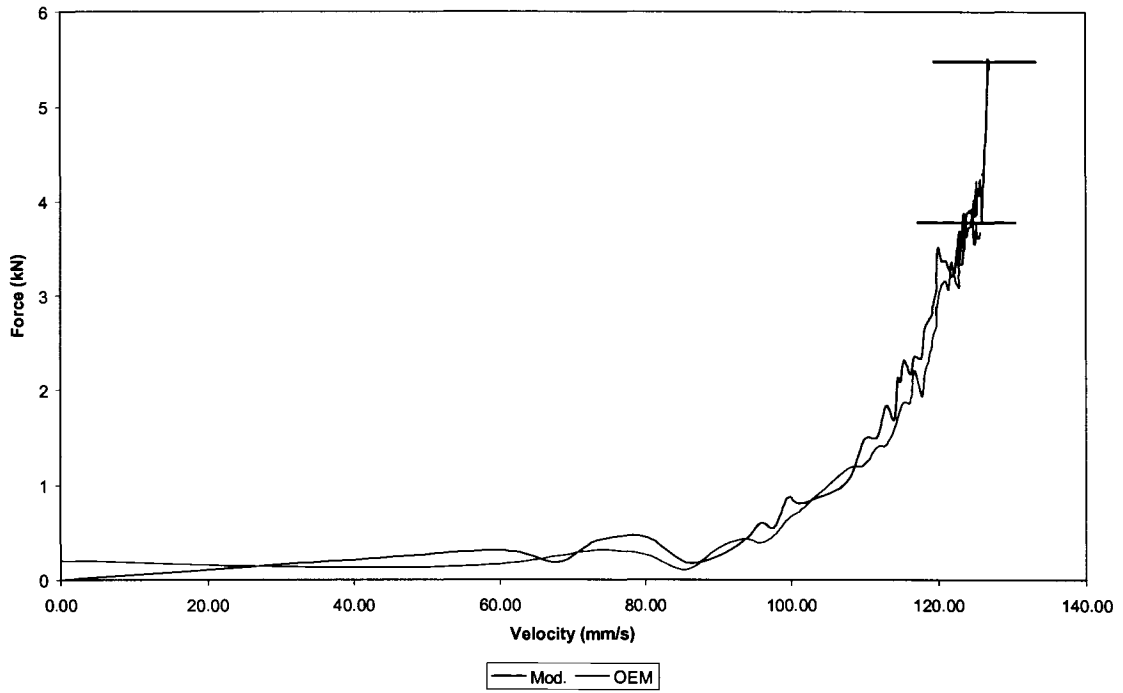
Force vs. Velocity (fq. 0.15)



Force vs. Velocity (fq 0.35)

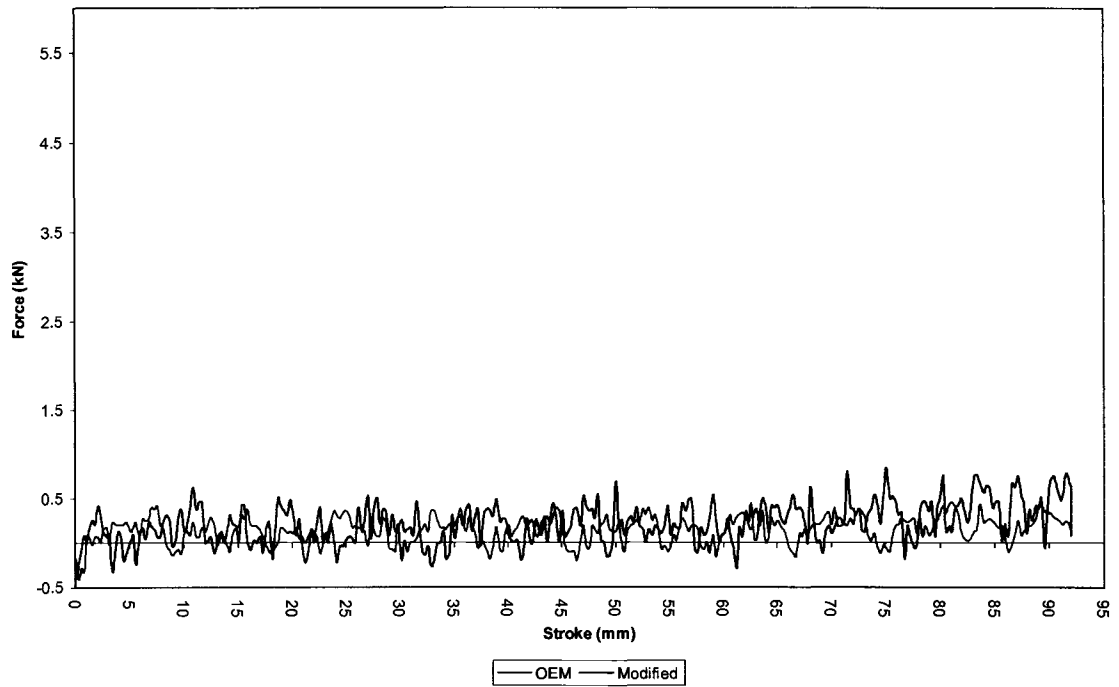


Force vs. Velocity (fq 0.7)

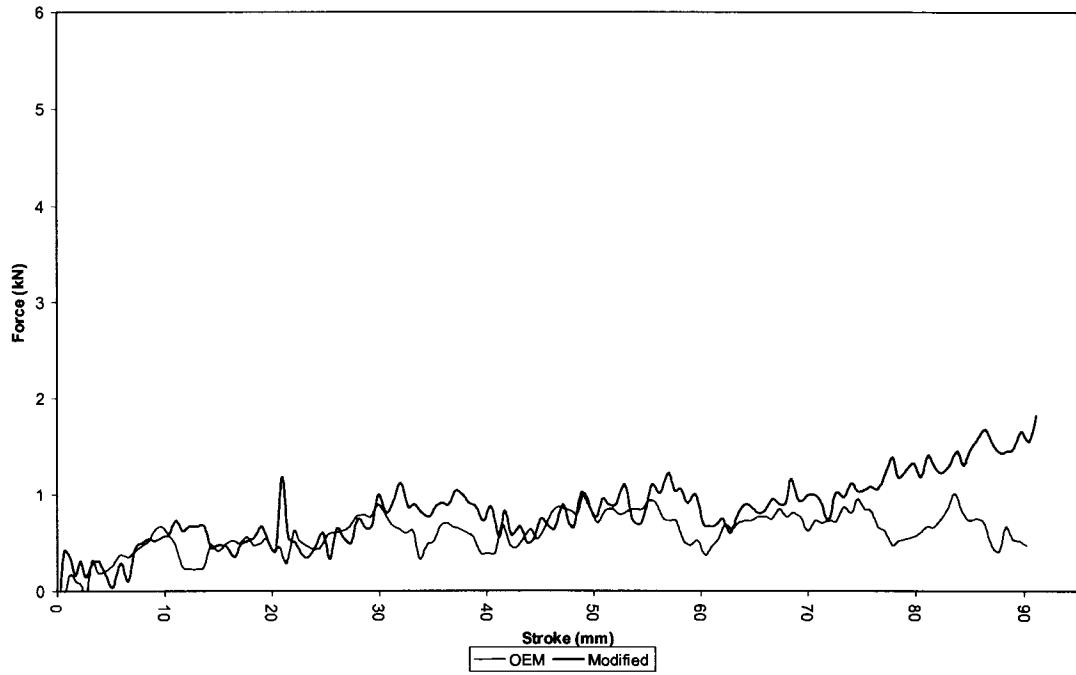


Dampening Force vs Stroke

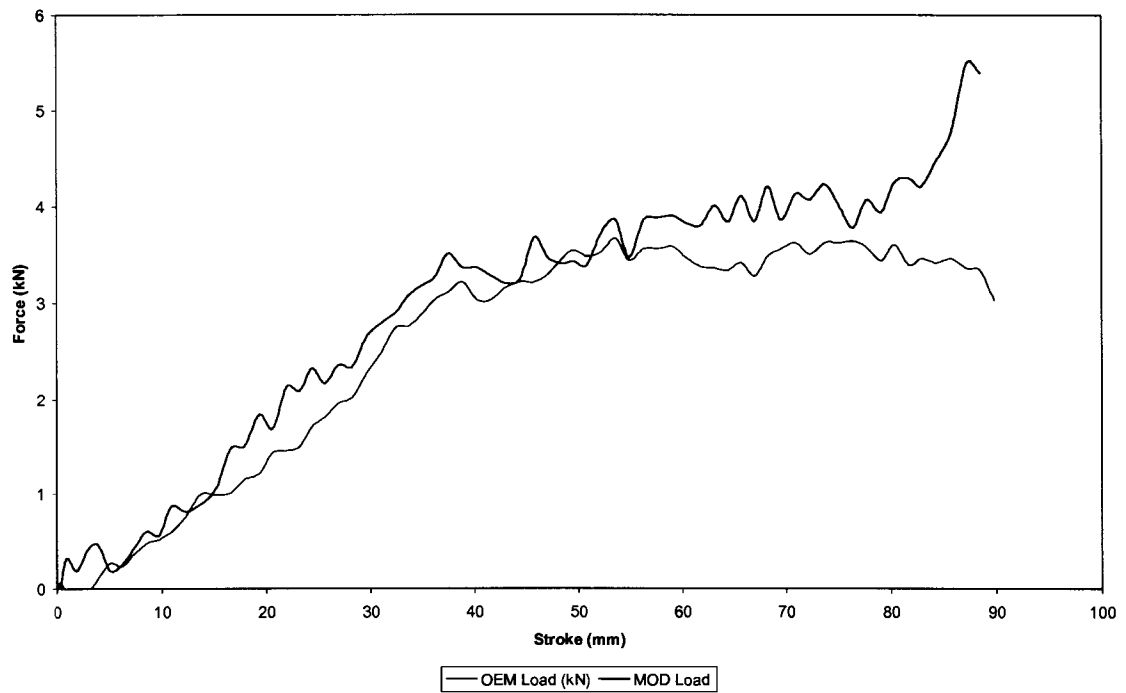
Hydraulic Dampening Force (fq 0.15)



Comparing Damping Force @ fq 0.35

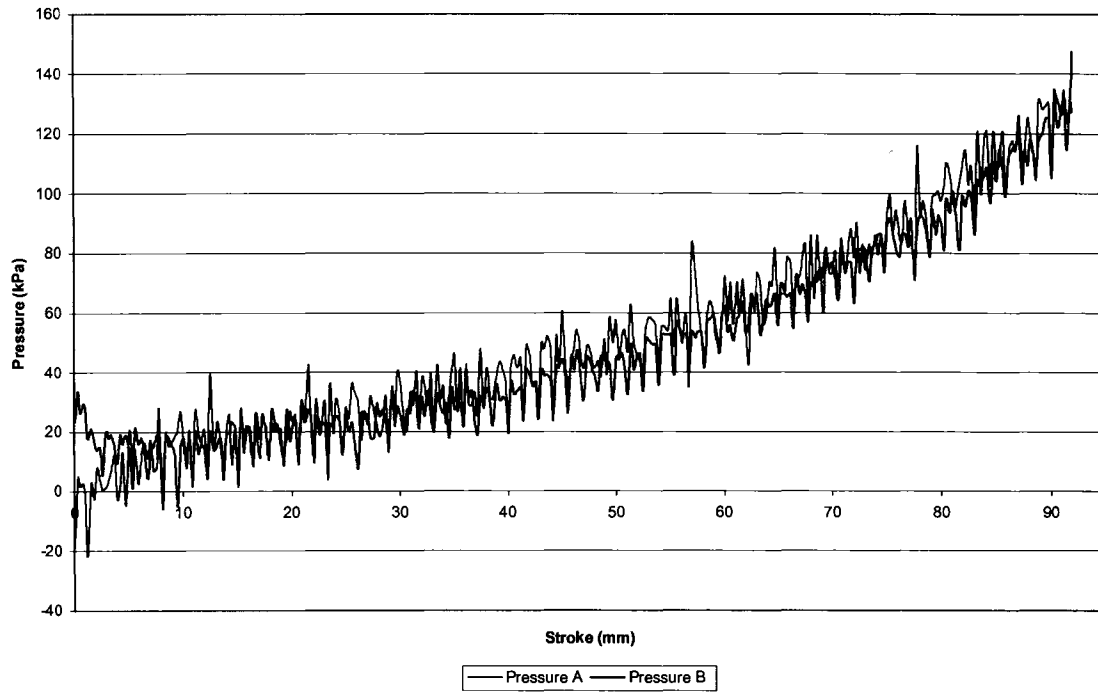


Damping Force (fq 0.7)

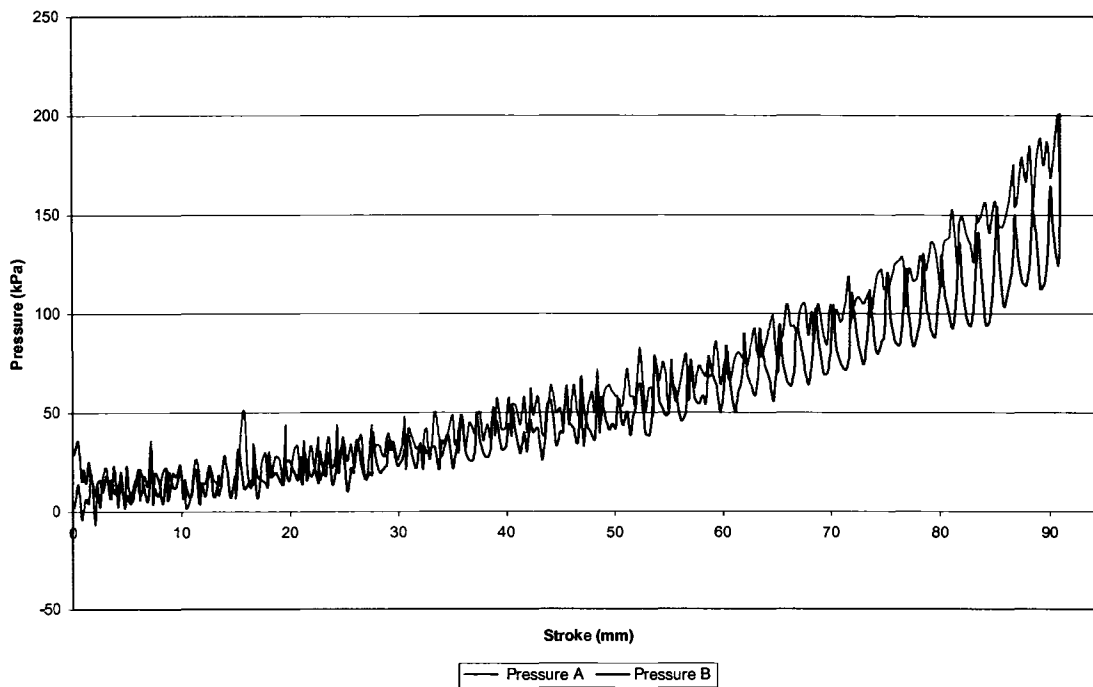


Pressure vs Stroke

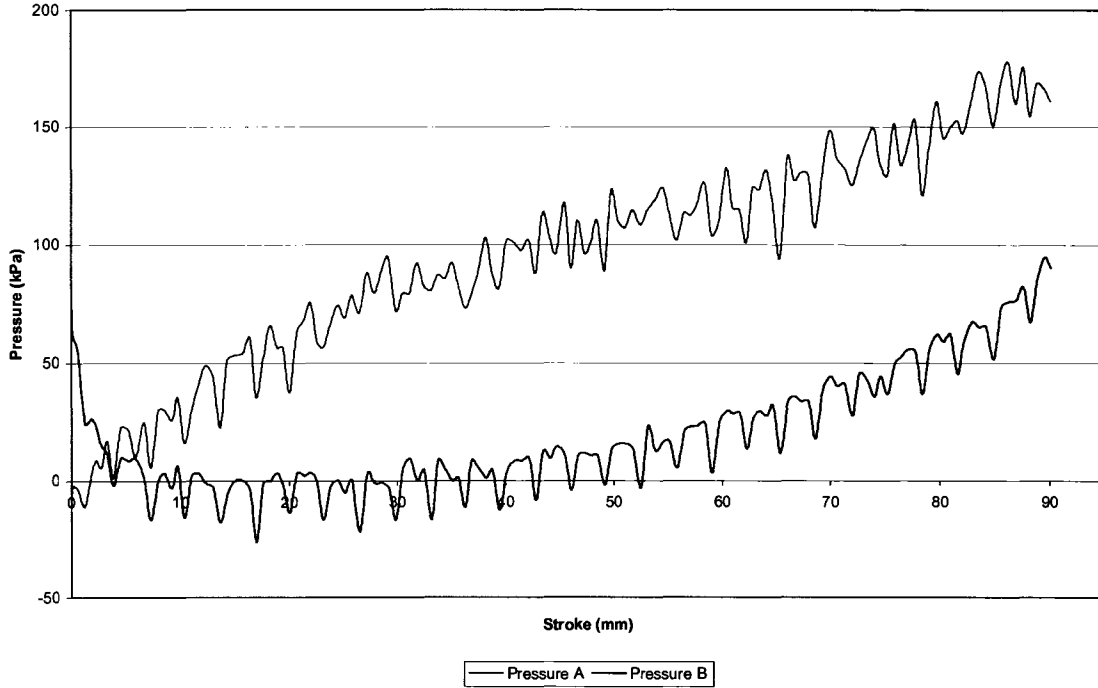
OEM: Stroke Vs. Pressure @ fq 0.15



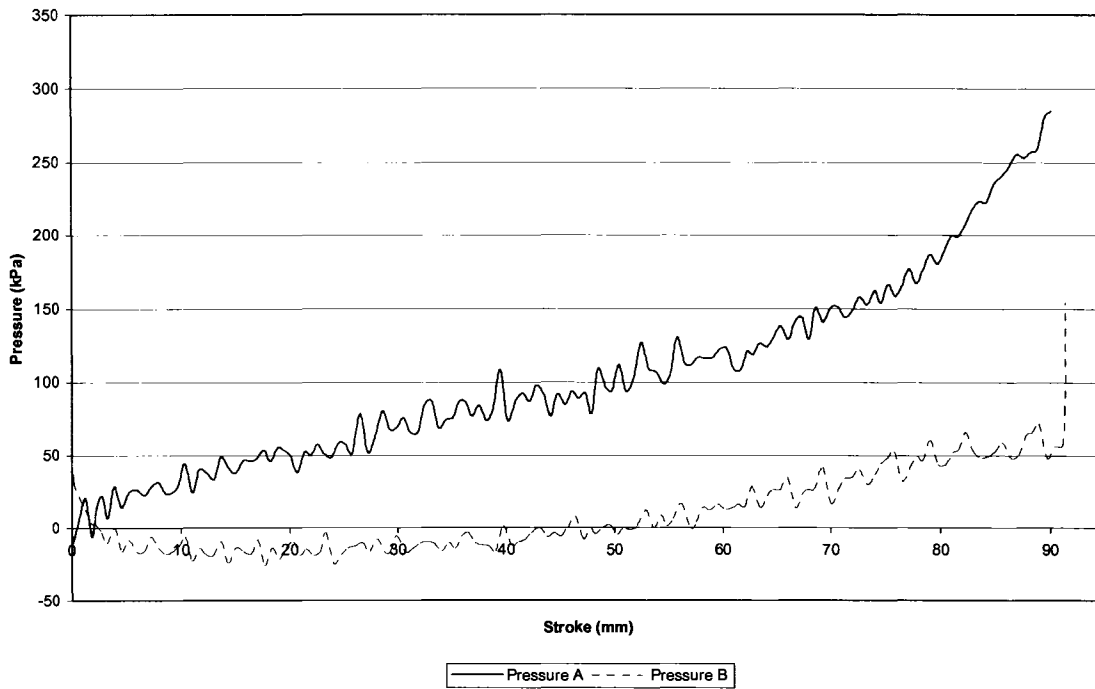
Modified: Stroke Vs. Pressure @ fq 0.15



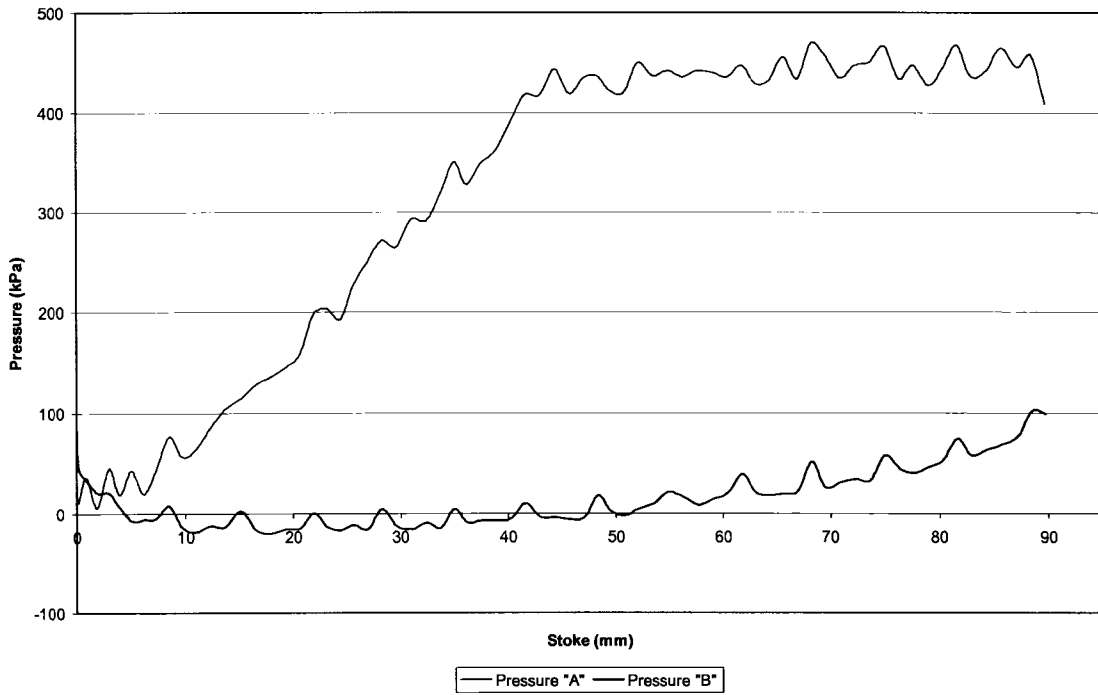
OEM: Pressure Vs. Stroke @ fq 0.35



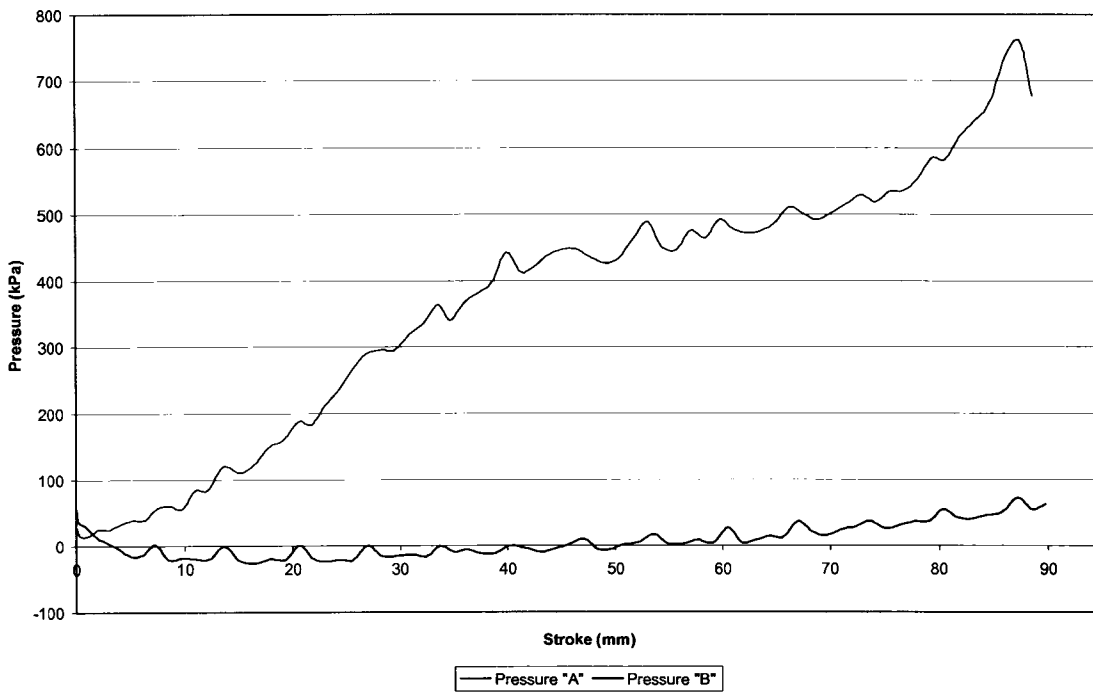
Modified: Pressure Vs. Stroke @ fq 0.35



OEM: Pressure-Stroke @ fq 0.7

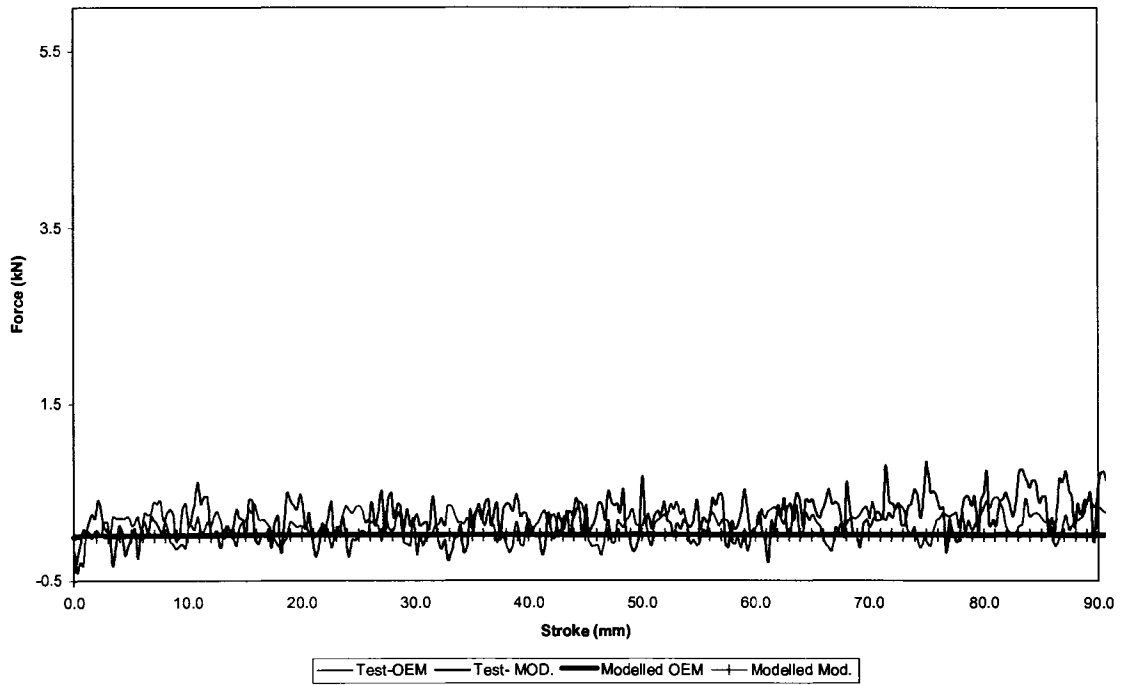


Modified: Pressure Vs. Stroke @ fq 0.7

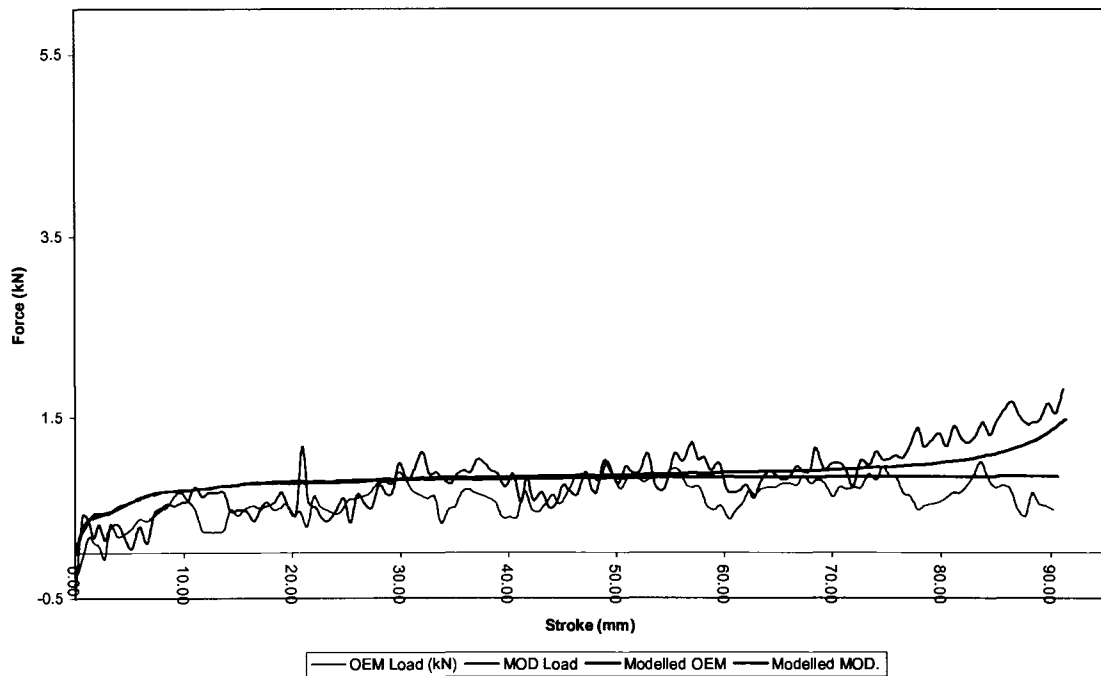


Modelled Vs Test Results

Modelled vs. Test @ fq 0.15

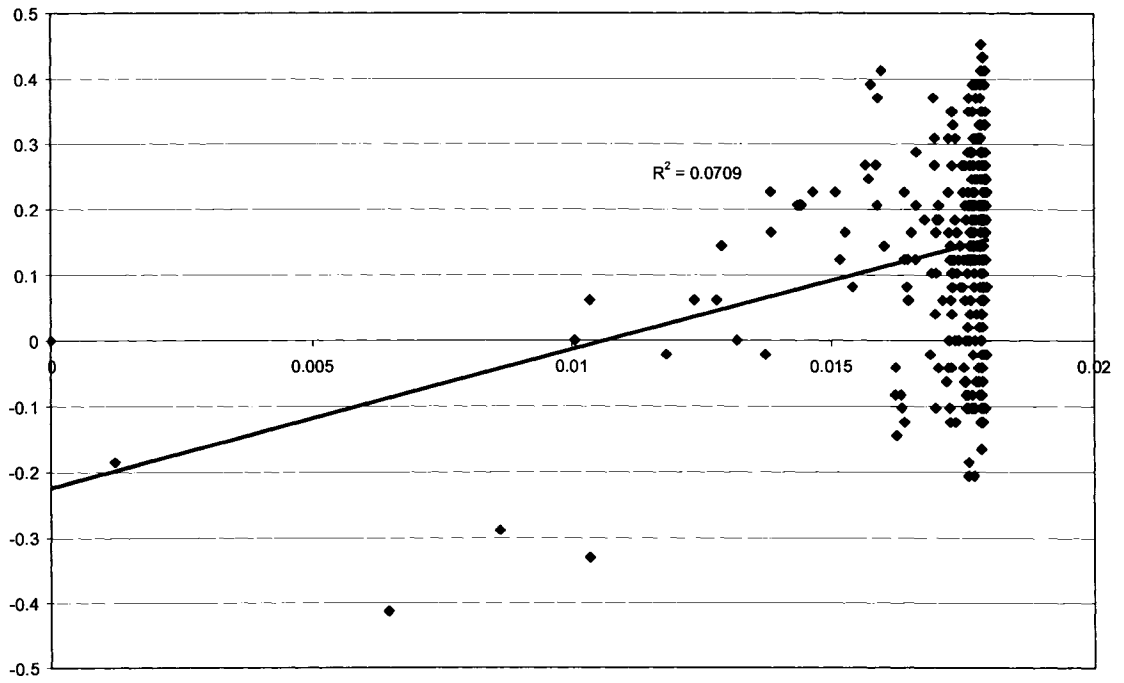


Modelled vs. Test @ fq0.35

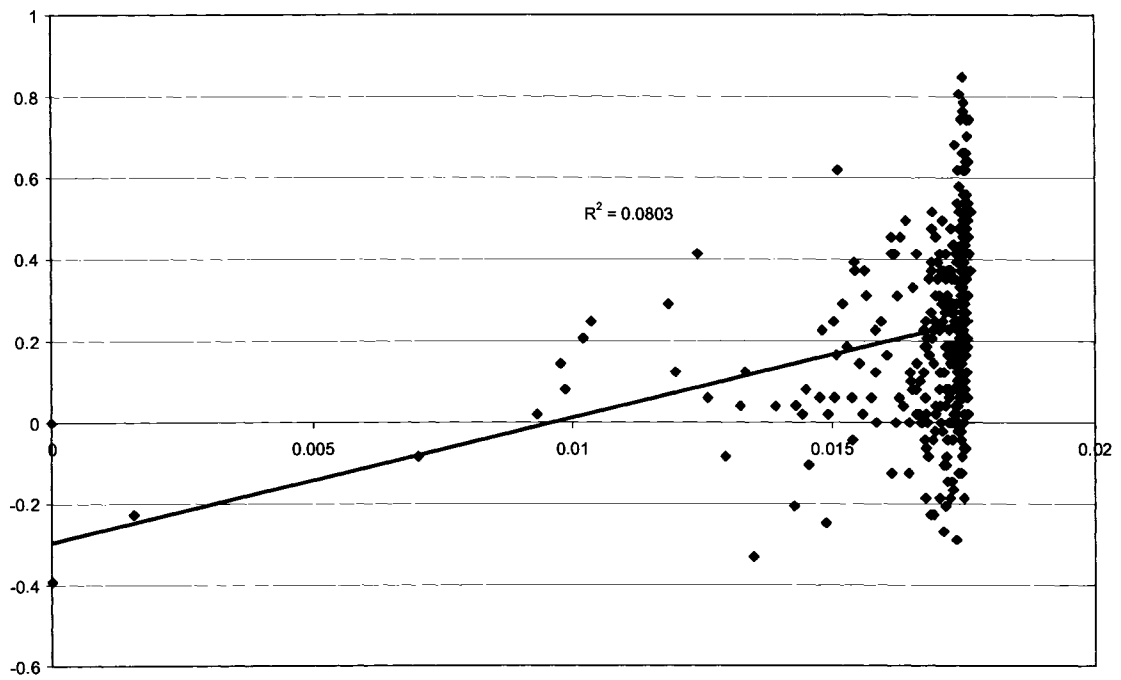


APPENDIX E
Regression Plots

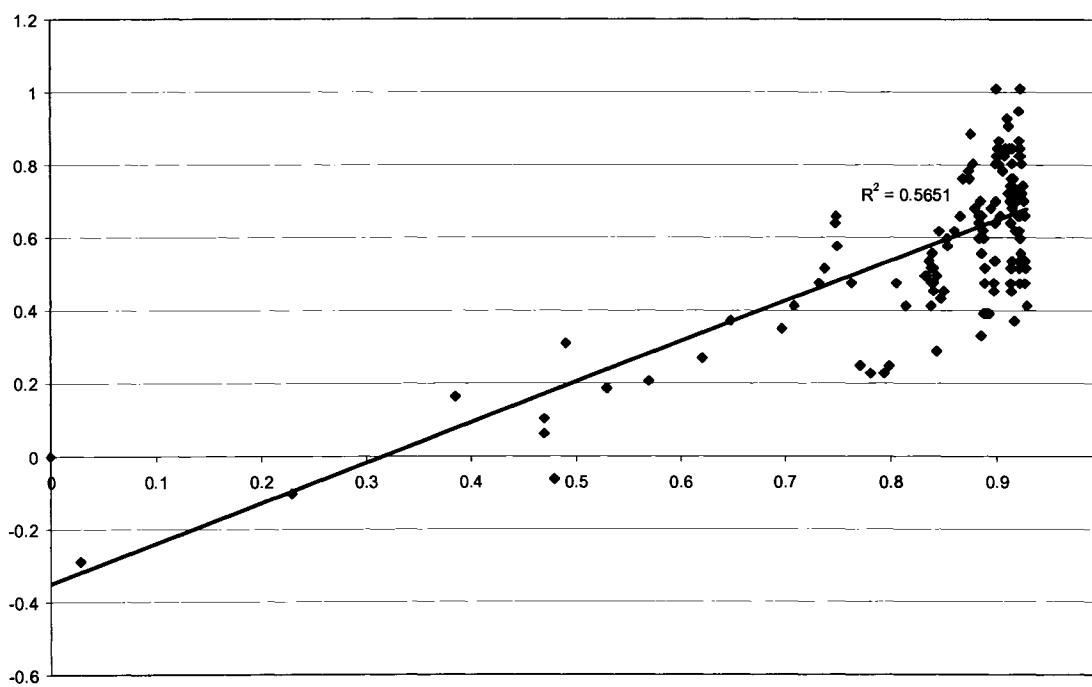
fq 0.15 (OEM)



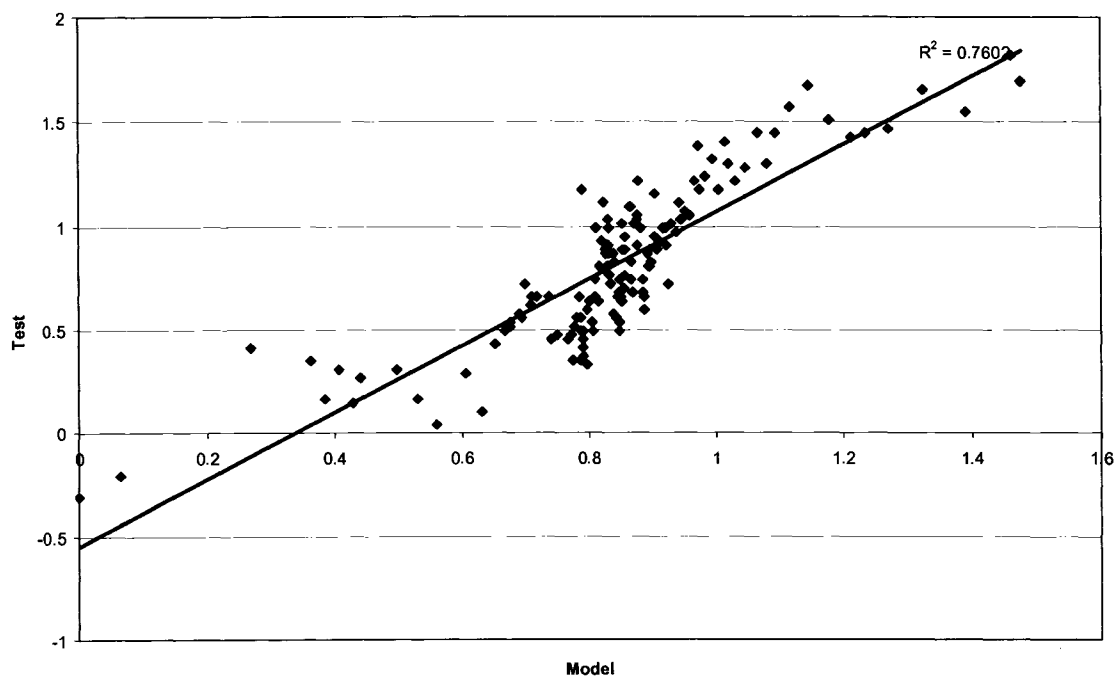
fq 0.15 (modified)



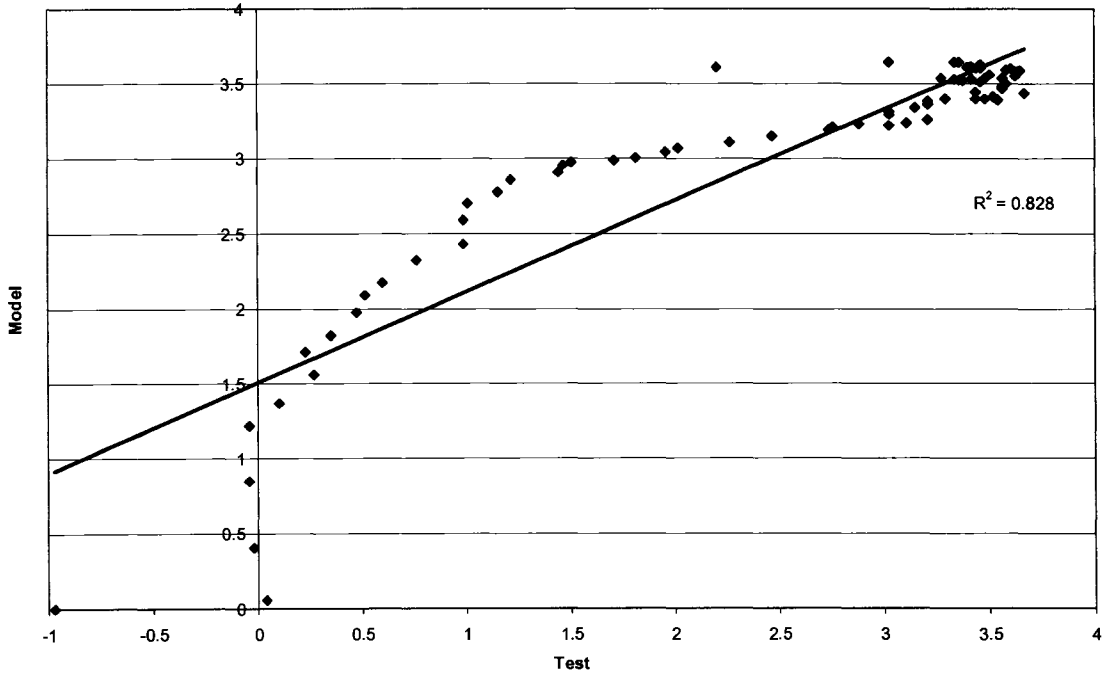
fq 0.35 (OEM)



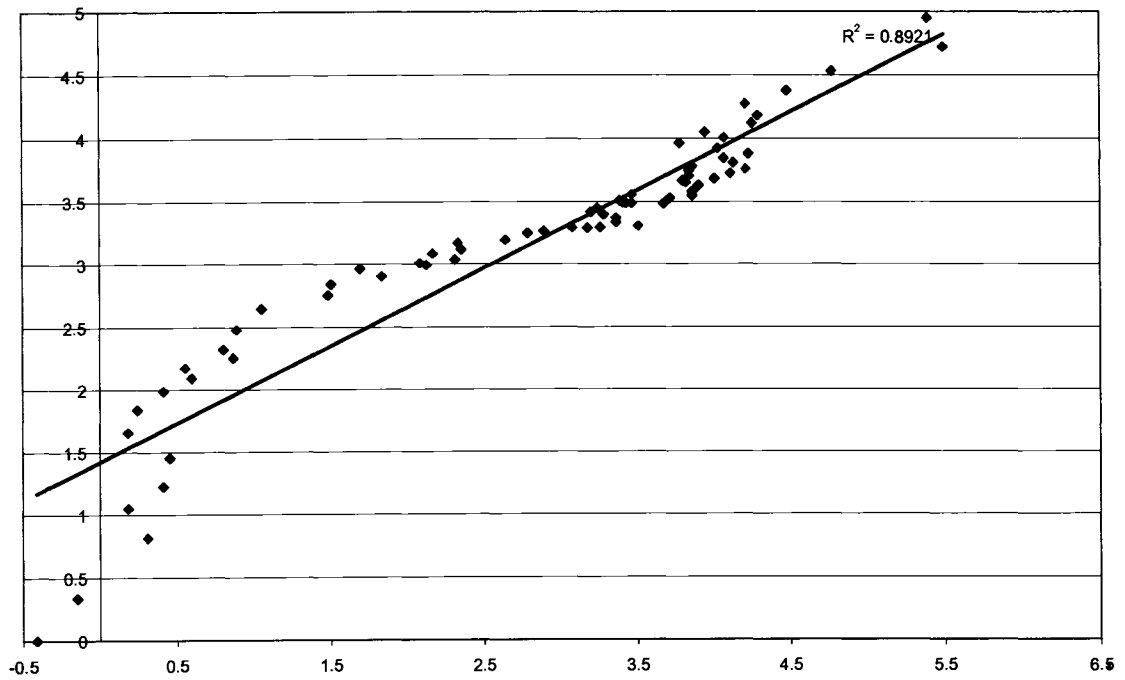
fq 0.35 (modified)



fq 0.7 (OEM)



fq 0.7 (modified)

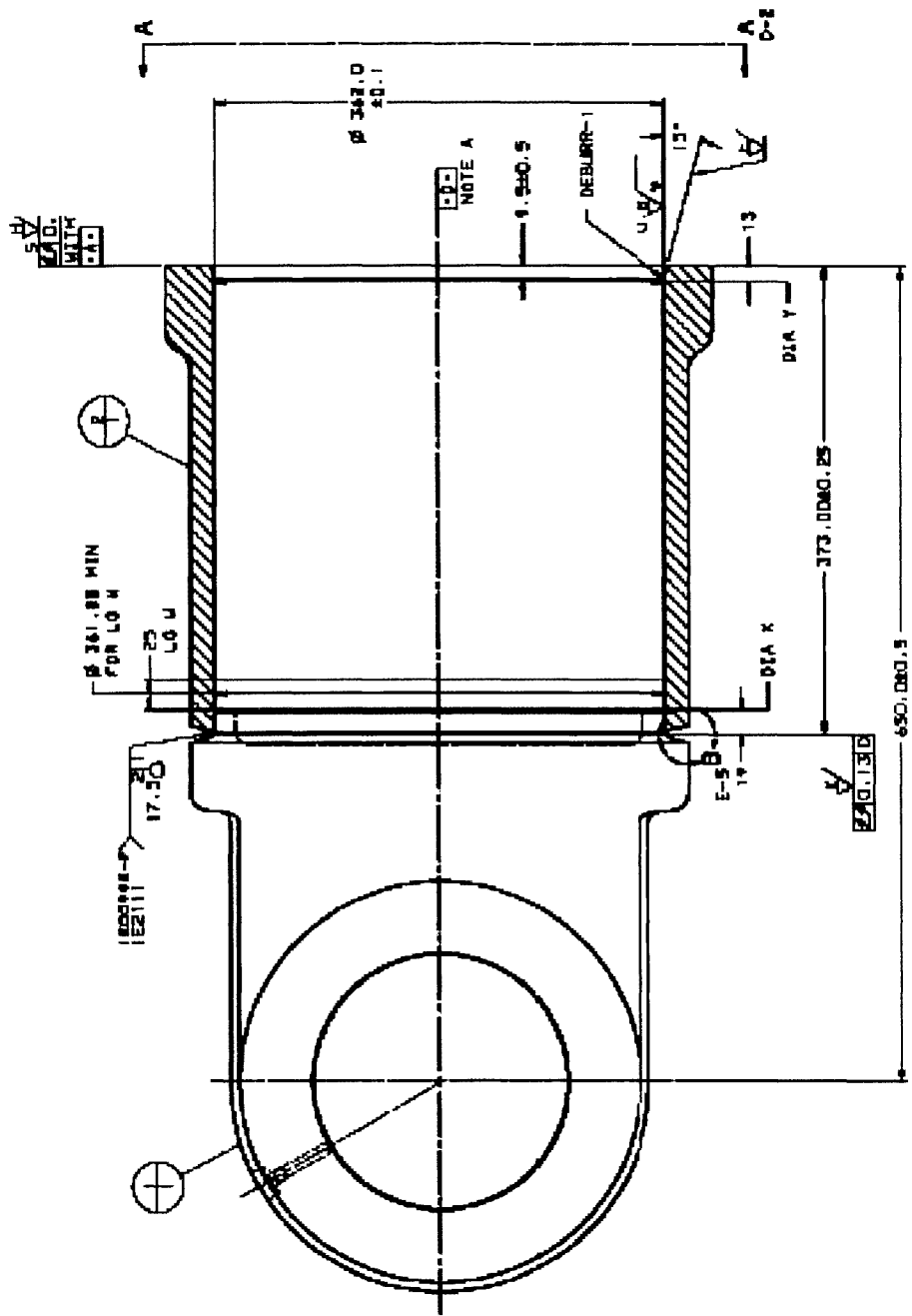


APPENDIX F
Full Scale Modeling

Input		Nitrogen Gas	
Suspension Dampert			
Inner shaft diameter	0.275 m	Initial vol.	9.34E+03 m ³
Piston diameter	0.368 m	Initial pressure	1.20E+06 Pa
Outer shaft diameter	0.318 m	Gamma	0.070693987
Inside piston height	0.478 m		1.3
Piston thickness	0.1163 m		
Cylinder diameter	0.361 m		
Total stroke	0.165 m		
Orifice Diameter	0.007 m		
Ball Check Diameter	0.0125 m		
Fluid			
Fluid Density	912 kg/m ³		
Fluid Viscosity	0.042 Ns/m ²		
Fluid Vol.	0.034 m ³		
Velocity [m/s]	0.6 m/s		

Time	Stroke [m]	V _z	V _{z,vel}	V _{z,acc}	Thickn [mm]	V _z	P _{gas}	P _{oil}	1/R _{eff} [1/R]	1/R _{ball check}	0	AP	P _z	Gas spring	Hydraulic Damping	Total	G-force
0	0.0000	0.0014	0.04315	0.00515	0.15409159	0.03286	1275000.00	1275000.00	0	0	0.00E+00	0	1275000	7.57E+04	0.00E+00	7.57E+04	0.88
0.01	0.0058	0.0017	0.04268	0.00668	0.146076041	0.03273	1402496.36	1402496.36	3.25E-12	1.39E-11	1.80E-04	10821424.76	8416828.405	4.59E+05	4.59E+05	6.42E+05	6.31
0.02	0.0628	0.0040	0.04220	0.00820	0.136052923	0.03260	1509368.01	1509368.01	3.25E-12	1.39E-11	1.80E-04	10821424.76	-9312056.752	4.59E+05	4.59E+05	5.48E+05	6.30
0.03	0.0698	0.0054	0.04172	0.00772	0.130029904	0.03246	1631543.45	1631543.45	3.25E-12	1.39E-11	1.80E-04	10821424.76	9048661.304	4.59E+05	4.59E+05	6.58E+05	6.47
0.04	0.0746	0.0067	0.04125	0.00725	0.122006986	0.03233	1772375.37	1772375.37	3.25E-12	1.39E-11	1.80E-04	10821424.76	9048661.306	4.59E+05	4.59E+05	6.58E+05	6.56
0.05	0.0800	0.0081	0.04077	0.00677	0.113863688	0.03219	1936241.42	1936241.42	3.25E-12	1.39E-11	1.80E-04	10821424.76	8662163.338	4.59E+05	4.59E+05	6.74E+05	6.68
0.06	0.0869	0.0094	0.04029	0.00629	0.105950449	0.03206	2128959.96	2128959.96	3.25E-12	1.39E-11	1.80E-04	10821424.76	8662163.338	4.59E+05	4.59E+05	6.86E+05	6.81
0.07	0.0928	0.0108	0.03982	0.00582	0.097937331	0.03192	2358422.89	2358422.89	3.25E-12	1.39E-11	1.80E-04	10821424.76	8463001.853	4.59E+05	4.59E+05	6.99E+05	6.97
0.08	0.0989	0.0121	0.03934	0.00534	0.089814213	0.03179	2635698.33	2635698.33	3.25E-12	1.39E-11	1.80E-04	10821424.76	8186906.427	4.59E+05	4.59E+05	7.15E+05	7.16
0.09	0.1048	0.0134	0.03886	0.00486	0.081891096	0.03166	2976984.71	2976984.71	3.25E-12	1.39E-11	1.80E-04	10821424.76	7845330.046	4.59E+05	4.59E+05	7.40E+05	7.40
0.1	0.1088	0.0146	0.03838	0.00438	0.073973976	0.03152	3402966.43	3402966.43	3.25E-12	1.39E-11	1.80E-04	10821424.76	7419429.332	4.59E+05	4.59E+05	7.69E+05	7.69
0.11	0.1162	0.0161	0.03791	0.00391	0.065846568	0.03140	3951627.52	3951627.52	3.25E-12	1.39E-11	1.80E-04	10821424.76	6919317.963	4.59E+05	4.59E+05	8.07E+05	8.07
0.1082	0.1236	0.0176	0.03743	0.00343	0.05761981	0.03124	4792789.89	4792789.89	3.25E-12	1.39E-11	1.80E-04	10821424.76	6076314.669	4.59E+05	4.59E+05	8.56E+05	8.56
0.131333	0.1296	0.0190	0.03695	0.00295	0.049393986	0.03103	5844296.36	5844296.36	3.25E-12	1.39E-11	1.80E-04	10821424.76	4261077.695	4.59E+05	4.59E+05	9.30E+05	9.30
0.1465	0.1367	0.0207	0.03647	0.00247	0.041693476	0.03103	6800347.16	6800347.16	3.25E-12	1.39E-11	1.80E-04	10821424.76	2338812.897	4.59E+05	4.59E+05	9.87E+05	9.87
0.176	0.1504	0.0224	0.03597	0.00200	0.034693654	0.03077	8480612.66	8480612.66	3.25E-12	1.39E-11	1.80E-04	10821424.76	684665.754	4.59E+05	4.59E+05	1.14E+06	11.21
0.176	0.1504	0.0224	0.03597	0.00200	0.034693654	0.03077	1506290.51	1506290.51	3.25E-12	1.39E-11	1.80E-04	10821424.76	684665.754	4.59E+05	4.59E+05	1.14E+06	11.21
0.176	0.1504	0.0224	0.03597	0.00200	0.034693654	0.03077	1754844.21	1754844.21	3.25E-12	1.39E-11	1.80E-04	10821424.76	6727419.449	4.59E+05	4.59E+05	1.50E+06	17.47
0.182	0.16	0.0238	0.03448	0.00148	0.012892277	0.03050	32917428.18	32917428.18	3.25E-12	1.39E-11	1.80E-04	10821424.76	2206603.42	4.59E+05	4.59E+05	2.41E+06	28.09
0.182	0.16	0.0238	0.03448	0.00148	0.003078406	0.03042	60440914.16	60440914.16	3.25E-12	1.39E-11	1.80E-04	10821424.76	4951965.4	4.59E+05	4.59E+05	4.06E+06	47.12

APPENDIX G
789B Damper Detail



Details of the Cylinder Tube

